ORGANIC CHEMISTRY FRONTIERS

REVIEW

View Article Online
View Journal | View Issue

Cite this: *Org. Chem. Front.*, 2022, **9**, 517

A brief overview of classical natural product drug synthesis and bioactivity

Gen Li,†[a] Mingliang Lou†[a] and Xiangbing Qi *[a,b]

Traditional medicines consisting of compounds derived from natural organisms have been used for human health care worldwide since ancient times. Since the last century, huge numbers of bioactive natural entities with diverse chemical scaffolds have been discovered, and some have been explored as clinical medications to treat various diseases. The advent of modern technologies has promoted the discovery of natural product-based pharmaceutical agents. The synthesis of natural products not only paves the way to confirm their molecular structures but also offers the structural modification opportunity to rationally optimize the drug-likeness parameters and evaluate the bioactivity of analogs. By providing a brief overview of a miscellaneous collection of complex natural products synthesis and the efforts of the structure–activity relationship, the present report aims to highlight the impact of chemical synthesis in natural product generation, diversification, bioactivity evaluation, and natural product-based drug development.

Received 8th September 2021,
Accepted 18th November 2021

DOI: 10.1039/d1qo01341f

rsc.li/frontiers-organic

1. Introduction

For millennia, nature has provided an invaluable source of traditional medicines from a variety of plants, animals, microorganisms, and minerals for humans to treat a wide spectrum of diseases. Since around 2600 BCE the successful use of natural medicines and remedies, particularly plant-originated substances, has been well documented in a large number of countries.[1] The World Health Organization (WHO) estimated in 1985 that more than 4000 million people in the world relied mainly on traditional medicines for their primary health care.[2] Since the 19th century, developments in the fields of phytochemistry and analytical chemistry have enhanced humans' ability to examine natural materials more deeply and to identify pure bioactive constitutes to further leverage the application potential of natural products.

Beginning with the isolation of morphine, the first active principle from the opium poppy, by German pharmacist

[a]*National Institute of Biological Sciences (NIBS), 7 Science Park Road ZGC Life Science Park, Beijing 102206, China. E-mail: qixiangbing@nibs.ac.cn*
[b]*Tsinghua Institute of Multidisciplinary Biomedical Research, Tsinghua University, Beijing 100084, China*
†These authors made equal contribution.

Gen Li

Gen Li was born in Xinjiang, China. He received his B.Sc. (2004) in Chemistry from Xinjiang University and his Ph. D. (2011) degree in Chemical Biology from Peking University under the supervision of Professor Xin-Shan Ye. After a seven year research stage at Xinjiang Technical Institute of Physics and Chemistry, CAS, as an assistant professor and associate professor, he joined Qi's group at the National Institute of Biological Science (NIBS) at the beginning of 2019. His research interests focus on the total synthesis of natural products, and medicinal chemistry.

Mingliang Lou

Mingliang Lou was born in Anhui Province, China. He received his BS degree in Biology from Nankai University in 2014. In 2020, he received his Ph.D. degree in Medicinal Chemistry from Peking Union Medical College under the direction of Professor Xiangbing Qi. Currently, he works in the National Institute of Biological Sciences (NIBS) and focuses on natural product synthesis and drug development.

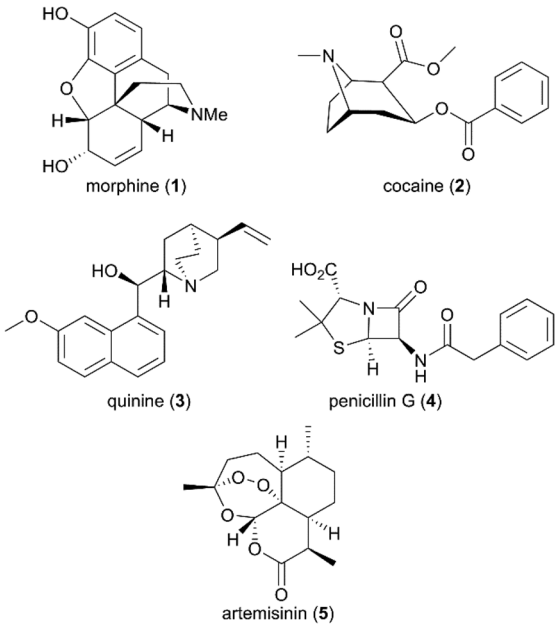

Fig. 1 Structures of morphine, cocaine, quinine, penicillin G, and artemisinin.

Friedrich Sertürner in 1806, and followed by its commercialization as an analgesic and sedative by Merck in 1827,[3] several active natural products were subsequently purified, such as cocaine and quinine from plant coca and cinchona, respectively (Fig. 1).[4] However, not until the last century did drug discovery-based natural products come of age due to the scientific breakthroughs in modern chemistry and medicine. The natural products pool was enriched with broader chemical structures and diverse spectrum bioactivities. Compared with conventional synthetic molecules, naturally generated products are characterized by more complex skeletons with a higher molecular mass and a larger number of sp^3-hybridized atoms, which can be advantageous for the exploration of small molecule and biomolecule interactions.

Despite the successful discovery of multiple drugs based on original natural products, such as morphine and artemisinin (Fig. 1), they still suffer from source and availability challenges. More importantly, the low success rate of the natural entity in approved drugs emphasizes the importance of structural optimization to improve natural products' drug-like characteristics during drug development. With the development of new synthetic strategies and methodologies, more complex natural products have been assembled by efficient total synthesis or semisynthesis. The complementation of total synthesis strategies with semisynthetic transformations has been applied widely in the diversity- and bioactivity-oriented synthesis of drug-like entities.

Natural products and their synthetically modified analogs have historically made a remarkable contribution to the development of new drugs. A number of reports and books have reviewed the development of natural product-based drugs,[1,5–13] including antibiotic drugs,[14–16] antitumor agents,[17–20] analgesics,[21,22] and antiparasitic drugs.[23–25] All the reviews mentioned above emphasize that original natural products play significant roles in the drug discovery and development process. This is also confirmed further in the recent survey provided in serial reviews from Newman and Cragg,[5,26–29] which reported that only 463 purely synthetic drugs accounted for 24.6% of 1881 approved new chemical entities between 1981 and 2019. The rest of the new drugs on the market were either derived from the original natural structure or inspired by the rigidly complex skeletons of natural entities; 427 naturally occurring products (N, Newman and Cragg's category) and their structural derivatives (ND) were approved over almost 39 years.

Even though these reviews summarized nicely the natural product-based new drug development, druggability-related synthesis was not intensively tackled. We proposed to provide a brief overview of a miscellaneous collection of complex natural products synthesis and the endeavors of structure–activity relationships (SAR) studies to highlight the impact of chemical synthesis in natural product medicinal chemistry. Given the large number of approved natural product drugs in history, only the representative complex natural products whose chemical synthesis played an important role during the related drugs development are selected here. We admit that some natural products drugs, such as penicillin, vancomycin, ciclosporin, and rapamycin, are also classical and complex, but these are not covered due to limited space. Herein, the total synthesis of eight natural entities that were approved as drugs is presented according to the structural features, and the roles that total synthesis played in drug discovery and development are overviewed. The SAR studies are also discussed extensively.

Xiangbing Qi

Xiangbing Qi was born in Shandong, China, and received his Ph.D. in chemistry and biochemistry from UT Southwestern Medical Center, Dallas, in 2005. After postdoctoral training at the University of Illinois Urbana-Champaign and medicinal chemistry research at UT Southwestern Medical Center, Dr Qi joined the faculty at the National Institute of Biological Sciences, Beijing, in 2013 and he is currently the Director of the Chemistry Center. The central theme of the research program is focused on the interface of synthetic chemistry, chemical biology, natural product total synthesis, and medicinal chemistry.

2. Morphine and morphine derivatives

Morphine (**1**), isolated in 1806 by a German pharmacist, Friedrich Sertürner, is used primarily to treat both acute and

chronic moderate-to-severe pain.[30–34] It functions through selective binding to the μ-type opioid receptor in the brain and spinal cord.[35,36] Many natural analogs and semisynthetic derivatives of morphine have been isolated or synthesized until now, some of which are presented in Fig. 2. The primary source of morphine and its congeners is isolation from the opium poppy, which is greatly affected by climate and political instability.[32,37] Although the morphine biosynthesis pathway has been elucidated and the laboratory scale production of morphine in yeast has been realized, major challenges remain to be addressed before the realization of practical strategies for industrial-scale production.[38,39] Therefore, total synthesis may be a plausible surrogate for extraction in the production of morphine and its derivatives.

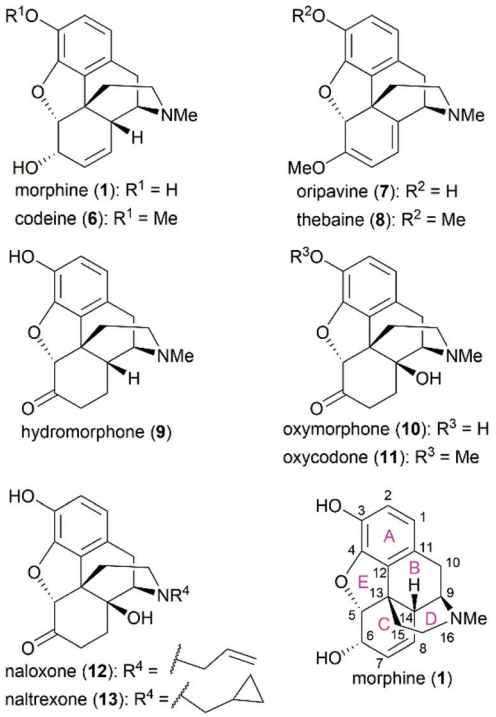

Fig. 2 Morphine and related compounds, and their ring lettering and carbon numbering system.

The structure of morphine was first proposed by Robinson in 1925, and this structure was supported by Gates' first total synthesis of morphine in 1952 and later by X-ray analysis in 1954.[40–43] As shown in Fig. 2, there are several intriguing structural features of morphine: a rigid pentacyclic bridged/fused ring structure (designated A, B, C, D, and E), five contiguous stereocenters (C5, C6, C9, C13, and C14) including one quaternary stereocenter (C13), an ether linkage between C4 and C5, two hydroxy groups (C3 and C6), a basic tertiary amine moiety, and a double bond between C7 and C8, which make its total synthesis a challenging task. The numerous studies on the synthesis of morphine alkaloids have led to over 40 synthesis routes, which have been summarized in several recent reviews.[31,33,34,37,44,45] Selected representative routes for catalytic asymmetric total synthesis of morphine alkaloids will be discussed in the following section.

2.1 Catalytic asymmetric total synthesis of morphine alkaloids

2.1.1 Overman's total synthesis of (−)-morphine. Overman and co-workers completed the first catalytic asymmetric synthesis of (−)-morphine (**1**).[46] In their synthesis, enantioselective reduction of ketone **14** with catecholborane in the presence of (*R*)-oxazaborolidine catalyst (**15**) and subsequent condensation of the alcohol with phenyl isocyanate produced **16** (Scheme 1). The latter was transformed into **18** through two

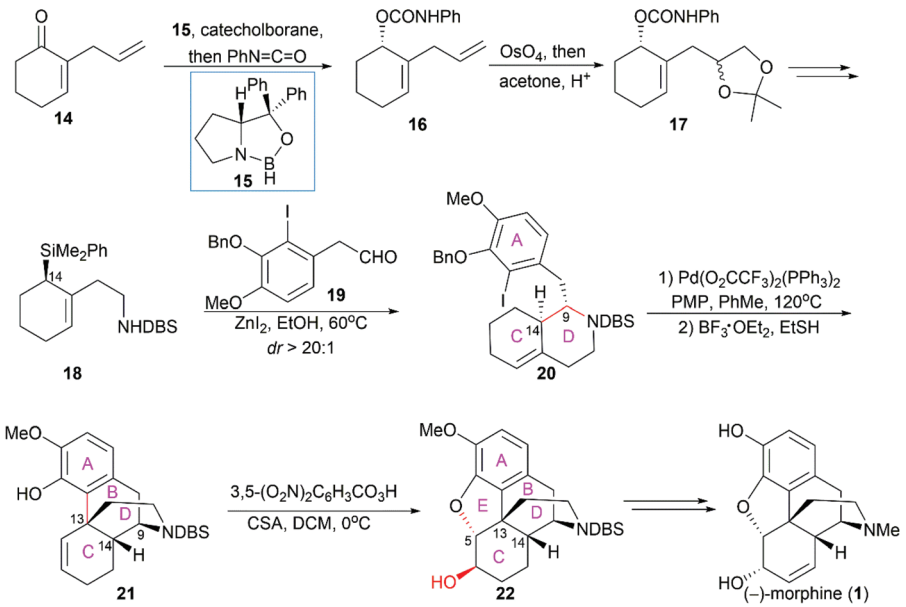

Scheme 1 Overman's synthetic route.

key operations: catalytic dihydroxylation of the terminal double bond and introduction of an allylsilane group, in which the desired C14 (following the numbering in morphine) stereocenter was established. Condensation of **18** with a tetrasubstituted A ring aldehyde **19** through the Mannich reaction generated ring D in **20**. An intramolecular Heck reaction within **20** and subsequent removal of the benzyl group gave the tetracyclic compound **21** concomitant with the construction of the crucial quaternary C13 stereocenter. Ring E was constructed through epoxidation of the double bond and an epoxide ring-opening cyclization sequence. The pentacyclic compound **22** was transformed into (−)-morphine (**1**) following Rice's method.[47]

2.1.2 White's total synthesis of (+)-morphine. In White's synthesis,[48] the phenanthrene ring system (ring A/B/C) was constructed first, and this ring system was used as a platform for the sequential introduction of the dihydrofuran ring E and piperidine ring D. The first chiral center (C9) was established through Rh-catalyzed enantioselective hydrogenation of the α,β-unsaturated ester **23** in the presence of (4*R*,5*R*)-MOD-DIOP **24** (Scheme 2). The following intramolecular Friedel–Crafts reaction and Robinson annulation provided the phenanthrene nucleus **28**. DBU-promoted cyclization yielded the tetracyclic compound **29**, which was transformed into the diazo ketone **30**. A Rh(II)-catalyzed carbenoid C–H insertion reaction was used to construct the challenging C13 all-carbon stereocenter in **31**. The cyclopentanone was transformed into the piperidine ring through Beckmann rearrangement, which completed the synthesis of the pentacyclic core skeleton **32**. Several functional group manipulations successfully led to the synthesis of (+)-morphine.

2.1.3 Trost's total synthesis of (−)-morphine. Trost's asymmetric total synthesis of (−)-morphine (**1**) features a series of Pd-catalyzed reactions.[49–51] By employing Pd-catalyzed asymmetric allylic alkylation of allylic ester **35** with 2-bromovanillin **34** in the presence of chiral ligand **36**, the aryl ether **37** with 87% to 88% ee and the desired stereo configuration at C5 was obtained (Scheme 3). Then, a Pd-catalyzed intramolecular Heck reaction was applied to construct the ring E accompanied by the establishment of the quaternary stereocenter C13 (**38** to **39**). Another intramolecular Heck reaction on **40** smoothly led to tetracyclic compound **41**, which was transformed into allyl alcohol **42**. The final piperidine ring D was constructed through an intriguing visible light-promoted hydroamination reaction. It should be noted that intramolecular Heck reactions were also used in Hudlicky's asymmetric total synthesis of (−)-codeine (**6**) to construct ring E and ring B, wherein the chiral starting material was derived from enzyme-catalyzed enantioselective dihydroxylation of β-bromoethylbenzene.[52,53]

2.1.4 Tu's total synthesis of (−)-morphine. In Tu's total synthesis of (−)-morphine (**1**),[54] chiral spiropyrrolidine (SPD) organocatalyst **44**-catalyzed asymmetric Michael addition within **43** and subsequent *p*-toluenesulfonic acid-promoted Robinson annulation were utilized to construct the A/C/E ring system with the establishment of the quaternary stereocenter C13 (Scheme 4). Introduction of an aldehyde group on **45** and subsequent polyphosphoric acid (PPA)-catalyzed Friedel–Crafts type cyclization led to the tetracyclic compound **46**. A Wharton reaction was used to transform α,β-unsaturated ketone **46** to allylic alcohol **47**. Introduction of the sulfonamide through a

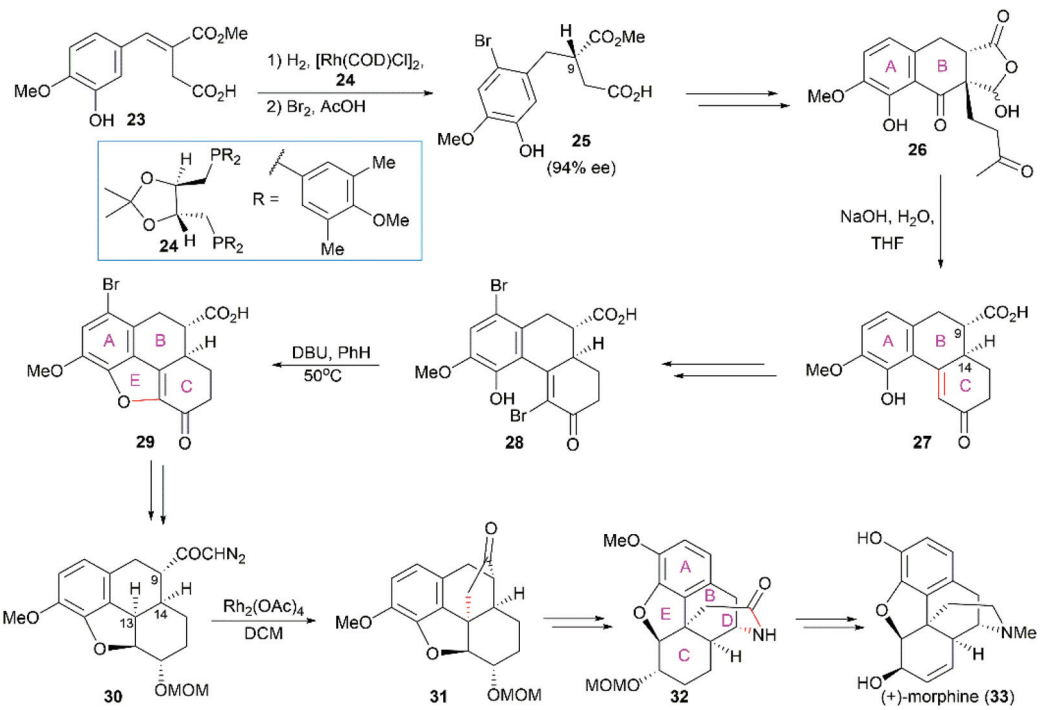

Scheme 2 White's synthetic route.

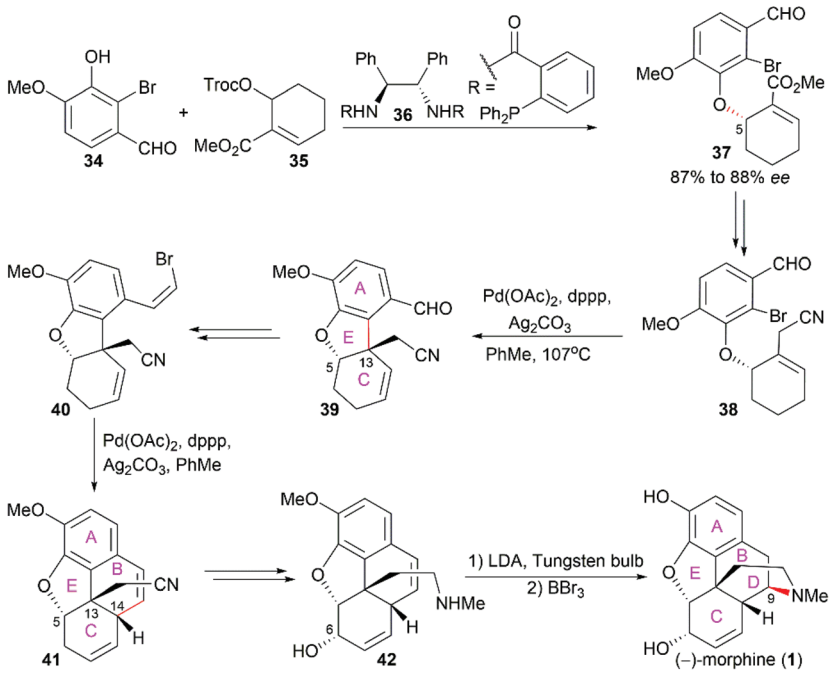

Scheme 3 Trost's synthetic route.

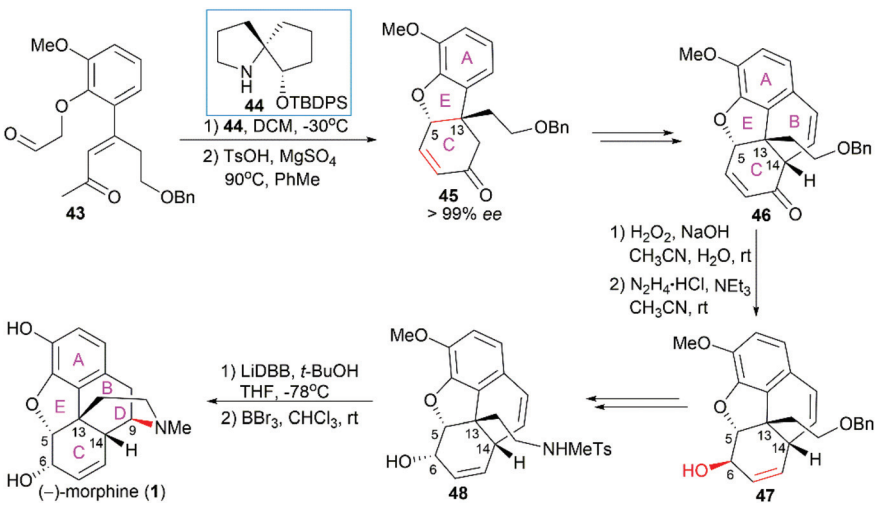

Scheme 4 Tu's synthetic route.

regioselective Mitsunobu reaction and configuration inversion of C6 hydroxy group *via* an oxidation/reduction process led to **48**, which was ready for the introduction of the final piperidine ring D. A lithium 4,4′-di-*tert*-butylbiphenylide (LiDBB)-promoted hydroamination reaction and a subsequent demethylation operation successfully led to (−)-morphine (**1**).

2.1.5 Dong's total synthesis of morphine alkaloids. Dong and co-workers developed a deconstructive strategy for the asymmetric total synthesis of morphine alkaloids (Scheme 5).[55] In their synthesis, the phenanthrene ring system in **51** was efficiently constructed through Rh-catalyzed "cut-and-sew" transformation between a sterically hindered trisubstituted alkene and benzocyclobutenone within **49** in the presence of the chiral bidentate phosphine ligand **50**. The chiral C13 and C14 centers with the desired stereo configuration were also set up. Then, BBr_3-mediated ether bond cleavage successfully yielded compound **53**, which was a suitable substrate for the introduction of the sulfonamide group in **54**. The piperidine ring was constructed through sodium naphthalenide-mediated removal of the Ts group and subsequent radical cyclization. Selective demethylation on one of the two MeO ethers using NaSEt led to compound **55**, which was a common precursor for the synthesis of morphine (**1**), codeine (**6**), and thebainone A.[55]

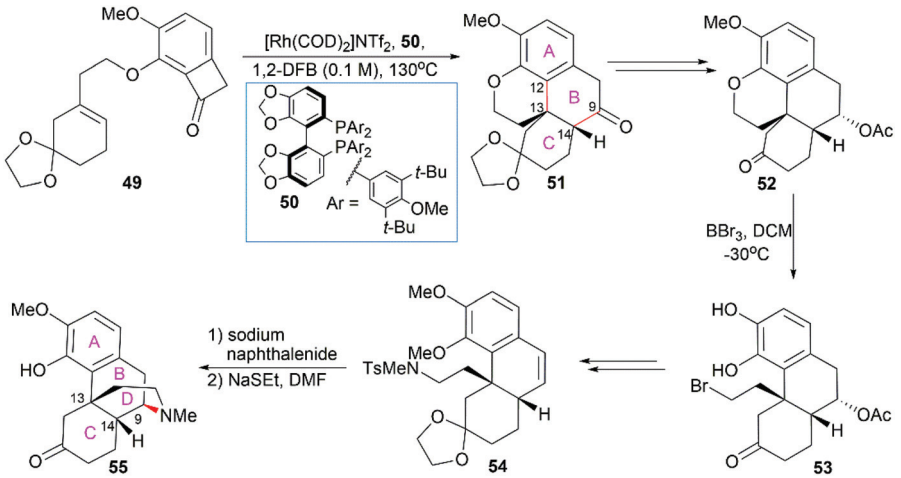

Scheme 5 Dong's synthetic route.

2.2 Structure–activity relationships of morphine derivatives

As the prototypical opioid agonist, morphine (**1**) has been intensively studied, which led to various types of morphine-related drugs. Representative pentacyclic morphine-based drugs are listed in Fig. 3. There are several structural features that are important for morphine's biological function: the C3 phenolic hydroxy group, C6 allylic hydroxy group and C7–C8 double bond, the B/C *cis*-fused ring system, the substitution groups at C14, and the amine group. Detailed SAR studies have been summarized previously[56] and a brief discussion is provided in the following paragraph.

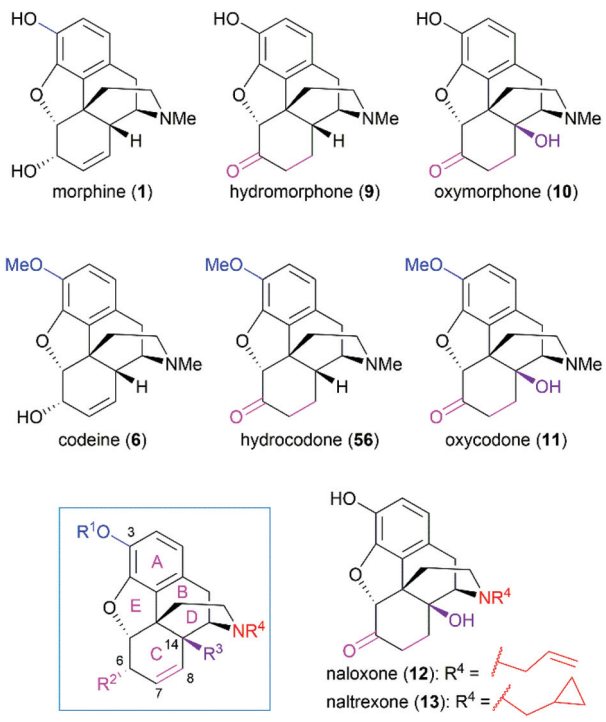

Fig. 3 Representative morphine-related drugs.

The C3 phenolic hydroxy group is essential for the binding of morphine with the μ receptor. Therefore, codeine (**6**), the C3 methoxy ether derivative of morphine, shows 10-fold lower potency than morphine.[57] However, codeine possesses greatly enhanced oral bioavailability. A similar relationship is observed between codeine-derivatized hydrocodone (**56**) and morphine-derivatized hydromorphone (**9**), which are the same as oxycodone (**11**) and oxymorphone (**10**).[56] These codeine-derivatives function as prodrugs and must undergo CYP2D6-mediated demethylation of their corresponding phenolic methyl ethers before binding to μ receptors.[56]

The C6 allylic hydroxy group is engaged in a weak hydrogen bond between morphine and its receptor.[58] However, removal of the hydroxy group increases the molecular lipophilicity and therefore leads to a 10-fold increase in activity.[59] If the alcohol is oxidized to ketone, a 3-fold decrease in activity is observed; further hydrogenation of the C7–C8 double bond led to hydromorphone (**9**) with more flexibility in ring C, which shows a 6-fold increase in potency compared with morphine.[56] Introduction of a β-hydroxy group at C14 transforms hydromorphone (**9**) into oxymorphone (**10**), which shows a 2- to 3-fold increase in receptor affinity when compared with hydromorphone (**9**).

The essential amino nitrogen functions in a protonated form by forming an electrostatic bond with the receptor. Substituents at this nitrogen atom have a great influence on its biological function. A methyl group is commonly observed in morphine-derived agonists; however, naloxone (**12**) and naltrexone (**13**), with allyl or cyclopropylmethyl group, respectively, are pure antagonists.

3. Tetracyclines

Following the discovery of chlortetracycline (**57**) by Duggar in 1945,[60] several other natural tetracyclines—oxytetracycline (**58**),[61] tetracycline (**59**),[62] and demeclocycline (**60**),[63]—were discovered in the following years (Fig. 4). The broad-spectrum

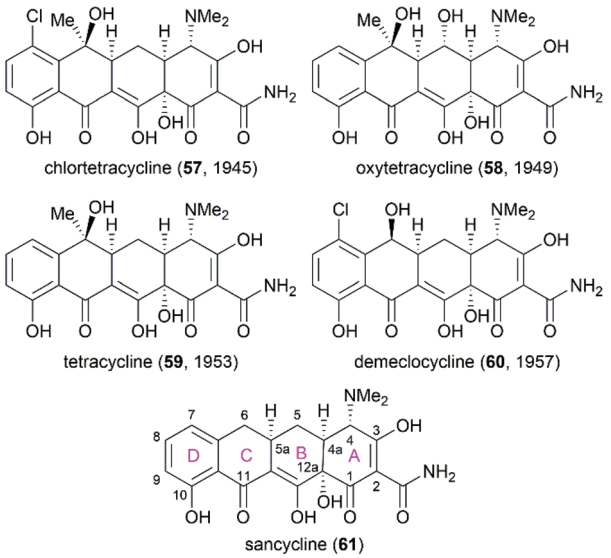

Fig. 4 Structures of natural tetracyclines and the core structure of tetracyclines.

activity and low side effects of tetracyclines make them one of the most important classes of antibiotics.[64] It is well established that tetracyclines function by binding to the 30S ribosomal subunit, which prevents the association of aminoacyl-tRNA with the bacterial ribosome and therefore inhibits bacterial protein synthesis.[65] Over 70 years of widespread use has resulted in the emergence of bacterial resistance to tetracyclines. There are three main mechanisms responsible for tetracycline resistance: (1) efflux pumps reduce the intracellular tetracycline concentration by exporting tetracycline from the cell; (2) ribosomal protection proteins protect ribosomes from tetracycline inhibition *via* various mechanisms; and (3) protection enzymes inactivate tetracycline through modification and degradation.[64,66–68] The growing problem of tetracycline resistance calls for much more investigation on the synthesis of tetracycline derivatives for the development of higher potency antibiotic drugs.

In the early 1950s, the structures of chlortetracycline (**57**) and oxytetracycline (**58**) were first determined by scientists from Pfizer with the help of Woodward.[69–71] Subsequent studies showed that the tetracyclines share one common nucleus, sancycline (**61**), which is composed of four linearly fused 6-membered rings (designated A, B, C, and D) with four stereocenters. A combination of different substitution groups, for example, chloride, hydroxy, and methyl, with the different substitution positions on the nucleus could lead to various tetracyclines with more structural complexity. The tetracyclines are frangible under an array of conditions: (1) the C6 hydroxy group undergoes dehydration in acidic media; (2) the C4 dimethylamino group epimerizes in mildly acidic conditions; and (3) the B and C rings undergo a retro-Dieckmann reaction in basic media.[72,73] The important biological functions and the complicated structural features of tetracyclines have attracted much attention of synthetic chemists.

3.1 Total synthesis of tetracyclines

3.1.1 Woodward and Shemyakin's total synthesis. One decade after they elucidated the structures of chlortetracycline (**57**) and oxytetracycline (**58**), Woodward and co-workers completed the first total synthesis of the prototypic tetracycline antibiotic, 6-demethyl-6-deoxytetracycline (**61**, sancycline).[74–76] Starting from methyl 3-methoxybenzoate (**62**), they constructed the four fused rings one by one in a D to A direction through sequential Friedel–Crafts acylation and Claisen-/Dieckmann-type condensation reactions (Scheme 6). At the final stage of their synthesis, C12a was selectively oxidized with O_2 in the

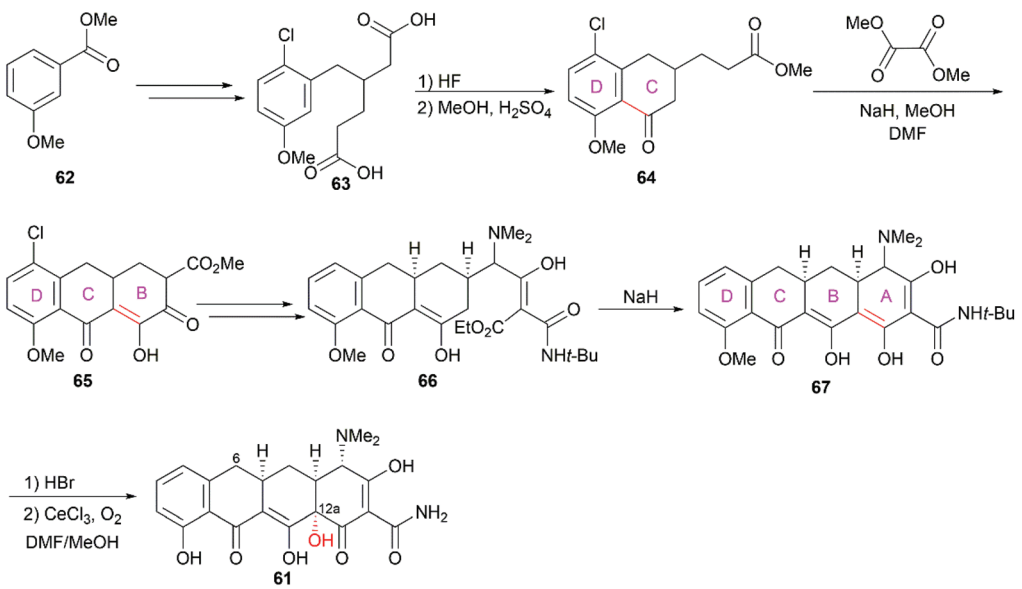

Scheme 6 Woodward's total synthesis of sancycline.

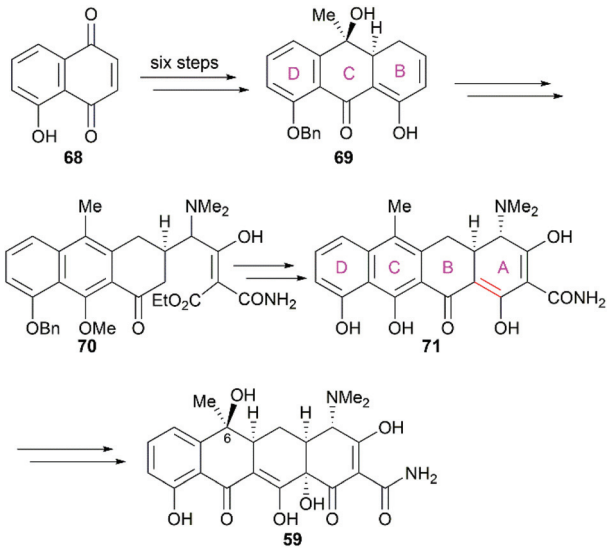

Scheme 7 Shemyakin's total synthesis of tetracycline.

presence of $CeCl_3$ to construct the hydroxy group, which gave the desired product sancycline.

Not long after Woodward's synthesis of sancycline, Shemyakin reported their synthesis of tetracycline.[77] Starting from juglone (**68**), they developed a synthetic strategy similar to that of Woodward (Scheme 7). It should be noted that the C6 hydroxy group was installed using a photooxidation method.[78]

3.1.2 Muxfeldt's total synthesis. In 1965, Muxfeldt and co-workers reported their total synthesis of sancycline (**61**).[79] Still performed in the D to A direction, their synthesis utilized 1-chloro-2-bromomethyl-4-methoxybenzene (**72**) as a starting material and the D/C ring fused compound **75** was synthesized (Scheme 8). Condensation of **75** with methyl *N*-*t*-butyl-3-oxo-glutaramate (**76**) in the presence of sodium hydride led to the tetracyclic product **77**. Notably, their strategy constructed the A and B rings in one step utilizing a cascade reaction consisting of intramolecular Michael addition and Dieckmann condensations. Further exploration of this strategy led to their achievement of the total synthesis of oxytetracycline (**58**).[80]

3.1.3 Stork's total synthesis. In Stork's total synthesis of tetracycline,[81] the C5a stereocenter was established using C6 hydroxy group-directed radical cyclization (**78** to **79**, Scheme 9), and the C4a stereocenter was correctly constructed in a substrate-controlled stereoselective Michael reaction to generate **80**. Dieckmann cyclization of **80** in the presence of potassium hydride smoothly led to the pentacyclic product **81**, which could be transformed into tetracycline (**59**) with hydrogenolytic opening of the isoxazole ring and incorporation of the C12a hydroxy group. It should be pointed out that when ring B was constructed first, trials to synthesize ring A were unsuccessful. Therefore, the authors proposed that ring A was formed prior to ring B in the transformation of **80** into **81**.

3.1.4 Tatsuta's total synthesis. There was no asymmetric total synthesis of tetracyclines until Tatsuta's seminal report on the completion of (−)-tetracycline in 2000.[82] Starting from **82**, which was derivatized from D-glucosamine, the functionalized ring A (**83**) was synthesized first (Scheme 10). The subsequent regio- and stereo-selective [4 + 2] cycloaddition reaction between **83** and the diene **84** successfully led to the A/B ring-fused bicyclic intermediate. The following tandem Michael-Dieckmann-type reaction between **85** and **86** constructed the ring C with the concomitant introduction of the ring D. In contrast to previous synthetic strategies, Tatsuta's synthesis builds the tetracyclic framework in the ring A to ring D direction.

3.1.5 Myers' total synthesis. In Myers' total synthesis of the FDA-approved drug (−)-doxycycline (**94**), the functionalized ring B **88**,[83] derivatized from benzoic acid, was transformed into compound **89**, which was a precursor of the tricyclic compound **90** with A/B-fused rings (Scheme 11). Like that in Stork's synthesis,[81] Myers and co-workers used a functionalized isoxazole as a precursor for the sensitive groups on ring A. Following a strategy similar to that used in Tasuta's total synthesis of (−)-tetracycline,[82] the cascade Michael-Dieckmann reaction between **91** and **92** successfully yielded the pentacyclic compound **93**, which could be efficiently transformed into (−)-doxycycline (**94**).

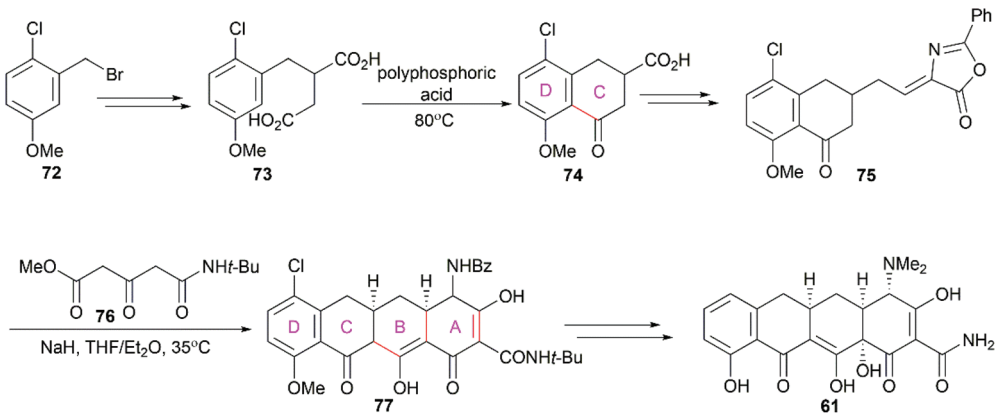

Scheme 8 Muxfeldt's total synthesis of sancycline.

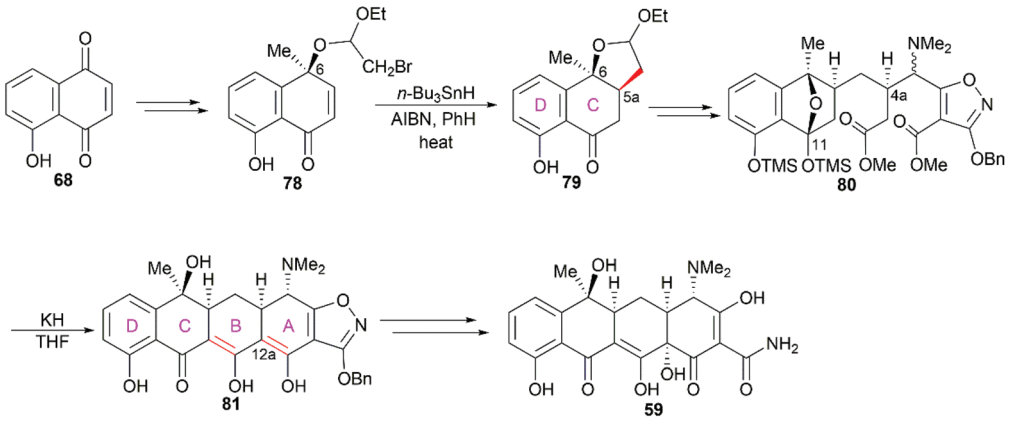

Scheme 9 Stork's total synthesis of tetracycline.

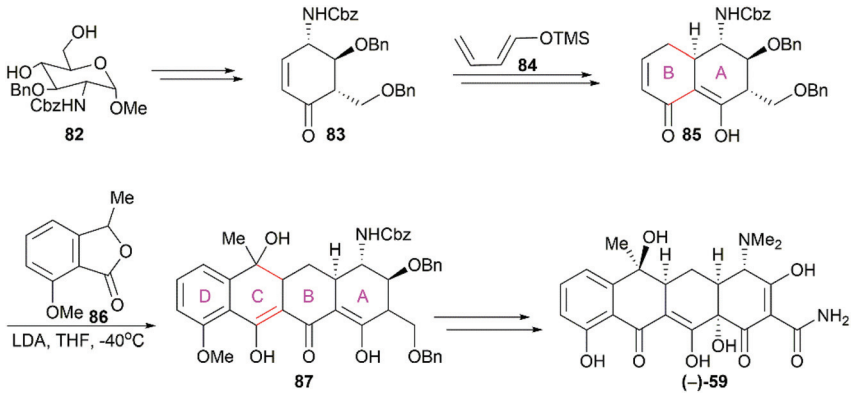

Scheme 10 Tatsuta's total synthesis of (–)-tetracycline.

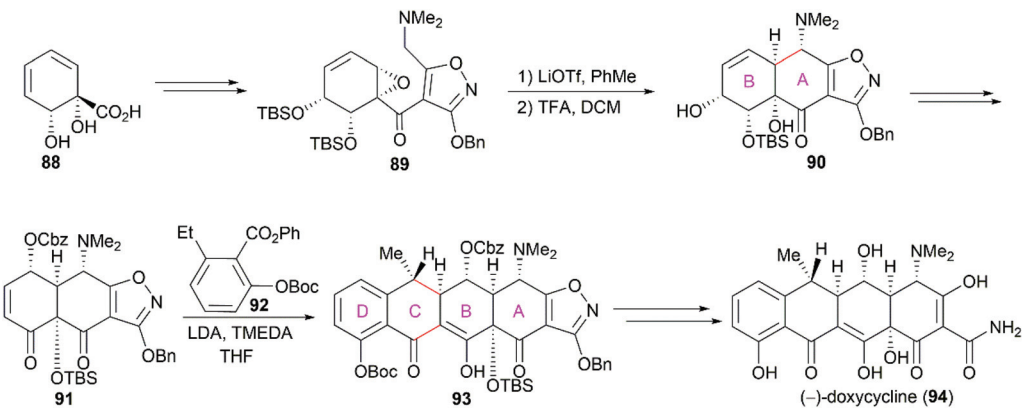

Scheme 11 Myers' total synthesis of (–)-doxycycline.

Previous X-ray crystallography studies on the interaction between tetracycline (**59**) and the 30S ribosomal subunit indicated that the D ring is suitable for modifications to generate more potent antibiotics.[65] Therefore, Myers' late-stage construction of ring C with the concomitant introduction of structurally varied forms of ring D is a promising strategy to synthesize tetracycline derivatives with modified D ring. With continuing optimization, this synthetic strategy is now suitable for industrial-scale application.[84–88] What's more, utilizing Myers' method, countless tetracycline derivatives, which are difficult to synthesize or are inaccessible by semisynthesis, can be constructed. Fig. 5 shows three representative tetracycline deriva-

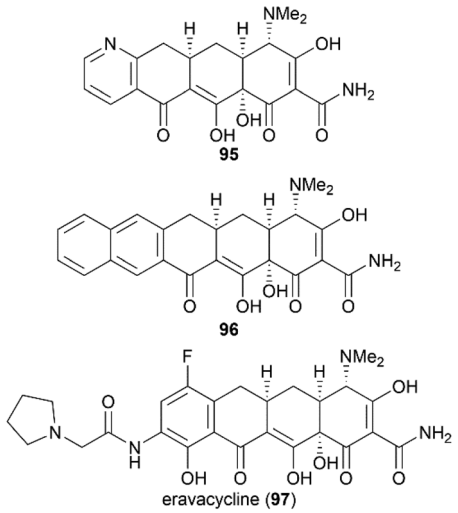

Fig. 5 Representative tetracycline derivatives synthesized based on Myers' strategy.

tives with different substitutions, the 7-azatetracycline **95**, the pentacycline **96**, and the fluorocycline **97**, among which **97**, the first fully synthetic tetracycline antibiotic, was approved in 2018.[89] To date, more than 3000 tetracycline derivatives have been synthesized based on Myers' strategy by a company named Tetraphase.[90] These tetracycline derivatives with diverse modifications make more detailed SAR studies possible.

3.2 Structure–activity relationships of tetracycline derivatives

Since the application of chlortetracycline (**1**) as the first broad-spectrum antibiotic, extensive efforts have been devoted to the SAR studies of tetracyclines, through natural tetracyclines to semisynthetic derivatives and then to fully total synthetic candidates. The tetracycline drugs can be roughly divided into four generations and representative members are presented in Fig. 6.

Naturally isolated tetracyclines are the main members of the first-generation drugs. These natural drugs share a common pharmacophore and comprise different substitution groups at C5, C6, and C7. Several structural features are important for their bioactivities. Maintenance of the four linearly fused six-membered carbocyclic skeleton and the α stereochemical configurations of C4, C4a, C5a, and C12a are essential for their high antibacterial activity.[64,91,92] Chelation with metal ions has a great influence on tetracyclines' activity, and the keto–enol systems (C1–C3 and C11–C12) and the carboxamide (C2), which are the sites of interaction with ions, are necessary.[64,91] Alkylation of the carboxamide (C2) generally decreases activity, whereas suitable substituents can increase the water solubility, as in the case of the prodrug lymecycline.[64,92] Removal of the C4 dimethylamino or its replacement with higher alkylamino groups reduces activity.[91] Furthermore, esterification of the C12a hydroxy group diminishes the activity.

However, as mentioned above, the C6 hydroxy group in these natural products is labile and undergoes dehydration in

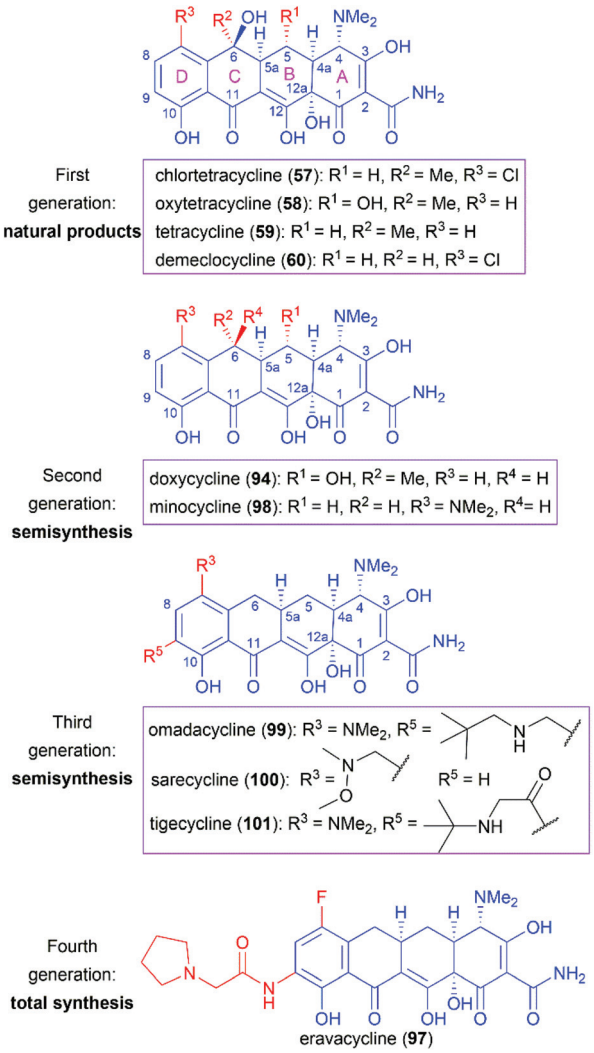

Fig. 6 Representative members of approved tetracycline drugs.

acidic media to produce anhydrotetracycline, which shows nephrotoxicity.[93] Therefore, removal of the C6 hydroxy group and further modifications through semisynthesis led to two second-generation drugs, doxycycline (**94**) and minocycline (**98**), which are more stable while maintaining similar or even higher antibacterial activity.[94,95]

The widespread use of tetracycline antibiotics has brought about serious resistance problems, which has led to the call for more-effective drugs. Investigations on C9-substituted tetracyclines led to the discovery of one glycylcycline named tigecycline (**101**), which is a derivative of minocycline (**98**).[96] Tigecycline (**101**) shows high potency on tetracycline-resistant strains that utilize the efflux and ribosomal protection mechanisms of resistance.[97] However, tigecycline (**101**) is only available in an injectable formulation.[91] Further modifications led to the discovery of omadacycline (**99**), which is a C9-aminomethylcycline. Compared with tigecycline (**101**), omadacycline (**99**) shows improved oral bioavailability while maintaining activity against tetracycline-resistant bacteria.[98] Another C7-

aminomethylcycline, sarecycline (**100**), was approved as a narrow-spectrum tetracycline for the treatment of acne.

The success of the second- and third-generation tetracycline drugs indicates the potential role of the tetracycline pharmacophore in developing new antibiotics. However, the use of semisynthesis, as opposed to total synthesis, for the modification of tetracyclines has inherent limitations. The power of total synthesis is demonstrated by the approval of eravacycline (**97**),[89,99] the first fully synthetic tetracycline drug. We believe that total synthesis will play a much more important role in the campaign against growing antibiotic resistance.

4. Macrolides

The macrolides, a series of macrocyclic lactones with 14-, 15- and 16-membered rings and decorated with one or two sugar moieties are primarily isolated from different *Streptomyces* spp. The first macrolide and wide-spread antimicrobial agent, erythromycin (**102**), was isolated in 1952 from the culture broth of *Saccharopolyspora erythera*, and its structure features, a highly substituted 14-membered lactone bearing 10 chiral carbon atoms, and configuration were successively defined by chemical and X-ray diffraction studies.[100–102] Inspired by its excellent and broad-spectrum activity against Gram-positive pathogens, the mechanism by which erythromycin binds to the 23S RNA of the 50S ribosomal subunit to hamper the exit peptide tunnel and inhibit protein synthesis was elucidated and confirmed further by determining the crystal structure of erythromycin bound to the 50S ribosomal subunit.[103,104] Since erythromycin was launched as Ilosone to treat bacterial infections of the respiratory tract, skin, and soft tissues, the problem of varying levels of resistance to macrolides has been uncovered; resistance was characterized as resulting from the expression of efflux proteins in Gram-positive pathogens,[105,106] a change in erythromycin binding site in mutated ribosomal proteins,[107] and bio-modifications of macrolides by methylase[108,109] and esterases.[110,111] In addition, erythromycin is unstable, especially in acidic environments, due to ketal formation between the C6 and C12 hydroxy groups and the C9 ketone; this undesired side reaction alters the structural properties and leads to low safety and bioavailability.[112] To effectively address these problems and improve the drug-likeness potential of natural macrolides, total synthesis and semisynthesis strategies for the macrolides and their structural analogs have been explored to develop novel lead structures with new molecular features and mechanisms of actions.

4.1 Total synthesis of macrolides

4.1.1 Woodward's total synthesis of erythromycin A. Only three groups in the world, including Woodward and Martin's teams, have completed the total synthesis of erythromycin A and B. The first route to erythromycin A (**102**) was reported by Woodward and co-workers using dithiohemiacetal as starting material, which was followed by 12 conversion steps to generate a common intermediate (**103**). Then, **103** was converted to intermediate **104** and aldehyde **105**, followed by aldolization in the presence of mesityllithium as a base, yielding diastereomeric aldols (**106**), which underwent a series of reactions, including deprotection, protection, and oxidation, to generate aldehyde **107**. The coupling of **107** with the enolate *tert*-butyl thiopropionate exclusively generated the "Cram" product with an undesired stereochemistry at C2. The desired stereochemistry at C2 was subsequently obtained in the presence of *t*-BuLi, to yield **108**, which was transformed into a single seco-acid derivative (**109**) decorated with 2-pyridyl-thioester as a precursor of macrocyclization. Next, **109** was subjected to Corey's method of lactonization to afford **110**, and this was followed by ten steps including two innovative glycosidation manipulations using D-desosaminide **112** and L-cladinoside **114** as Königs–Knorr glycosyl donors, which finally led to the production of erythromycin A (**102**) in 48 steps (Scheme 12).[113–115]

4.1.2 Martin's total synthesis of erythromycin B. A decade after Woodward's approach to erythromycin A synthesis was reported, the formal synthesis of erythromycin A was reported by Oishi's group and a highly efficient strategy for semisynthesis of erythromycin A from its natural aglycon was accomplished by Tatsuta using altered glycosidation strategy. In 1997, Martin completed the total synthesis of erythromycin B (**116**), a congener of erythromycin A lacking a hydroxy group at C12 (Scheme 13).[116] Based on known trihydroxy intermediate **118** prepared according to a reported method, synthesis of ketone **119** was achieved *via* interconversions of protecting groups and oxidation. This step was followed by aldolization with aldehyde **120** to generate intermediate **121**. A macrocyclization precursor, seco-acid (**122**), was prepared from **121** with highly stereoselective aldolization as a critical conversion step. Using excellent Yamaguchi's macrolactonization, synthesis of the macrolide core skeleton (**123**) was achieved with a high yield. After multiple steps of protecting group transformations accompanied by two steps of glycosidation using Woodward's protocol, erythromycin B (**116**) was obtained in 23 steps.

4.1.3 Kang's total synthesis of azithromycin. The approved drug azithromycin (**124**), a semisynthetic analog, is prepared from erythromycin A in four steps. Considering its clinical use as a first-line antibiotic, Kang and co-workers used a novel synthetic plan instead of using erythromycin A as the precursor to construct azithromycin (**124**) (Scheme 14).[117] According to the strategy, the triol (**125**) was converted to alkanolamine intermediate (**126**) in 11 steps using desymmetric mono-benzoylation and epoxide chemistry as key reactions. The eastern building block (**130**) with a carboxylic acid, was obtained by homologation, desymmerization, crotylation, and reduction and glycosidation using the known chiral moiety (**127**) as starting material. The alkanolamine (**126**) was coupled with an aldehyde by reductive amination under hydrogenation conditions, and amino methylation was completed in the presence of formaldehyde to give *seco*-acid (**131**). These and the following steps, including Yamaguchi macrocyclization, glycosidation, and deprotection, yielded azithromycin (**124**) in a total of 18 steps.

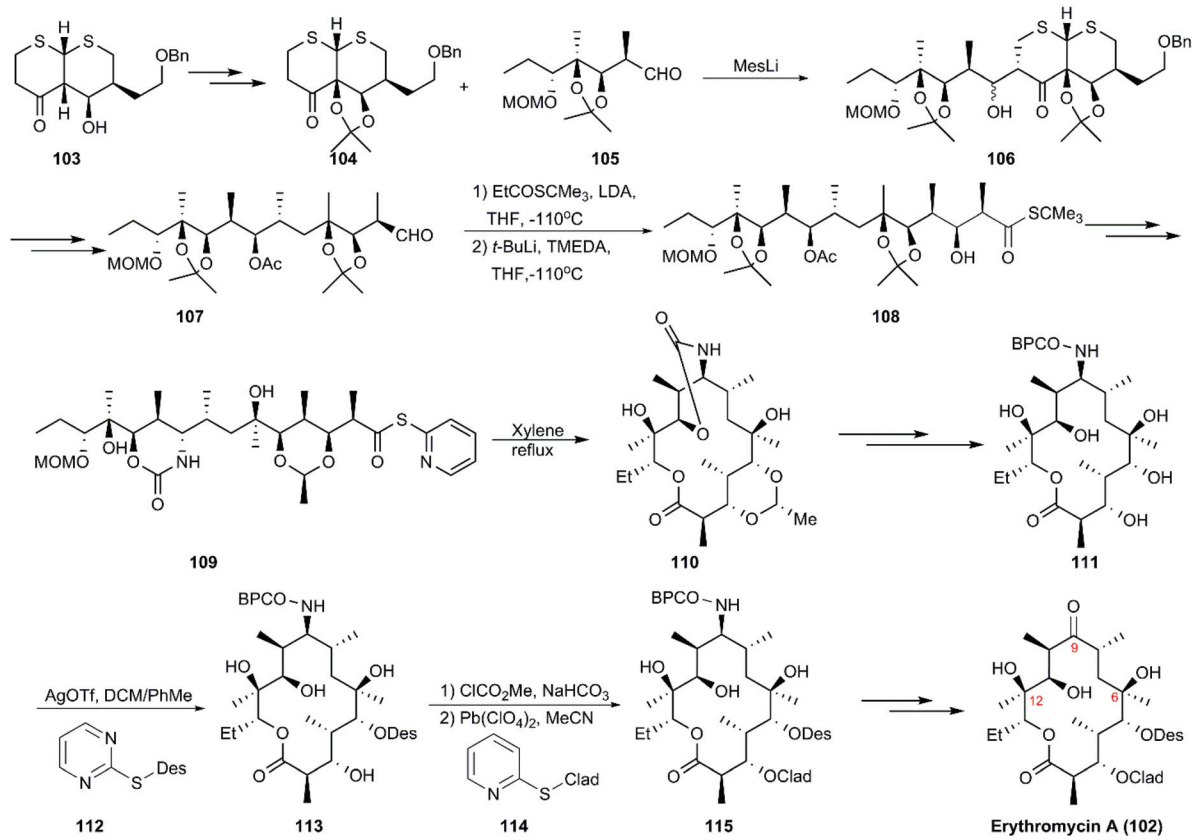

Scheme 12 Woodward's synthesis of erythromycin A.

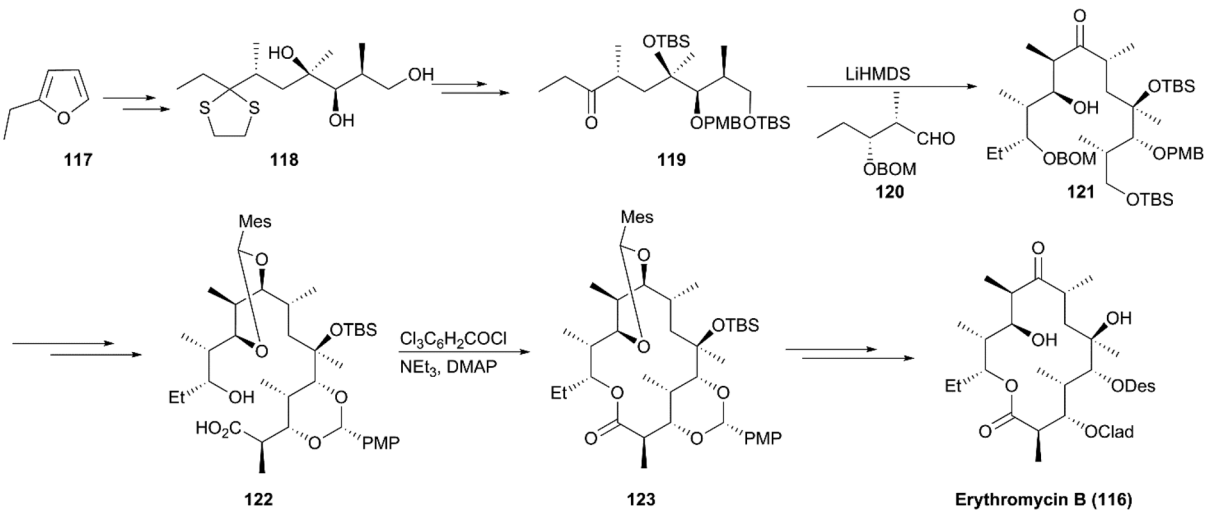

Scheme 13 Martin's synthesis of erythromycin B.

4.2 Structure–activity relationships of macrolide derivatives

Since the discovery of erythromycin as the first macrolide with broad-spectrum antibacterial activity, the development of more potential novel antibiotic candidates has been spurred, leading to the preparation and testing of hundreds of macrolide derivatives. As mentioned above, spiroketal formation between the ketone at C9 with hydroxy groups at C6 and C11 under acidic conditions contributes to the low stability of erythromycin. To avoid this unpleasant side effect, a more acid-resistant and powerful derivative with a 6-*O*-methyl group was developed by Ōmura and co-workers in 1984; six years later

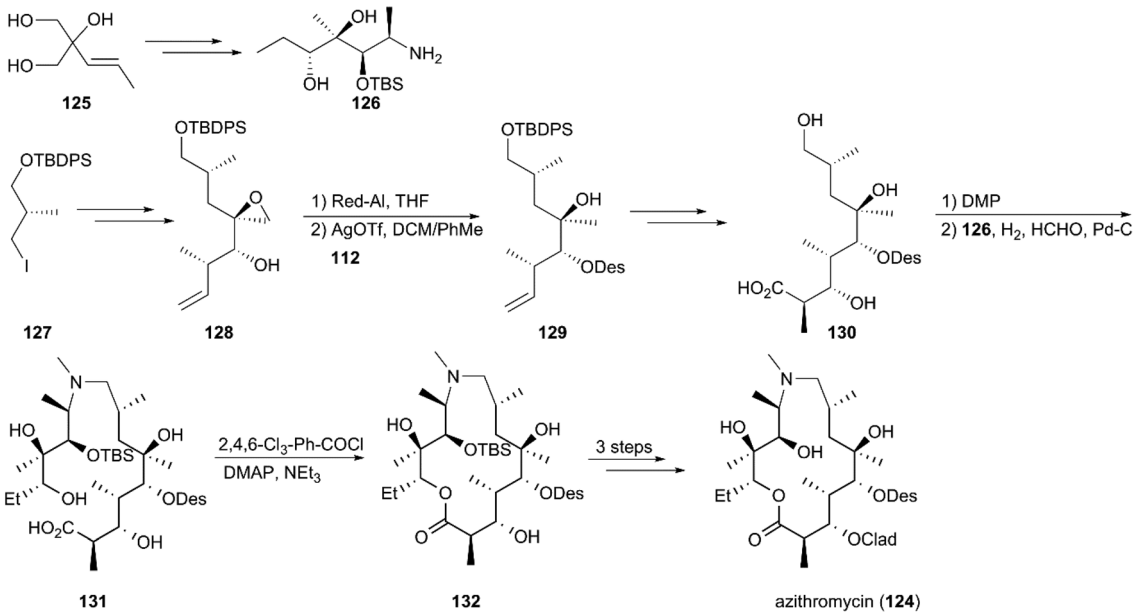

Scheme 14 Kang's total synthesis of azithromycin.

this derivative, clarithromycin (**133**), was approved for clinical use (Fig. 7).[118] Meanwhile, a 15-membered ring of azamacrolide was furnished through Beckmann rearrangement of erythromycin A oxime at C9. This new strategy from Lazarevski's group led to a novel chemical scaffold with excellent stability and activity; this chemical was approved as a new drug in 1988, named azithromycin (**124**). In addition, the C3-cladinose moiety was shown to be unnecessary for protein contact.[119] The success of the marketed drug telithromycin (**134**) showed that its ability to bind to the ribosome was improved by the introduction of a C11/C12 carbamate ring with an extended aryl substituted alkyl chain, and binding was also improved by oxidation of the C3 hydroxy group to give C3 ketone without sugar.[120–122] However, a more effective antibiotic is urgently needed because of the serious drug resistance problem induced by the widespread use of the antibiotic. The development of more drug-like candidates for clinical applications, such as cethromycin (**135**) and solithromycin (**136**), is currently underway.

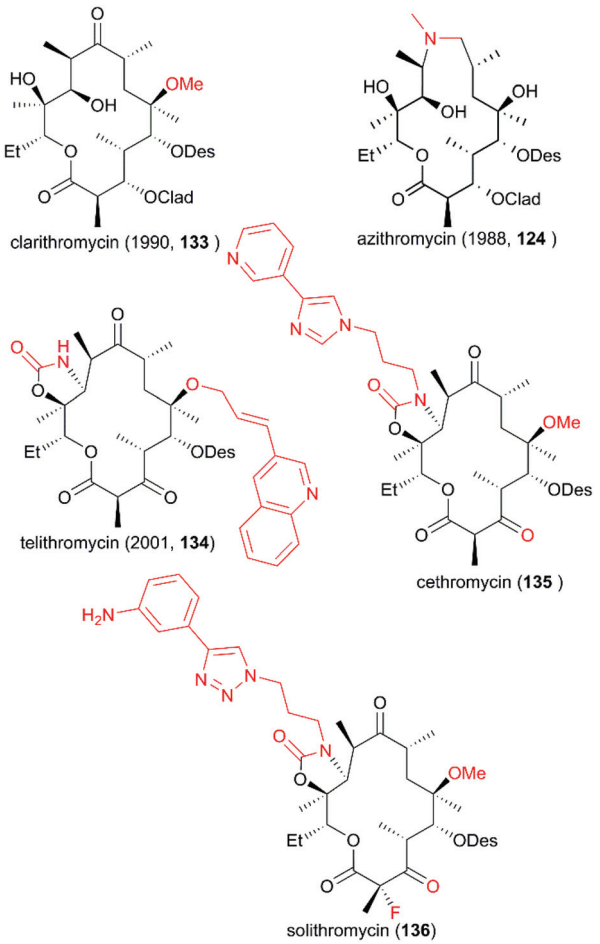

Fig. 7 Derivatives of erythromycin A.

5. Vinca alkaloids

Vinblastine (**137**) and vincristine (**138**) are characteristic members of the biologically important *vinca* alkaloids (Fig. 8). Along with these two alkaloids, derivatives of these alkaloids, including vindesine (**139**), vinorelbine (**140**), and vinflunine (**141**), have been widely applied as well-known antitumor drugs. These molecules function through binding to tubulin, which disrupts microtubule function and results in mitotic arrest and apoptosis.[123–127]

Vinblastine and vincristine were isolated from the leaves of *Catharanthus roseus* in 1958 and 1961,[128–130] respectively, and

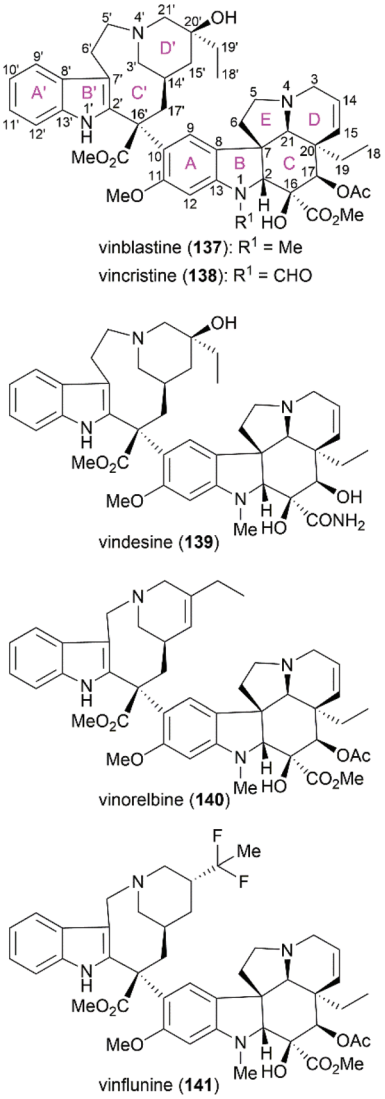

Fig. 8 Representative vinca alkaloids and related derivatives used as antitumor drugs and their ring lettering and carbon numbering system.

their absolute configuration was determined by X-ray crystallography in 1965.[131] Both vinblastine and vincristine possess an upper velbanamine subunit and a lower vindoline or vindoline-derived subunit. For vinblastine, the lower vindoline subunit contains a pentacyclic skeleton (ABCDE rings), which bears six contiguous stereocenters on ring C with two quaternary chiral centers. The upper velbanamine subunit is composed of four rings, including one 9-membered ring C′. There are three stereocenters in the upper subunit, including the C16′ quaternary chiral center resulted from the linkage between the two subunits. The pharmaceutical importance combined with their intriguing structural features make this kind of alkaloid attractive synthetic targets, and great endeavors from the synthetic community in the past several decades have resulted in several elegant total syntheses of vinblastine and vincristine. These strategies are discussed in the following section.

5.1 Total synthesis of vinca alkaloids

5.1.1 Potier and Kutney's total synthesis of (+)-vinblastine. Inspired by the proposed biogenetic pathway for the synthesis of vinblastine, Potier and Kutney developed a pioneering strategy for direct coupling of catharanthine (**142**) with vindoline (**144**), which are the precursors of vinblastine (Scheme 15).[132–134] In their synthetic design, catharanthine (**142**) was first oxidized to *N*-oxide **143**, which underwent fragmentation to give bis-iminiumion **145** through a TFAA-promoted Polonovski reaction. Then, the coupling of **145** with vindoline (**144**) successfully produced iminiumion **146** with the desired stereoconfiguration at C16′. Careful examination of reaction parameters showed that the C16′ diastereoselectivity was temperature- and concentration-dependent: low temperature and high concentration gave better diastereoselectivity.[132]

Potier and Kutney applied different strategies for the transformation of iminiumion **146** into vinblastine (**137**). In Kutney's one-pot operation, a 1,4-reduction of **146** with the carefully designed reductant **147** yielded enamine **148**, which was successfully oxidized with O_2 in the presence of $FeCl_3$ to establish the C20′ hydroxy group.[134] Potier's 1,2-reduction of iminiumion **146** with $NaBH_4$ produced anhydrovinblastine **149**, which is a naturally occurring vinca alkaloid. Hydrogenation of the C15′–C20′ double bond and oxidation gave **150**. The following Polonovski reaction transformed **150** into enamine **148**. Installation of the C20′ hydroxy group was achieved through $Tl(OAc)_3$ mediated oxidation followed by reduction with $NaBH_4$.[133]

5.1.2 Kuehne's total synthesis of (+)-vinblastine. Kuehne's enantioselective synthesis of vinblastine commenced with the construction of the chiral aldehyde **152** through catalytic asymmetric Sharpless epoxidation (Scheme 16).[135,136] A Pictet–Spengler reaction between **152** and indoloazepine **151** produced the bridged azepines **153**, which underwent benzylation and subsequent rearrangement *via* proposed intermediate **154** to give tetracyclic compound **155** with 1 : 1 dr. It should be noted that the diastereoselectivity of this transformation could be improved to 4 : 1 dr when **152** was condensed with **162** which contained a chiral naphthylethyl group. Chlorination of **156** with *tert*-butyl hypochlorite provided imine compound **157**, which coupled smoothly with vindoline (**144**) in the presence of $AgBF_4$ to give **158** with the desired stereoconfiguration at C16′. KBH_4-mediated reductive ring-opening of **158** provided tricyclic compound **159**, which possessed the 9-membered ring C′.

The final D′ ring of the upper unit was constructed by heating the precursor tosylate **159** in MeOH at reflux for 48 h. It is worth noting that no cyclized product was found when **159** was heated in toluene at reflux for two weeks. Hydrogenolytic debenzylation followed by removal of the TMS group led to a higher energy atropisomer of vinblastine, which was transformed into vinblastine (**137**) by heating at reflux in toluene. An alternative reaction sequence including the epoxide intermediate **161** can also transform **159** into vinblastine (**137**).

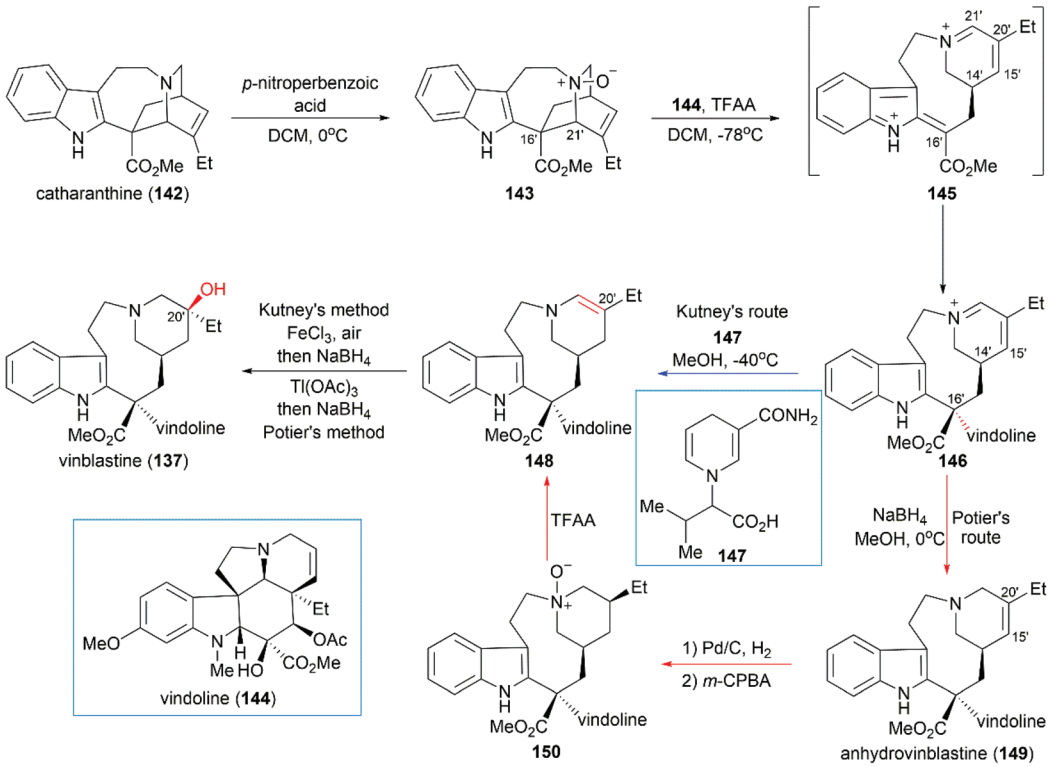

Scheme 15 Potier and Kutney's synthetic route.

5.1.3 Magnus' total synthesis of (+)-vinblastine. In Magnus' total synthesis of vinblastine (**137**), condensation of L-tryptophan (**163**) with diester ketone **164** produced the tetracyclic lactam **165** through Pictet–Spengler reaction (Scheme 17).[137] Aldol condensation of **166** with chiral aldehyde **167** provided **168**, which could be converted to **169** with the required C14′ stereo configuration after dehydration, desulfurization, and hydrogenation. When **169** was treated with $ClCO_2CH_2C_6H_4NO_2$-*p*, carbamate formation followed by fragmentation led to delocalized carbocation **170**, which was trapped by vindoline (**144**) to give the coupled product **171**. Their study showed that the stereochemistry of the newly generated C16′ chiral center was influenced by temperature, reaction solvent, and nucleophilicity of the aromatic partner. The best diastereoselectivity could be achieved in a ratio of 84 : 16 (C16′ *S*/*R*) when the reaction was run in CH_3CN/H_2O (15 : 1) at −15 °C. Hydrolysis of **171** followed by mono-oxidation of the diol and subsequent cyclization through reductive amination provided vinblastine (**137**).

5.1.4 Fukuyama's total synthesis of (+)-vinblastine. Fukuyama's total synthesis of vinblastine started with the enantioselective synthesis of the lower (−)-vindoline (**144**) subunit (Scheme 18).[138,139] Ring-opening of 7-mesyloxyquinoline (**173**) with thiophosgene followed by reduction with $NaBH_4$ provided isothiocyanate **174**, which was transformed into thioanilide **175**. Following the protocol developed in their laboratory, **175** was converted to indole compound **176** through radical-mediated cyclization. Further elaboration of **176** led to **177**, which was transformed into pentacyclic compound **178** upon hydrolysis in the presence of TFA followed by removal of DNS protection and subsequent cyclization. Further manipulations including dehydration to construct the C14–C15 double bond, and introduction of the C16 and C17 hydroxy groups successfully provided (−)-vindoline (**144**). The synthesis of the upper subunit also relied on a radical-type indole synthesis method developed by Fukuyama and co-workers to provide epoxide **180**, which was a precursor of the eleven-membered-ring compound **181**. When treated with *tert*-butyl hypochlorite, **181** was smoothly converted to chloroindolenine **182**, which was coupled with (−)-vindoline (**144**) in the presence of TFA to yield **183** with the desired stereoconfiguration at C16′. It is worth noting that the diastereoselectivity of this transformation was very high and no other stereoisomer was found. The final D′ ring was synthesized through deprotection of the tertial alcohol, removal of the Ns protection, and subsequent cyclization. This strategy was also applied to the synthesis of (+)-vincristine and vinblastine derivatives in the Fukuyama laboratory.[140,141]

5.1.5 Boger's total synthesis of (+)-vinblastine. Boger's concise synthesis of vinblastine utilized a powerful cascade cycloaddition reaction developed in their laboratory.[142,143] When heated at a high temperature, the advanced intermediate oxadiazole **184** underwent an inverse electron demand Diels–Alder reaction to give **185**, which was transformed into the bridged cycloadduct **187** after the loss of N_2 and subsequent 1,3-dipolar cycloaddition (Scheme 19). It should be

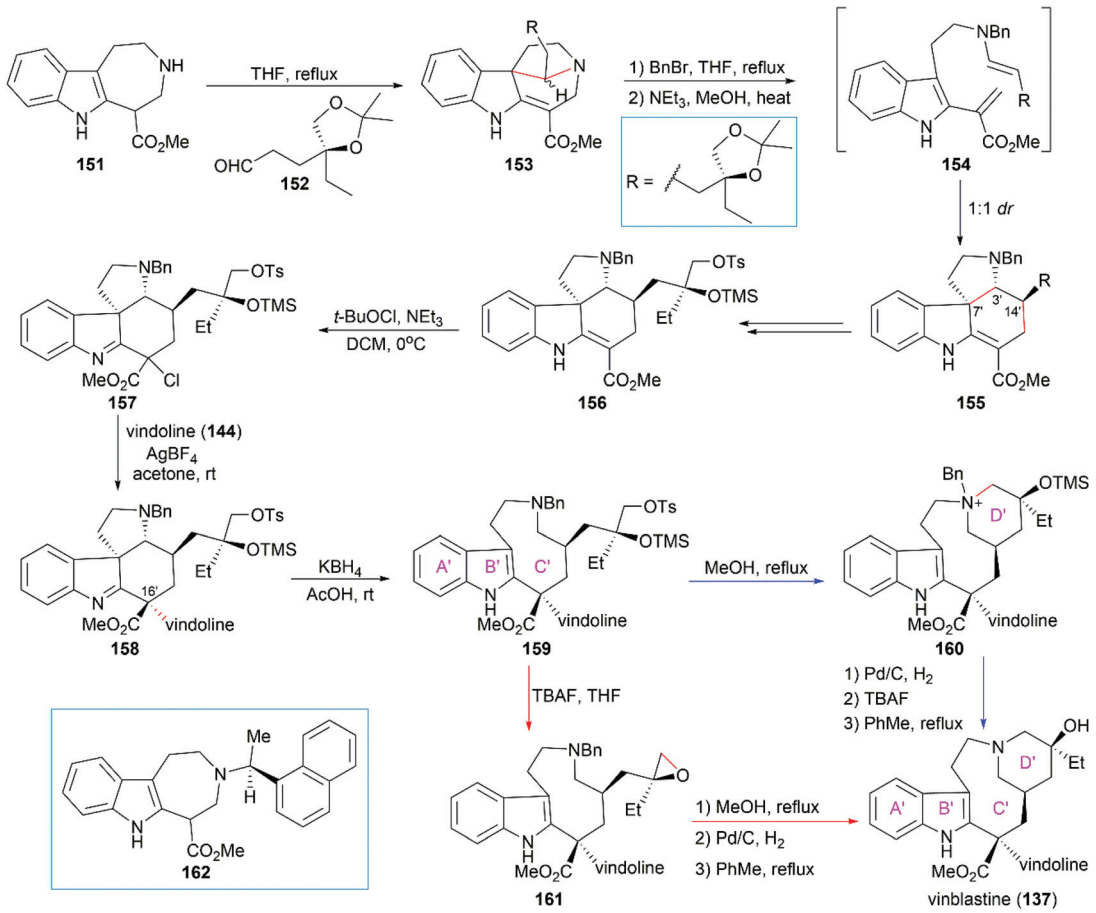

Scheme 16 Kuehne's synthetic route.

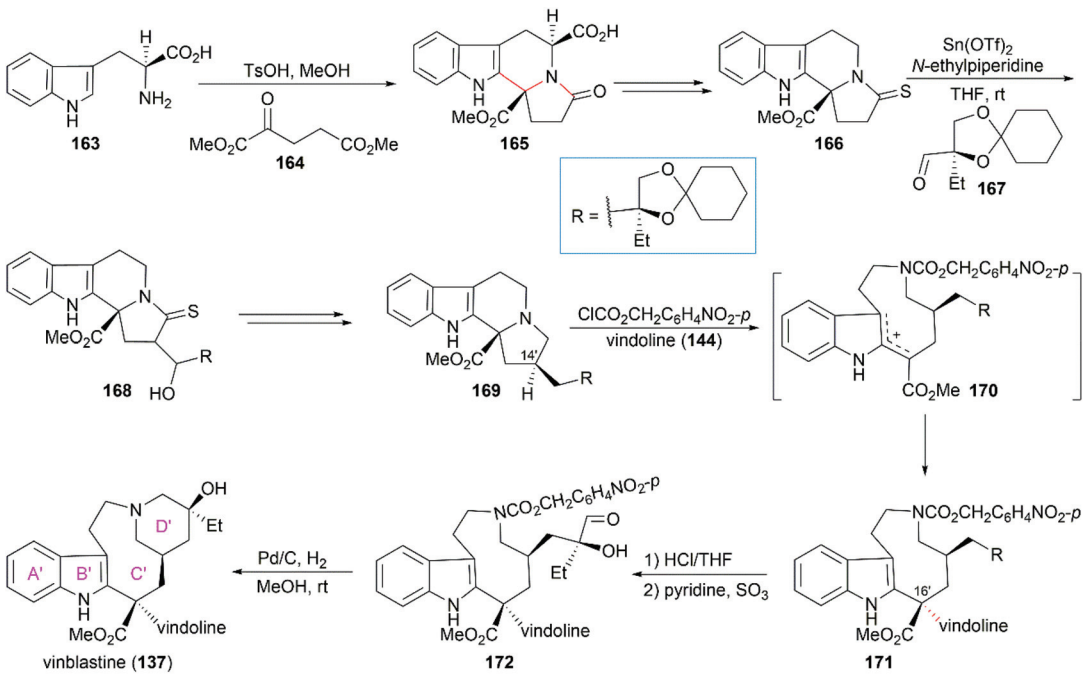

Scheme 17 Magnus' synthetic route.

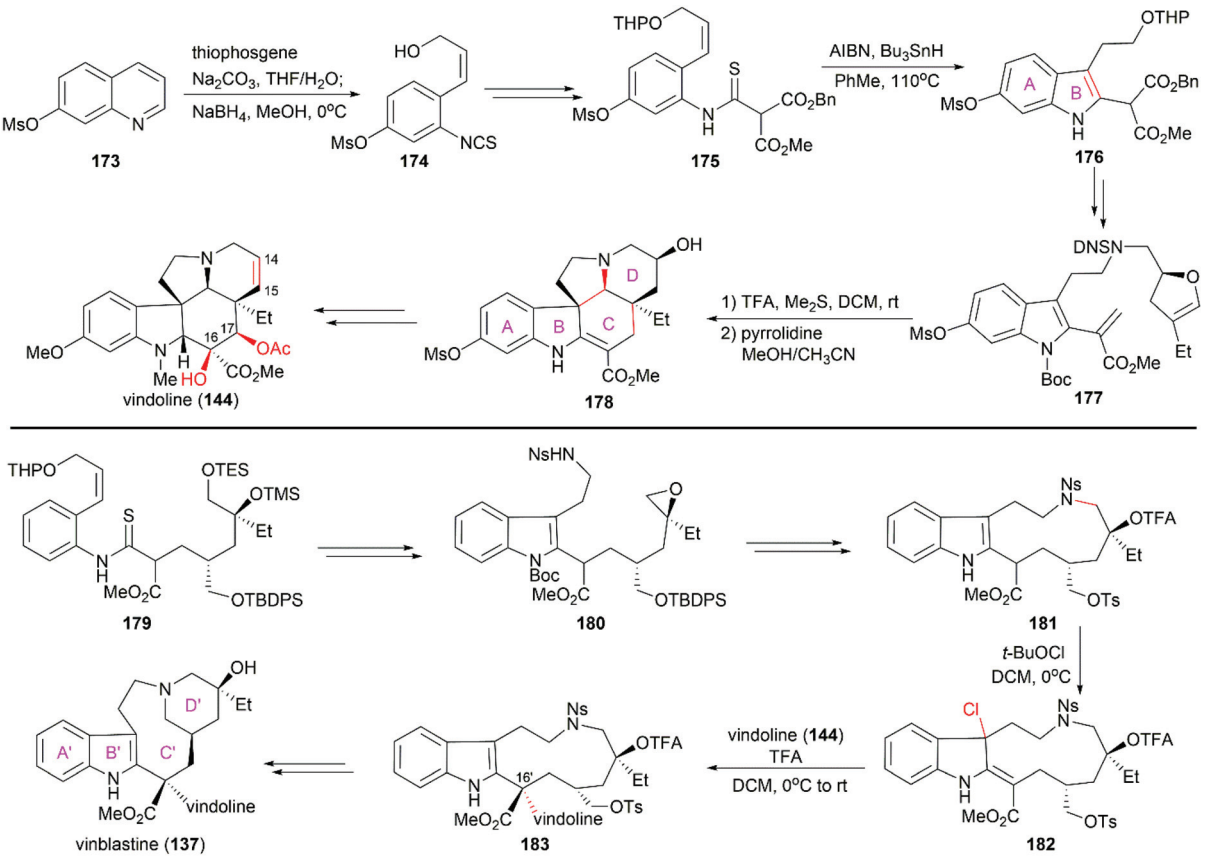

Scheme 18 Fukuyama's synthetic route.

noted that this elegant cascade cycloaddition reaction constructed four C–C bonds and three rings concomitant with the establishment of the six stereocenters with high diastereoselectivity. Hydrogenolytic cleavage of the oxygen bridge in **188** followed by silyl ether cleavage and subsequent dehydration under Mitsunobu reaction condition successfully produced (−)-vindoline (**144**). The following Fe(III)-mediated coupling of (−)-vindoline (**144**) with catharanthine (**142**) and installation of C20′ alcohol successfully produced vinblastine (**137**). According to their preliminary mechanistic studies, a plausible radical pathway was proposed for the coupling reaction: in the presence of $FeCl_3$, **142** was oxidized to radical cation **189**, which underwent radical addition to the aromatic ring of vindoline at C10 to yield **190**.[144] Further oxidation for rearomatization and subsequent reduction of the iminiumion provided anhydrovinblastine (**149**). They also proposed another Fe(III)-mediated radical pathway for the installation of a hydroxy group at C20′.[145] They applied this elegant strategy to the syntheses of vinblastine-related natural products and analogs.[144,145]

5.1.6 Jiang's total synthesis of (+)-vinblastine. Jiang's total synthesis of vinblastine started with inverse-electron-demand Diels–Alder cycloaddition of pyrone **191** with chiral enamide **192** to give bridged lactone **193**, which constructed the C20 and C21 chiral centers (Scheme 20).[146] Further manipulations on **193**, including decarboxylation, reductive ring-opening, installation of the ester group, and oxidation, led to α,β-unsaturated ketone **194**. A challenging Fischer indolization on **194** for the introduction of the A/B rings and the C7 quaternary chiral center was optimized to give tetracyclic compound **196** with excellent diastereoselectivity and regioselectivity. Pd(0)-catalyzed installation of the ester group provided **197**, which was transformed into pentacyclic compound **198** through a Pd/C-catalyzed one-pot cascade reaction including lactamization to construct ring D. Reintroduction of the C14–C15 double bond and reduction of the amide produced **199**, which was an advanced intermediate in Fukuyama's total synthesis of (−)-vindoline (**144**).[138] Coupling of vindoline with catharanthine (**142**) following Boger's protocol successfully provided vinblastine.[143]

5.2 Structure–activity relationships of vinblastine derivatives

Extensive SAR studies on vinblastine and related natural or synthesized derivatives led to the approval of several important antitumor drugs, some of which are listed in Fig. 8. However, the emergence of drug resistance caused by overexpression of the drug efflux pump phosphoglycoprotein (Pgp) calls for more potent vinblastine derivatives to be synthesized and evaluated in the future. Since several review papers have given a detailed summary of the SAR results,[147–150] we briefly discuss

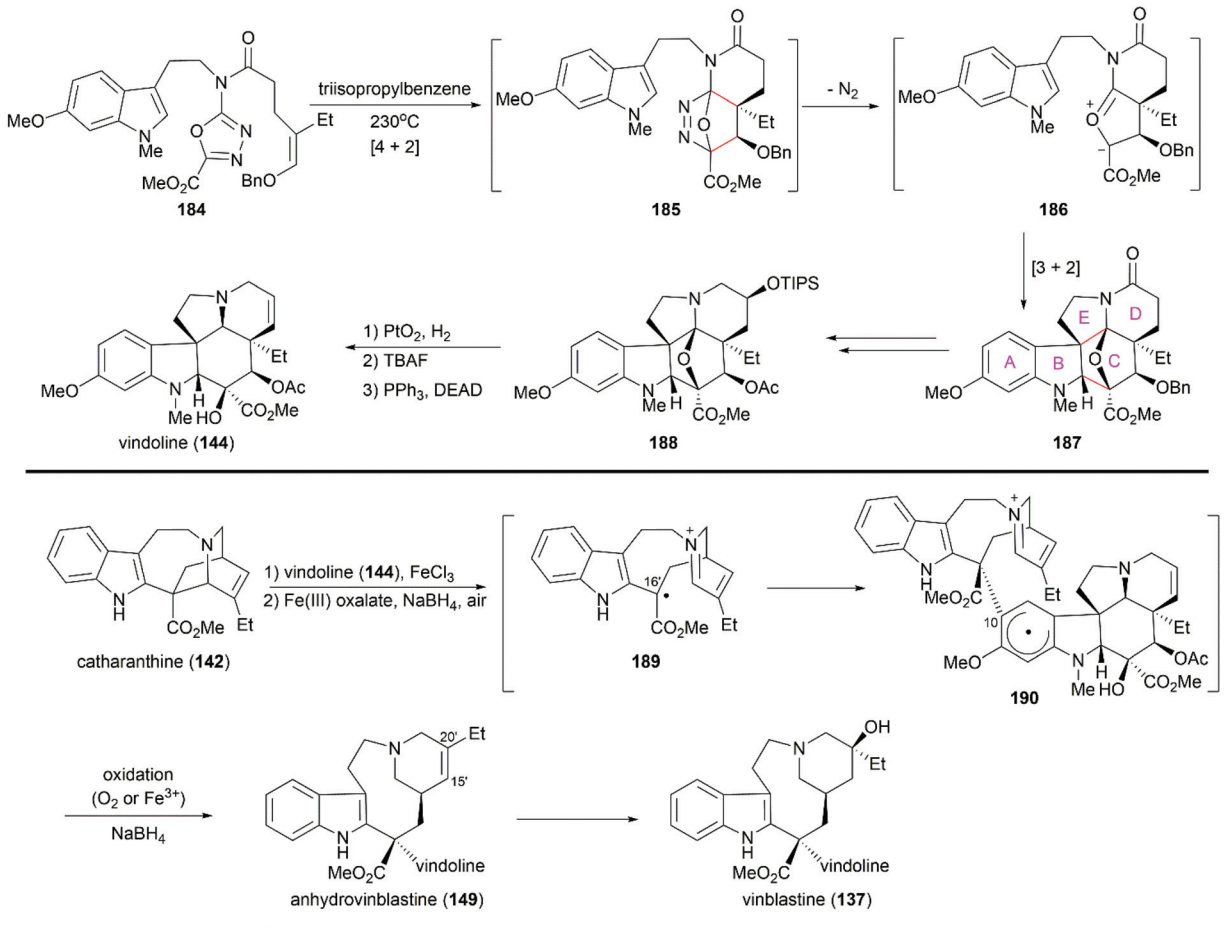

Scheme 19 Boger's synthetic route.

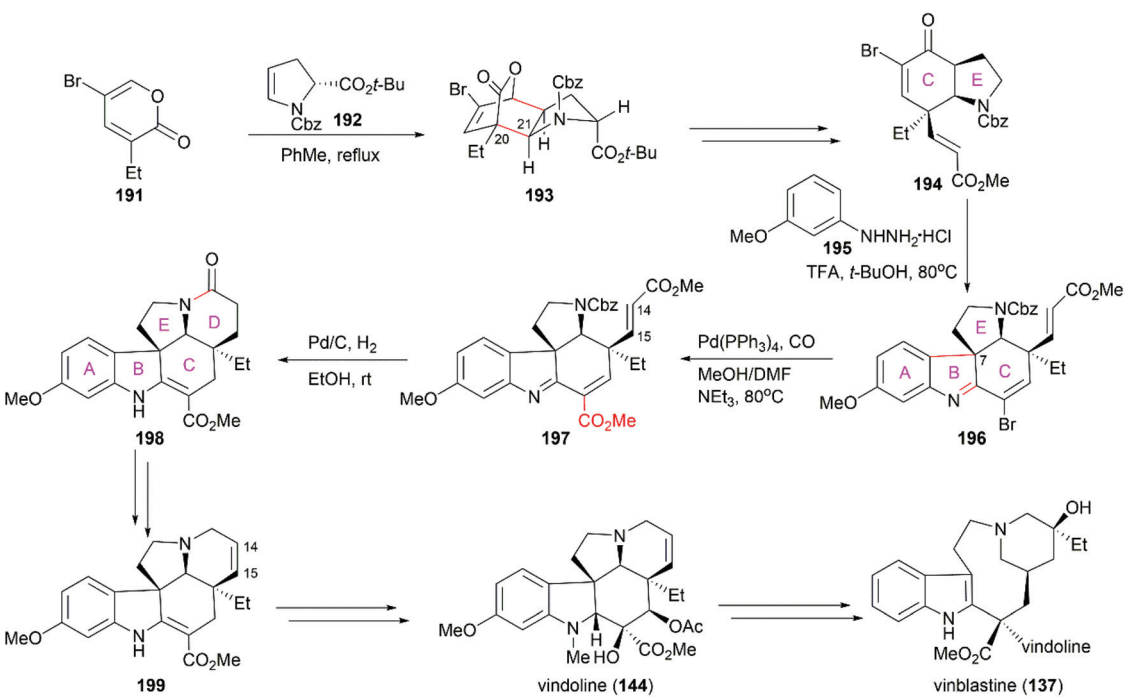

Scheme 20 Jiang's synthetic route.

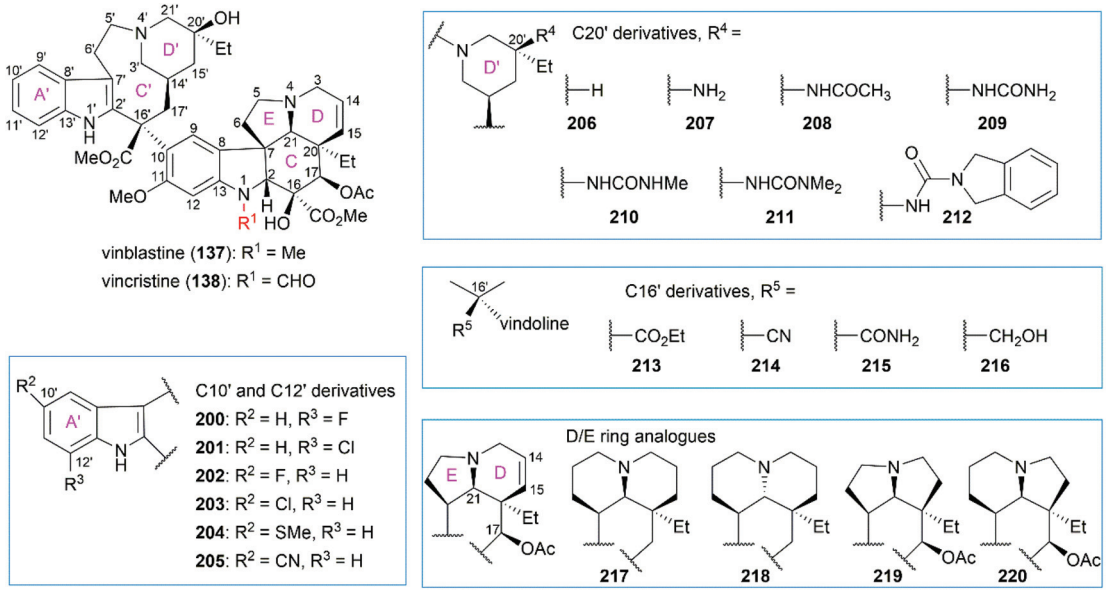

Fig. 9 SAR studies of vinblastine-related compounds.

research progress achieved in recent years, especially those in Boger's laboratory (Fig. 9 and Table 1).

Although substitution at the C12′ position of ring A′ in the upper velbanamine subunit (**200** and **201**) often led to reduced activity, substitution at the C10′ gave promising candidates.

Table 1 Cytotoxicities of vinblastine and related derivatives to three carcinoma cell lines[a]

		IC_{50} (nM)		
Entry	Compound	L1210[b]	HCT116[b]	HCT116/VM46[b]
1	Vinblastine (**137**)	6.0	6.8	6.0×10^2
2	**200**	50	65	7.3×10^2
3	**201**	3.3×10^2	2.2×10^2	5.0×10^3
4	**202**	0.70	0.80	80
5	**203**	6.2	7.6	7.2×10^2
6	**204**	50	50	7.8×10^2
7	**205**	6.3×10^2	6.2×10^2	$>1.0 \times 10^4$
8	**206**	—	60	6.0×10^2
9	**207**	—	6.0×10^2	$>1.0 \times 10^4$
10	**208**	—	90	7.5×10^3
11	**209**	40	7.5	4.4×10^3
12	**210**	—	0.82	5.3×10^2
13	**211**	5.9	2.8	80
14	**212**	0.51	0.60	7.5
15	**213**	60	70	8.3×10^2
16	**214**	6.3×10^2	6.7×10^2	7.4×10^3
17	**215**	$>1.0 \times 10^4$	$>1.0 \times 10^4$	$>1.0 \times 10^4$
18	**216**	6.5×10^3	5.8×10^3	$>1.0 \times 10^4$
19	**217**	5.7×10^3	7.4×10^3	$>1.0 \times 10^4$
20	**218**	55	80	9.0×10^2
21	**219**	5.6×10^2	80	7.8×10^3
22	**220**	7.2	6.5	4.5×10^2

[a] Values given are IC_{50} in nM and original activity data can be found in ref. 150–155. [b] L1210: murine leukemia cell line; HCT116: human colon cancer cell line; HCT116/VM46: resistant human colon cancer cell line, Pgp overexpression.

Applying their one-pot Fe(III)-mediated coupling and oxidation reaction, Boger and co-workers synthesized a series of vinblastine derivatives including the C10′-substituted ones.[151] These derivatives exhibited activity that correlated with the size and shape of the substituents: 10′-chlorovinblastine **203** matched the potency of vinblastine; 10′-fluorovinblastine **202** exhibited an 8-fold increase in activity against both a sensitive (HCT116) and a vinblastine-resistant tumor cell line (HCT116/VM46); in contrast, derivatives bearing the larger (SMe, **204**) or rigidly extended (CN, **205**) substituents were 10–100-fold less potent. According to the X-ray structure of vinblastine bound to tubulin[127] and the results of activity assays, the authors proposed that the 10′-fluorine substituent interacts with the protein at a hydrophobic site uniquely sensitive to steric interactions.[151]

Initial substitution of the C20′ hydroxy group with a hydrogen atom (**206**) or free amine (**207**) gave derivatives with less potency.[152,153] Acetylation of the free amine (**208**) resulted in activity improvement, and a derivative with the urea group (**209**) showed comparable potency with vinblastine. However, these derivatives exhibited a further decrease in activity against a resistant HCT116/VM46 cell line compared with vinblastine. Further substitution of the terminal nitrogen led to improved activity against both sensitive and resistant cell lines (**210** and **211**). Finally, they found that the isoindoline-substituted compound **212** exhibited a 10-fold increase in activity against the sensitive HCT116 cell line and an 80-fold increase in activity against the resistant HCT116/VM46 cell line.

Replacement of the C16′ methyl ester with an ethyl ester (**213**), a cyano group (**214**), a primary carboxamide (**215**), or a hydroxy group (**216**) dramatically reduced the activity against both sensitive and resistant cell lines.[154] Derivatives (**217–220**) containing 6,6-, 5,5-, and 5,6-membered DE ring systems,

instead of the vindoline 6,5-DE ring, were synthesized.[155] Among these analogs, **220** and **218** matched the potency of vinblastine and C17-deacetoxyvinblastine, respectively. Studies also showed that the *N*1-methyl group, C20 ethyl group, C14–C15 double bond, and C11 methoxy group were all essential to vinblastine's cytotoxic activity.[150]

6. Taxol

One of the most famous natural taxane products, taxol (**221**, paclitaxel) was first isolated from the stem bark of Pacific yew by Wall and Wani in 1966, and in 1971 its complex structure was elucidated by NMR techniques and X-ray crystal structural analysis as a diterpenoid with a unique 6-8-6 tricyclic carbon skeleton bearing 11 stereocenters, an unusual oxetane ring, and a β-phenylisoserine chain ester at C13 (Fig. 10).[156] Because of its potent anticancer activity, the worldwide academic and industrial research communities have developed different taxane agents for clinical use in the treatment of various cancers, including the marketed Taxol® and Anzatax®, as well as the synthetic structural derivatives under the tradenames Taxotere®, Jevtana®, and Abraxane®. In addition to its unique structure, taxol also demonstrates modes of action different from those of known anticancer agents. Mechanistic studies showed that during cancer cell mitosis, taxol diffuses through nanopores in the microtubule to bind the β-tubulin subunit on the inner surface of the microtubule, thereby inhibiting the microtubule depolymerization process and arresting the cell in the late G_2/M phase, which blocks the cell division and leads to apoptosis. Cancer cells are believed to have a higher cell division rate than "normal" cells; therefore, they are more sensitive to taxol.[157–159] As observed for other target-specific anticancer drugs, the mechanism of action discussed above and the long-term use as a first-line treatment have given rise to resistance against taxane anticancer agents. The actual resistance mechanisms are unclear, even though many of these mechanisms have been uncovered in different cell lines. For example, the over-expression of the *mdr1* gene gives rise to the drug efflux of the membrane-bound *P*-glycoprotein. The abnormal expression of microtubule-associated proteins leads to drug resistance.

Scarcity of the natural resources of taxane entities hampers the development of taxane-derived anticancer agents, and scientists from academia and industry never stop procuring the taxane products on an industrial scale. Research groups around the world have been working on the synthesis of taxanes and testing accessible synthetic strategies for the construction of the 20-carbon skeleton of the taxane family.

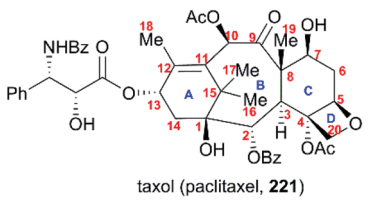

taxol (paclitaxel, **221**)

Fig. 10 The structure of taxol.

6.1 Total synthesis of taxol

6.1.1 Holton's total synthesis of taxol. In 1994, nearly three decades after the discovery of taxol (**221**), Holton's group reported the first total synthesis strategy using the readily available camphor derivative **222** as a starting material (Scheme 21).[160,161] This derivative underwent epoxidation and alcohol fragmentation followed by protection at C13 to construct the B ring of taxusin intermediate **223**, which was subjected to the aldol condensation and a series of oxidations and reduction to give **224** with a ketocarbonyl at C2. With ketone **224** in hand, Chan's rearrangement in the cyclic system was applied to produce trans-fused hydroxy lactone **225** in the presence of LTMP at low temperatures. Then, multi-step transformations gave rise to intermediate **226**, which was converted to the C ring-fused enol ester **227** through Dieckmann cyclization. Subsequent decarbomethoxylation and oxidation at C5 and the introduction of C4/C20 dihydroxys led to **228**, which was further converted to the D ring-attached precursor **229**. Additional functionality interconversions produced 7-BOM baccatin III **230**, which was lithium alkoxided and treated with β-lactam **231** to successfully produce taxol (**221**) after deprotection of C7 BOM.

6.1.2 Nicolaou's total synthesis of taxol. Soon after Holton's report, significant work on the total synthesis of taxol from Nicolaou and co-workers was published.[162] In their strategy (Scheme 22), two pivotal intermediates, **234** and **237**, with the ring A and ring B present in taxol, were both prepared by Diels–Alder cyclization between commercially available **232** and **233** and between **235** and **236**, respectively; **234** and **237** were further decorated with functional groups. Then, they were subjected to Shapiro coupling to obtain a single diastereoisomer of hydroxy compound **238**, which underwent epoxidation, regioselective reduction, deprotection, and oxidations to create dialdehyde **239**. Subsequent optimal McMurry coupling resulted in the construction of the taxoid 6-8-6 ring skeleton **240** with 23% yield, and the configurations of the newly generated centers were confirmed by X-ray crystallographic analysis. After hydroboration-oxidation and interconversion of protecting groups, the important intermediate **241** with trihydroxy installed at C4, C5, and C20 was produced. During the next stage, the oxetane ring was built by sequential monosilylation of the primary hydroxy, triflation of the second hydroxy at C5, and acid treatment to produce a tetracyclic ring system. The allylic oxidation at C13 and benzoylation of C2-OH generated 7-TES-baccatin III **243**, which was subjected to the protocol they previously reported using NaHMDS for C13 alkoxidation and consecutive treatment with β-lactam **231** to finally produce taxol (**221**).[163]

6.1.3 Danishefsky's total synthesis of taxol. Different from the approaches previously reported, in which oxetane was constructed at a later stage, Danishefsky and co-workers prepared it at the beginning of their strategy using partially protected

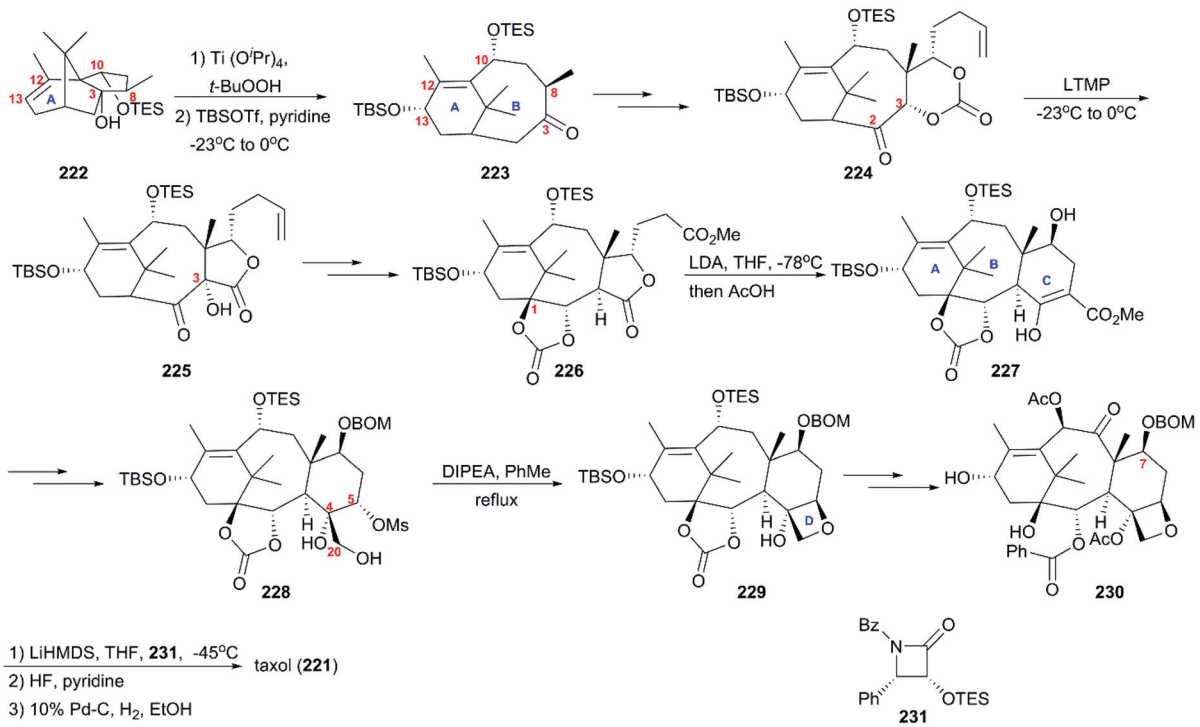

Scheme 21 Total synthesis of taxol by Holton.

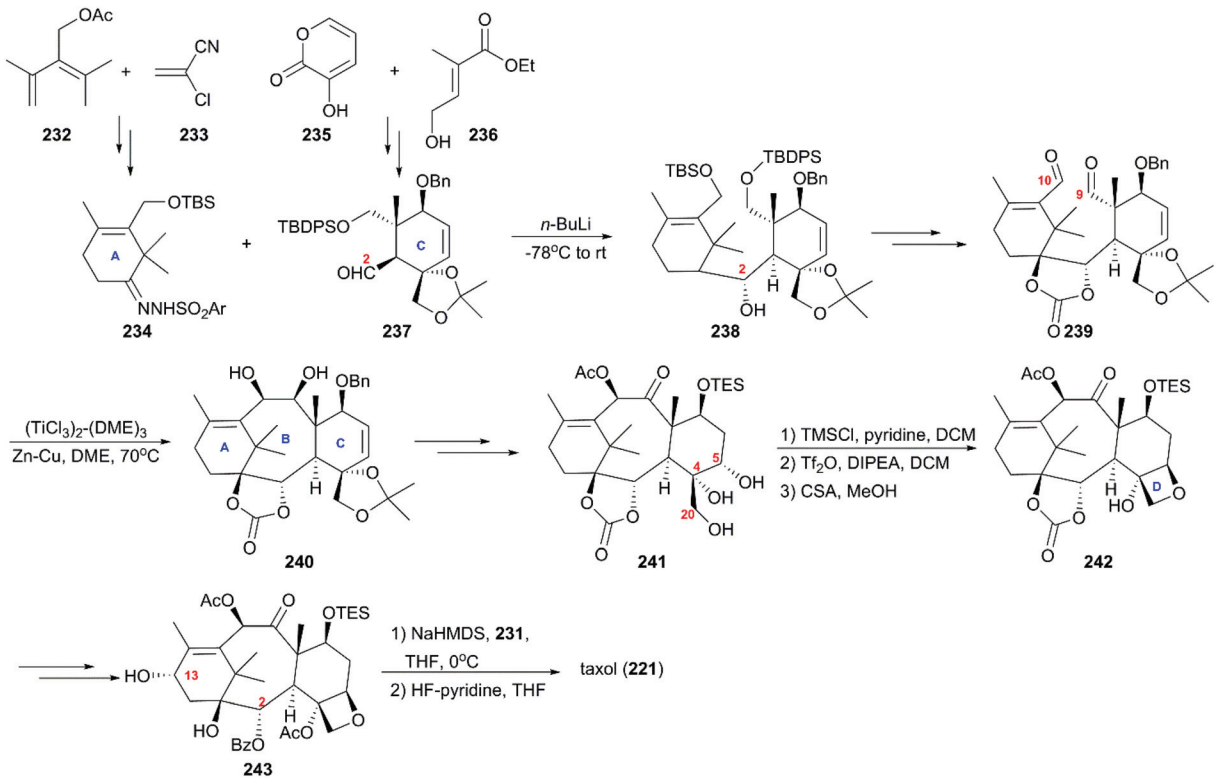

Scheme 22 Total synthesis of taxol by Nicolaou.

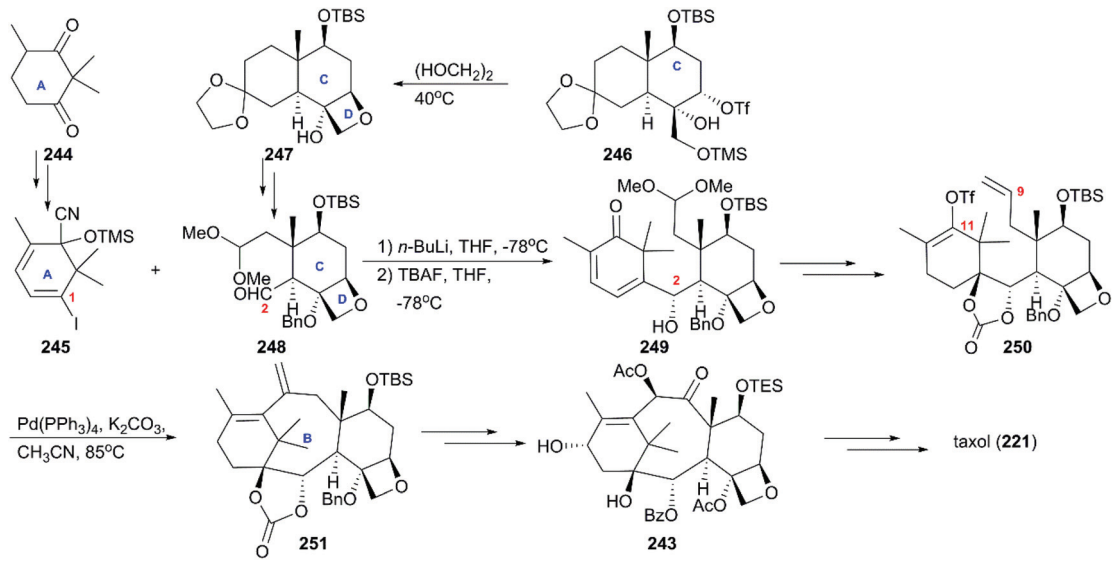

Scheme 23 Total synthesis of taxol by Danishefsky.

triol **246**, which was obtained from a Wieland-Miescher ketone (Scheme 23).[164] With the intermediate **247** in hand, additional functionalization led to the B ring precursor **248**, which coupled with **245** derived from dione **244** to give rise to a single carbinol **249**. After a series of conversions including epoxidation, hydrogenation, deprotection, and Wittig olefination, the precursor of cyclization **250** was obtained. In the next phase of synthesis, the intramolecular Heck reaction was employed to construct the tetracyclic skeleton **251**, which was converted to the building block **243** used by Nicolaou through successive oxidation and protection reactions. By following previously described protocols for the final steps, the total synthesis of taxol was completed.

6.1.4 Wender's total synthesis of taxol. The synthesis strategy from the Wender team used verbenone **252**, the air oxidation product of pinene, as the starting material (Scheme 24).[165,166] Reactions consisting of the major transformations of alkylation, photorearrangement, and nucleophilic addition produced the subunit tricyclic **253** as a supplier of the A–B ring system and source of chirality of the taxol core. Then, **253** was successfully converted to the A–B bicyclic ketone **254** *via* hydroxy-epoxide fragmentation induced by DABCO. After installation of the hydroxy at C1 and the alkyl with aldehyde group at C4, the intermediate **255** was subjected to intramolecular aldol cyclization in the presence of DMAP to construct the C ring. In the next phase, compound **256** underwent stereoselective bromination at C5 and dihydroxylation at C4/C20 to give rise to precursor **257**, which directly closed to afford compound **258** with the D ring. After the protecting group interconversions, baccatin III (**259**) reacted with β-lactam **231** following previously reported procedures to produce the target taxol (**221**).

6.1.5 Kuwajima's total synthesis of taxol. In the strategy developed by Kuwajima's group (Scheme 25),[167,168] the starting materials **261** and **263**, which were used as suppliers of the A ring/C2/C10 and C ring/C9, were prepared from compounds **260** and **262**, respectively. In the presence of Mg(II) ions, the coupling reaction of **261** with the lithiated **263** yielded a single diastereoisomer, which was converted to the cyclization precursor **264** through the protection of the newly produced vicinal diol as a boronate. Several Lewis acids were optimized to induce cyclization, and, finally, $TiCl_2(OiPr)_2$ was selected as the most powerful one for the construction of the B ring. This step was followed by the removal of a protecting group, generating the tricarbocycle **265**. After generation of hydroxy at C7 and ketocarbonyl at C4, cyclopropanation of the double bond between C3 and C8 was induced to give cyclopropyl ketone **266**, which was exposed to the SmI_2/HMPA/methanol reductive system to smoothly produce **267** with a newly angled methyl group at C8. Functionalizations of **267** generated **268** as the precursor of oxetane, and in the presence of DBU, the tetracycle **269** was generated. In the final phase, Kuwajima and colleagues also applied previously reported protocols with some modifications to finish the total synthesis of taxol (**221**).

6.1.6 Mukaiyama's total synthesis of taxol. In 1999, Mukaiyama's group applied a novel approach to taxol using optically active polyoxy linear unit **272** to prepare the B ring of taxol at the early stage of the plan (Scheme 26).[169] The cyclic precursor **272** prepared from amino acid **271** by repeated intermolecular aldol reactions, was converted to the 8-membered ring smoothly in the presence of SmI_2, and followed by dehydration, α,β-unsaturated cyclooctanone **273** was provided. Introduction of the alkyl aldehyde at C3 produced **274**, which was converted into the desired bicyclic compound **275** by the intramolecular aldol reaction in the presence of NaOMe. After transformations of the functional groups and protections of newly formed hydroxy groups, diketone **276** was given and it subsequently was subjected to the intramolecular pinacol

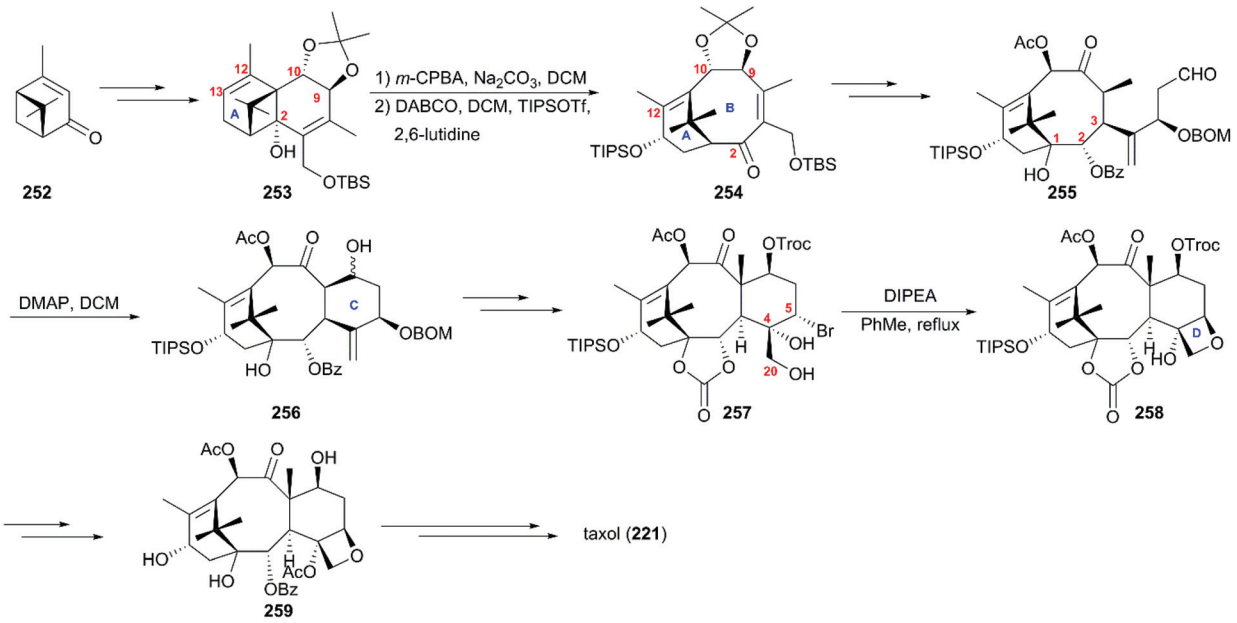

Scheme 24 Total synthesis of taxol by Wender.

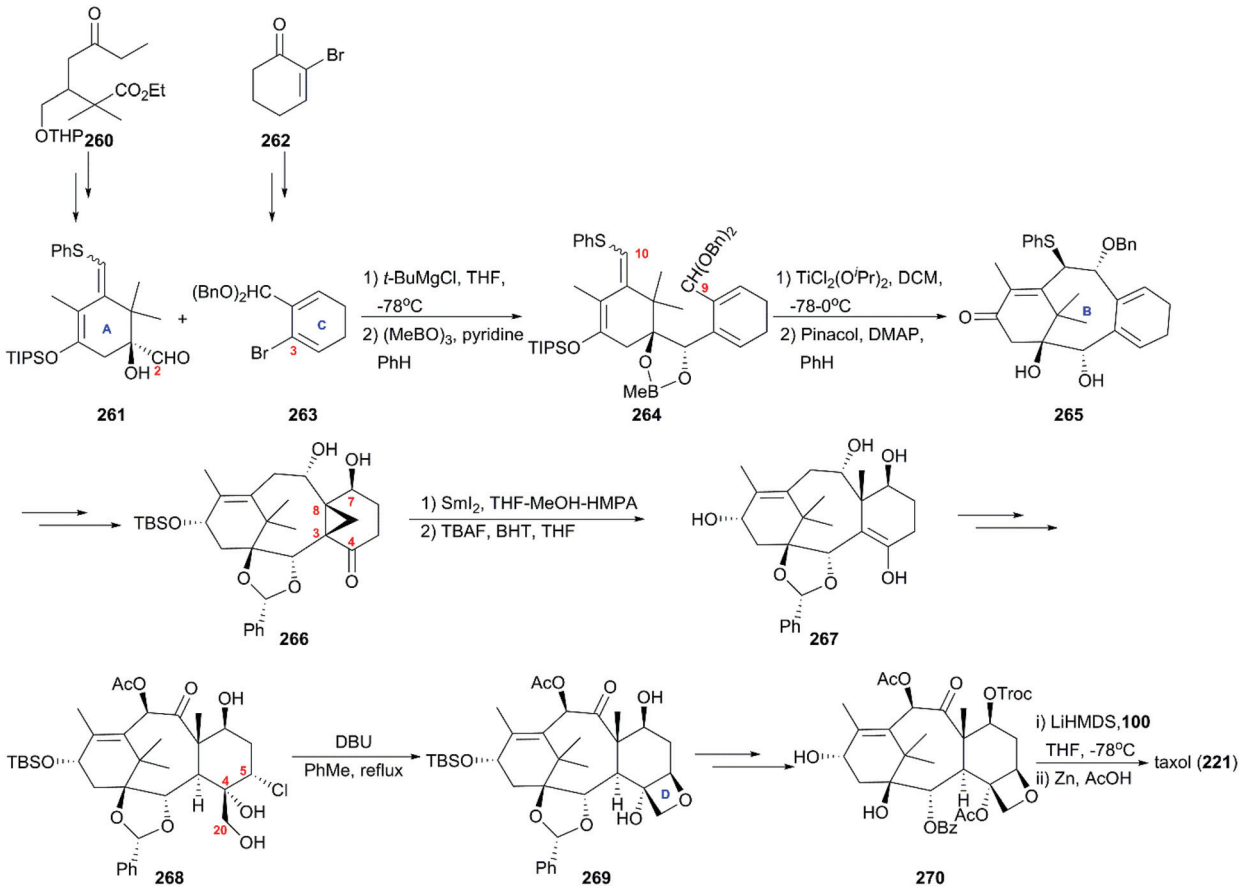

Scheme 25 Total synthesis of taxol by Kuwajima.

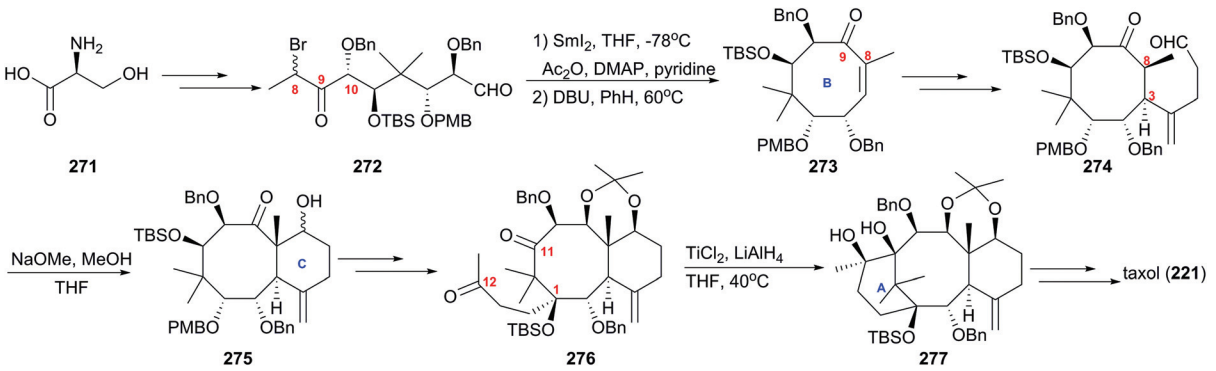

Scheme 26 Total synthesis of taxol by Mukaiyama.

coupling reaction to produce the desired pinacol **277** in the presence of low valent titanium. At the next stage, the protocols used previously were applied here to get taxol (**221**).

6.1.7 Baran's total synthesis of taxol. Except for the formal syntheses of taxol reported by Takahashi,[170] Nakada,[171] and Chida,[172,173] no synthetic approach was reported in the past two decades before Baran's work. The conventional convergent approaches to taxol proved not to be practical in the pharmaceutical industry; on the contrary, the relatively linear natural route used to synthesize taxol is efficient and the oxidation sequence of taxol biosynthesis could produce more natural analogs of taxol.[174,175] Inspired by the taxol biosynthetic approaches, including the generation of C–C bonds by the first type of enzymes in a "cyclase-phase" and installation of C–O bonds by the second type of enzyme in an "oxidase-phase", Baran's team presented a two-phase synthesis scheme for taxol.[176,177] As shown in Scheme 27, in the first "cyclase phase",[178] the cyclization precursor **280** was prepared on a decagram scale by the Lewis acid-modified organocopper 1,6-addition of known compounds **278**, **279**, and a subsequent aldol reaction and oxidation. With mixture **280** in hand, the tricyclic intermediate **281** was generated in the presence of $BF_3{\cdot}OEt_2$. At the beginning of the "oxidase phase", regioselective allylic oxidation was more feasible at C13 than at C10 in the presence of the Cr(v)-based oxidant. After bromination at C5, compound **283** experienced radical oxidation and nucleophilic substitution at C10 to generate **284**, which was subjected to sequential elimination of C5 bromide, the addition of MeMgBr at C4, and reduction of the C2 and C13 ketone groups accompanied by TBS installation to give the oxidation precursor **285**. The oxidant DMDO was employed to produce the epoxy-triol **286** using $CHCl_3$ as an optimal solvent, followed by TPAP-mediated oxidation of C2 to afford **287**, which was reduced using Na/*i*-PrOH and exposed to triphosgene to produce carbonate **288**. After sequential iodine-oxidation in the presence of $TBAI/BF_3{\cdot}OEt_2$ and elimination and epoxidation by DMDO, **288** was converted to epoxy-taxane **289**. After the reductive opening of epoxide, BOM protection, and Burgess dehydration of C4, allylic alcohol **290** was generated in moderate yield. The intermediate with a hydroxy group activated by MsCl at C5 was unstable and immediately exposed to OsO_4 to obtain the oxetane precursor **291**, which was subjected to oxetane ring formation to generate tetracyclic carbonate **292**. Then, $(PhSeO)_2O$ was applied to introduce a hydroxy group at C9 in the present of *t*-BuOK to deliver **293**. Finally, synthesis of the target molecule **221** was achieved using previously reported protocols.

6.2 Structure–activity relationships of taxol derivatives

The discovery of taxol as one of the most potent anticancer agents spurred a large number of academic and industrial researchers to investigate the SAR for identifying lead compounds with drug-likeness potential. However, the complex structure of taxol, a heavily oxygenated polycyclic diterpenoid, presents a huge challenge for pharmaceutical studies that call for a substance-rich library. A number of studies have uncovered the still-incomplete SAR information about taxol. This information has been described by several reviews,[179–183] and is summarized here in Fig. 11.

Studies on the modifications at C1, such as removal and esterification, revealed that the C1-OH is not essential for the activity of taxol.[184] In addition, C7-OH, C9-C=O, and C10-OAc play insignificant roles in the anticancer activity of taxol.[185–188] SAR studies have shown that the benzoyl group at C2 is necessary for activity; 2-deoxy-taxol displayed decreased antitumor activity,[189] and 2-benzoate analogs did not lead to any remarkable improvement in biological activity in a microtubule assay or cytotoxicity test.[189] The acetoxy group at C4 was also demonstrated to be essential for activity, and the analog 4-deoxytaxol was inactive on several tumor cell lines.[190,191] However, oxetane plays a critical role in the bioactivity of taxol, and analogs in which the oxygen atom was replaced by nitrogen, sulfur, or other heteroatoms did not significantly enhance antitumor activity.[192,193]

SAR studies revealed that the *N*-benzoyl-β-phenylisoserine side chain is essential for the antitumor activity of taxol, and this chain has attracted more extensive investigation than any other functional group of taxol.[194–198] A number of analogs with a modified side chain exhibit stronger activity than taxol, some of which are listed in Fig. 12, including two marketed drugs, docetaxel (Taxotere®, 1995) and cabazitaxel (Jevtana®, 2010).

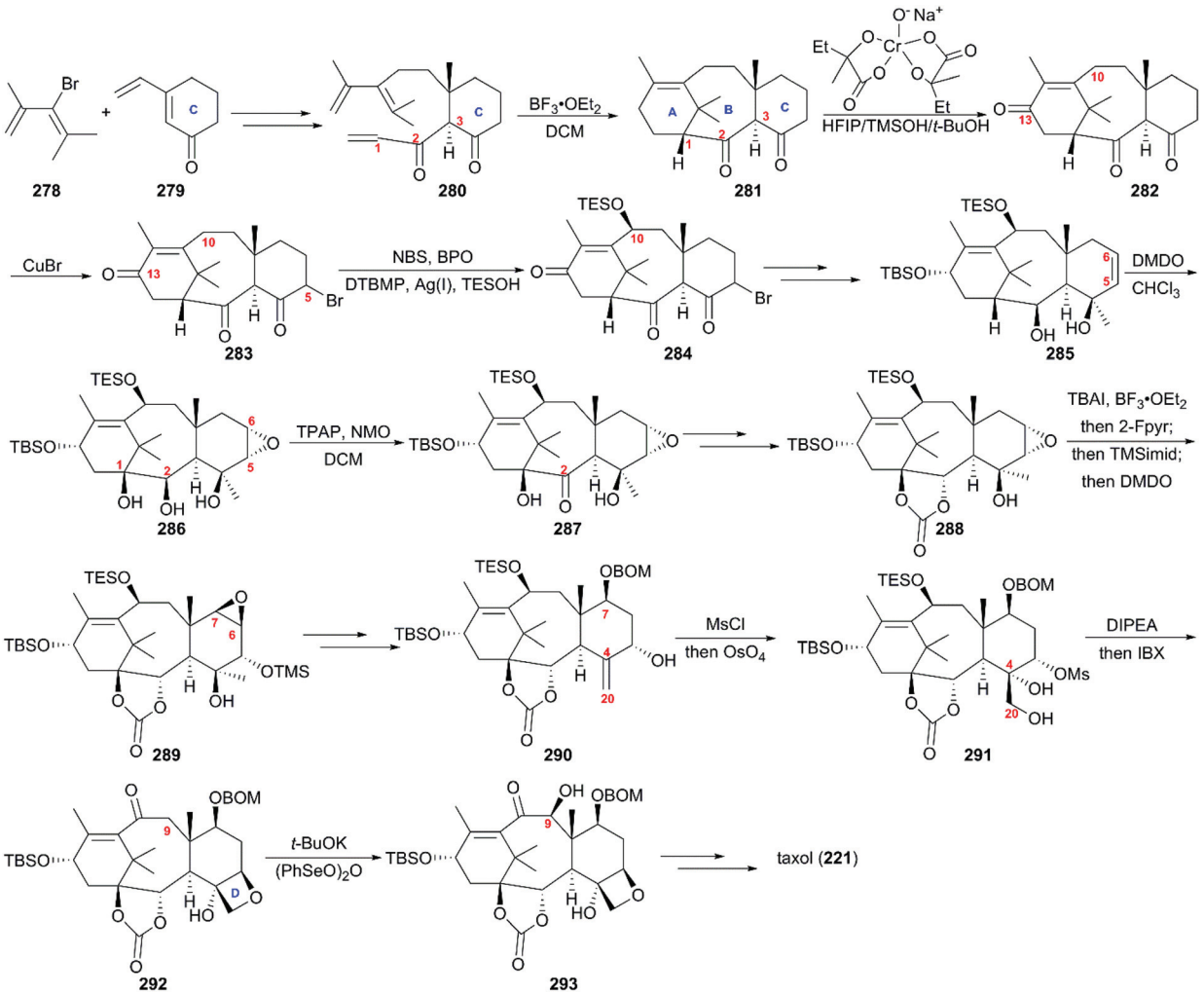

Scheme 27 Total synthesis of taxol by Baran.

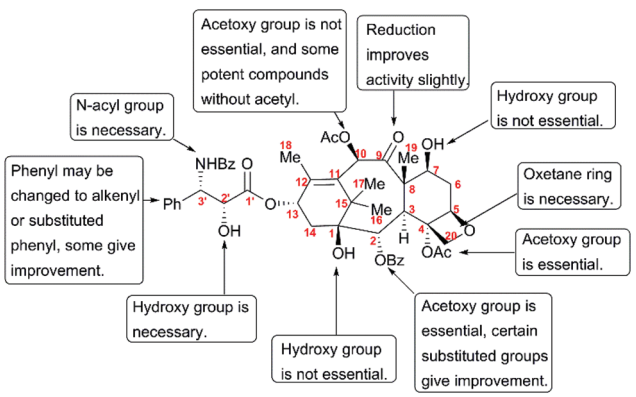

Fig. 11 Structure–activity relationships of taxol.

7. Artemisinin

(+)-Artemisinin (QingHaoSu) (Fig. 13, **5**), the most used drug against malaria worldwide, was isolated from the traditional Chinese medicine plant *Artemisia annua* L. in 1972 by Youyou Tu, who shared the 2015 Noble Prize for this discovery,[199] and (+)-artemisinin-based combination therapy is advocated by WHO. Artemisinin is a sesquiterpene lactone, and its structure is characterized by a unique 1,2,4-trioxane moiety, a pharmacophore that is a necessary endoperoxide bridge for the development of novel antimalaria drugs through semisynthesis of (+)-artemisinin. So far, pharmacological studies have not fully elucidated the exact mechanism of action of (+)-artemisinin, which is believed to be a pro-drug of carbon-centered free radical that plays a substantial role in antimalarial produced by cleavage of its endoperoxide ring inside erythrocytes. Upon bio-activation, the binding of (+)-artemisinin with low valent ions in hemin leads to reduction of the endoperoxide ring to produce an O radical, which subsequently generates a carbon free radical. This free radical is suggested to alkylate heme in the late stage of the parasite life cycle and react with reduced glutathione (GSH) in the early life-ring stage, after which cellular targets are selectively damaged.[200–205] Due to its different mechanism of action, (+)-artemisinin shows higher efficacy

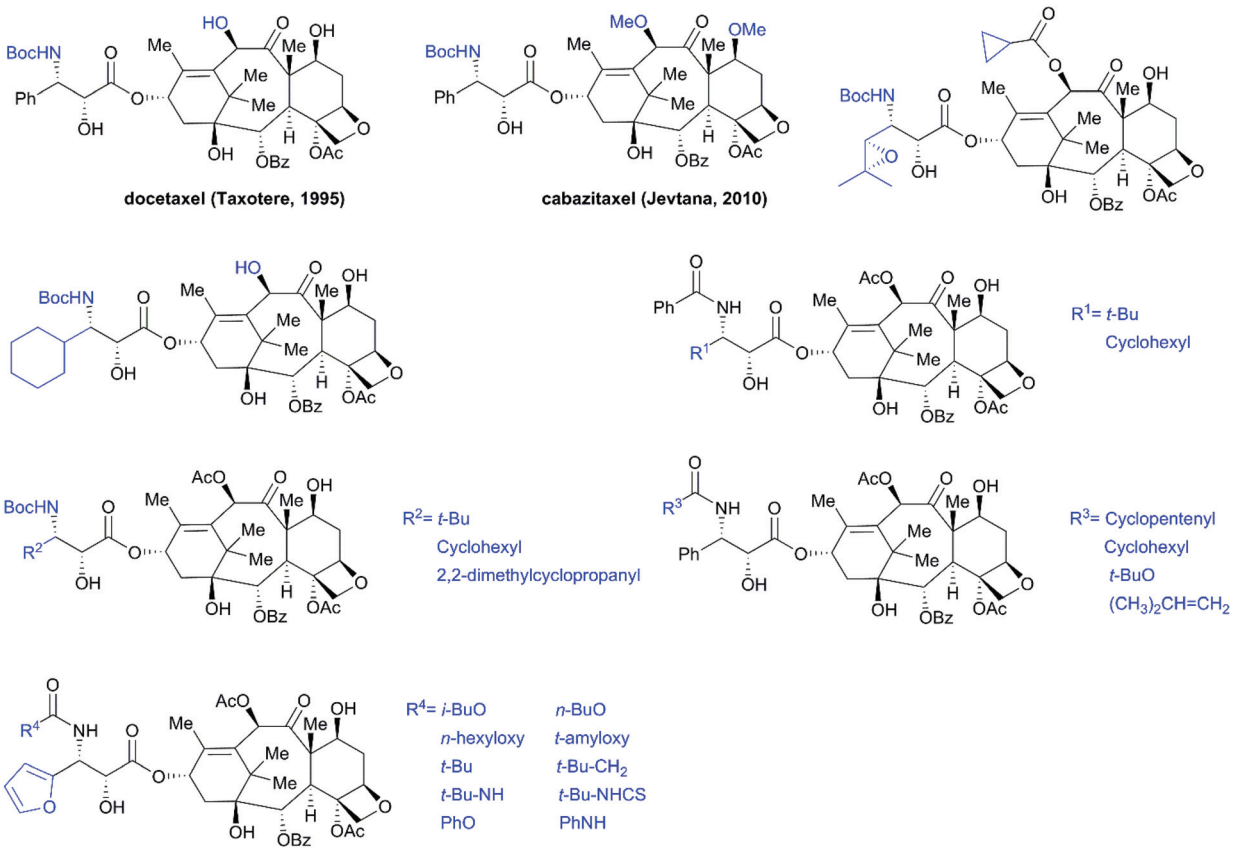

Fig. 12 Examples of potent taxol analogs.

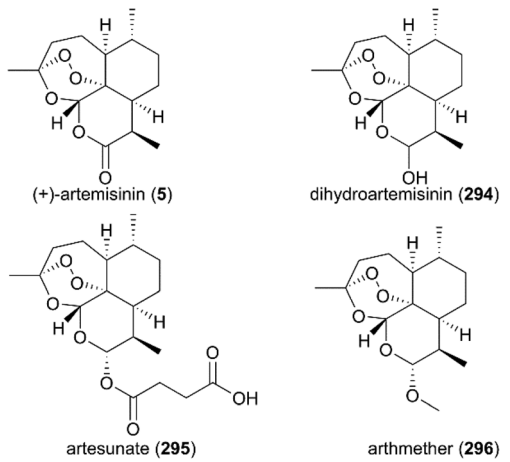

Fig. 13 (+)-Artemisinin and its derivatives.

against multi-drug-resistant malaria compared with the old antimalarial agent quinine and synthetic drug chloroquine. However, along with the widespread use of (+)-artemisinin-based combination therapy in the world have come reports of resistance from different regions. The mechanism of artemisinin-resistance is unclear enough and mainly attributed to the C580Y mutation in Kelch13 (K13) of parasites, and associated elevation of the lipid product phosphatidylinositol-3-phosphate (PI3P). It may influence host remodeling, functions of the apicoplast and food vacuole, all of which protect the parasites against artemisinin challenge.[206,207] Therefore, there is an urgent need to develop novel drugs with new chemical scaffolds and, of course, different mechanisms of action would be excellent. But (+)-artemisinin is still sourced from plants with low yield, which limits the development of more efficient drugs. Therefore, exploring chemical synthesis methods, especially for the total synthesis of (+)-artemisinin, is important for academia and the pharmacy industry.

7.1 Total synthesis of artemisinin

7.1.1 Schmid and Hofheinz's total synthesis of (+)-artemisinin. In the half-century since the discovery of (+)-artemisinin as an antimalarial drug with an unprecedented endoperoxide bridge structure, more than ten teams have completed its total synthesis.[208,209] In 1983, scientists from Roche, Schmid and Hofheinz, first reported a 13-step route to synthesize artemisinin using (−)-isopulegol (**297**) as a starting material (Scheme 28).[210] The alkylated menthone **298** was obtained from **297** with a 6 : 1 diastereomeric ratio in five steps of protection, oxidation, and alkylation reactions. Following the nucleophilic addition of a substituted trimethylsilane reagent, accompanied by deprotection and oxidation, enol ether **299**

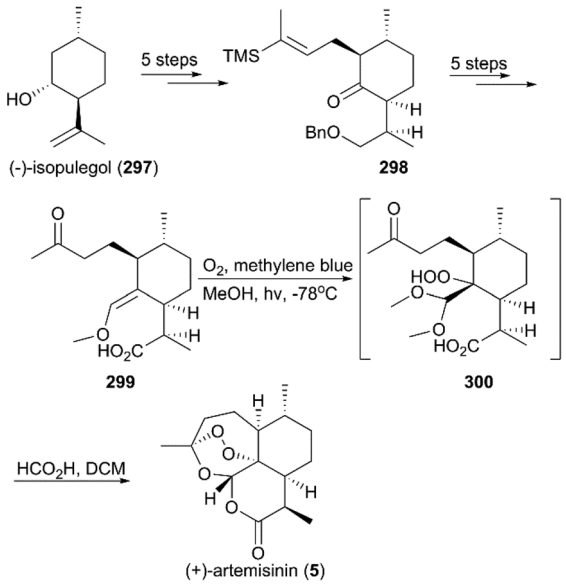

Scheme 28 Total synthesis of (+)-artemisinin by Schmid and Hofheinz.

was generated after desilylation. With the key intermediate **299** in hand, photooxygenation was carried out at −78 °C, and the crude oxidation mixture was treated with acid; the target (+)-artemisinin (**5**) was achieved in 30% yield after crystallization.

7.1.2 Zhou's total synthesis of (+)-artemisinin. Three years later, Zhou and co-workers finished the total synthesis of (+)-artemisinin using *R*-(+)-citronellal (**301**) as raw material (Scheme 29).[211] *R*-(+)-citronellal (**301**) was subjected to two intramolecular cyclizations to produce α,β-unsaturated ketone **302**, which was converted to aldehyde-ketone **303** *via* eight consecutive steps. Subsequently, enol ether **304** was afforded by protecting group manipulations and the condensation of aldehyde carbonyl with trimethyl orthoformate. Photooxidation of the methanolic solution of **304** in the presence of oxygen and Rose Bengal at −78 °C provided intermediate **305**, which was hydrolyzed in 70% $HClO_4$ to give (+)-artemisinin (**5**) in 28% yield.

7.1.3 Avery's total synthesis of (+)-artemisinin. Soon after Zhou's work, Avery and co-workers reported their method for the total synthesis of (+)-artemisinin (Scheme 30).[212] The known chiral sulfoxide **306** was used as the starting material, and five conversion steps gave rise to the diastereomerically pure silyl-acetate **307**, which was converted to the cyclohexyl-acetate **308** by the exclusive Ireland–Claisen ester enolate rearrangement in the presence of lithium *N*-isopropylcyclohexylamide (LICA) as the base. Successive methylation, hydrolysis, and deketalization reactions generated the desired keto-acid **309**. After exposure of the keto-acid **309** to ozone at −78 °C, the crude product was acidified with trifluoroacetic acid (TFA), and the synthesis of artemisinin was finished in a total of 12 steps. In 1992, Avery and co-workers completed the stereoselective total synthesis of **5** again, utilizing an optimized strategy with 10 steps.[213]

7.1.4 Ravindranathan's total synthesis of (+)-artemisinin. In 1990, Ravindranathan and co-workers utilized commercially available monoterpene (+)-car-3-ene as raw material to prepare the precursor enol ether **310**, which was subjected to high temperature for 3 days to undergo an intramolecular Diels–Alder reaction, generating an epimeric mixture of ether **311** in a ratio of 3 : 2 (Scheme 31).[214] After sequential oxidations, hydrolysis and methylation, the ketone-aldehyde **312** Zhou reported previously was obtained, and, followed by Zhou's protocol, the synthesis of (+)-artemisinin (**5**) was completed.

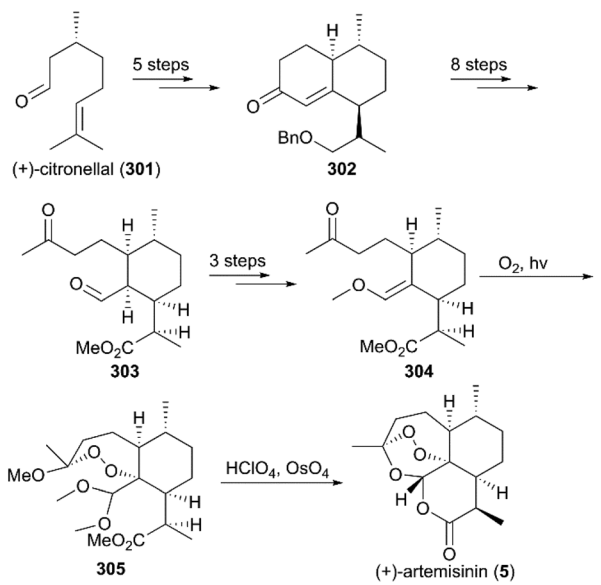

Scheme 29 Total synthesis of (+)-artemisinin by Zhou.

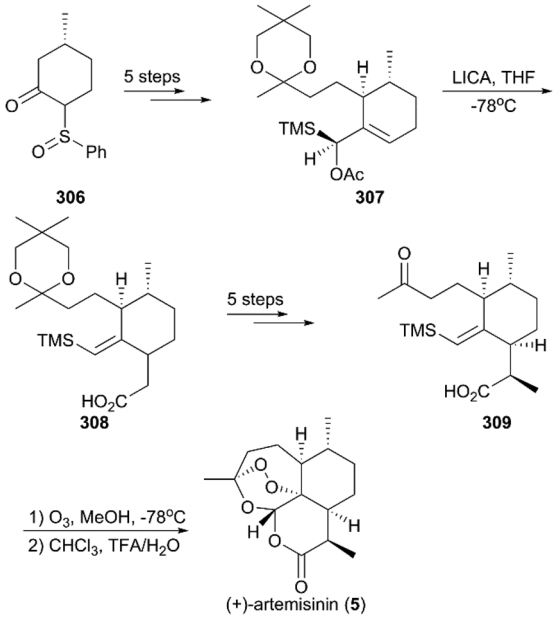

Scheme 30 Total synthesis of (+)-artemisinin by Avery.

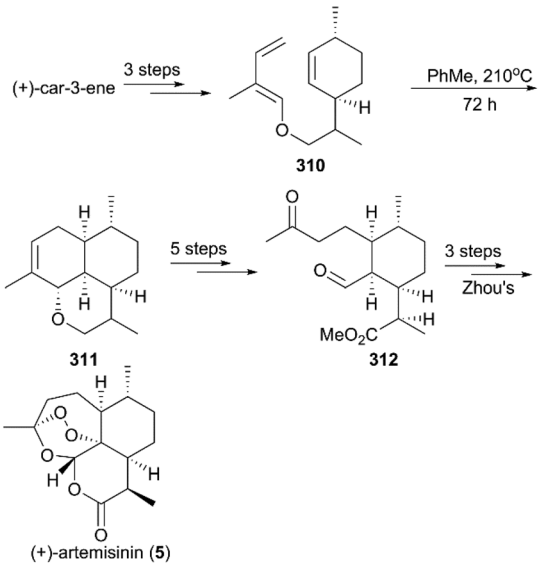

Scheme 31 Total synthesis of (+)-artemisinin by Ravindranathan.

7.1.5 Liu's total synthesis of (+)-artemisinin. As shown in Scheme 32,[215] the total synthesis of (+)-artemisinin by Liu and co-workers began with a $ZnCl_2$-catalyzed intermolecular Diels–Alder addition of (+)-enone ester **313**, followed by photooxygenation in the presence of 5,10,15,20-tetraphenyl-21*H*,23*H*-porphine and oxygen to give enedione **314**, which was subjected to protection, fragmentation of the cyclobutane ring, and a Wittig reaction to generate a mixture of enone ethers (**315**). After nine conversion steps, including deprotection, reduction, a Mitsunobu reaction, and selective hydroboration–oxidation reaction, the ester **316** was obtained as a single stereoisomer. Finally, Schmid and Hofheinz's protocol for photooxygenation was applied to finish the preparation of **5**.

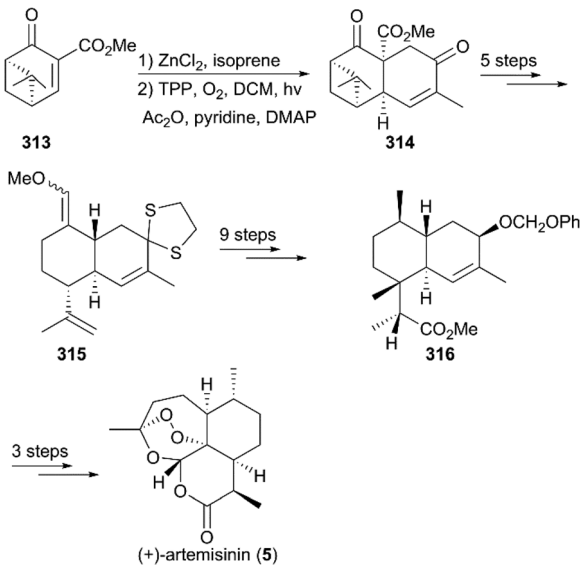

Scheme 32 Total synthesis of (+)-artemisinin by Liu.

7.1.6 Bhonsle's total synthesis of (+)-artemisinin. In Bhonsle and co-workers' synthesis strategy (Scheme 33),[216] (−)-menthol (**317**) was used as the starting material to prepare **318** by Jones oxidation, α-formylation, condensation with ethyl acetoacetate, epoxidation, and regioselective reductions, along with chemoselective acetylation. With intermediate **318** in hand, photooxygenation in the presence of lead tetraacetate and I_2 was used to generate **319** as a major isomer. Next, alcohol **320** was obtained by consecutive saponification, oxidation, nucleophilic addition, and dehydration. Then, the natural product **5** was achieved using previously reported methods.

7.1.7 Constantino's total synthesis of (+)-artemisinin. In 1996, Constantino and co-workers presented the total synthesis of **5**, also using (−)-isopulegol (**297**) as the starting material (Scheme 34).[217] In their strategy, diketone was obtained through oxidations and alkylation, and after condensation, dehydration, and some of the procedures from Bhonsle's work, acid **323** was generated and synthesis of (+)-artemisinin was achieved using a photooxygenation and

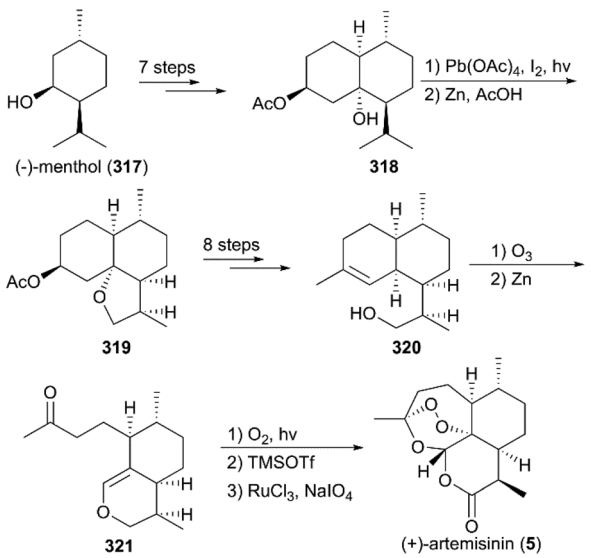

Scheme 33 Total synthesis of (+)-artemisinin by Bhonsle.

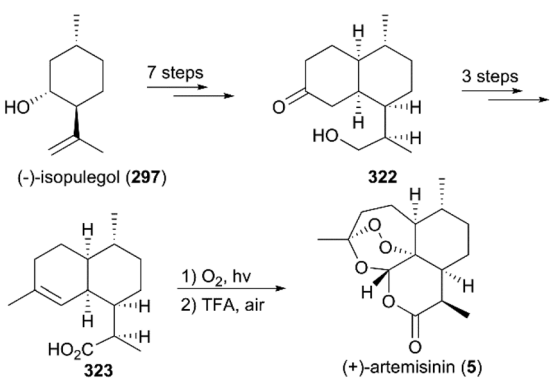

Scheme 34 Total synthesis of (+)-artemisinin by Constantino.

additional oxidation by oxygen in the presence of trifluoroacetic acid.

7.1.8 Yadav's total synthesis of (+)-artemisinin. In 2003, Yadav and co-workers reported the total synthesis of natural product **5** in 11 steps using (+)-isolimonene **324** as a raw material (Scheme 35).[218] In their strategy, an intermolecular radical reaction on the intermediate iodolactone **325** and a Wittig reaction on a ketone **327** were critical transformations. After deprotection and photooxygenation, synthesis of (+)-artemisinin was completed using previously reported procedures.

Seven years later, Yadav and co-workers altered the synthetic strategy by using (*R*)-(+)-citronellal **329** as a starting material instead of (+)-isolimonene **324** (Scheme 36).[219] Their new route involved asymmetric 1,4-addition, aldol condensation, ene reaction, and regioselective hydroboration as key steps; synthesis of target molecule **5** was finished in 11 steps.

7.1.9 Cook's total synthesis of (+)-artemisinin. In 2012, Zhu and Cook reported a highly efficient route for (+)-artemisinin synthesis in just five pots and a total of nine steps (Scheme 37).[220] Their strategy began with the conversion of the simple and inexpensive starting material cyclohexenone **332** to α,β-unsaturated aldehyde **333** in five steps, including a one-pot conjugate addition/alkylation sequence and formylation of the sulfonylhydrazide in the presence of *n*-BuLi and *N*,*N*-dimethylformamide (DMF). A [4 + 2] annulation was explored for the installation of the six-membered lactone to generate enol ether **334**. Different from the procedure that was previously reported, they applied a singlet oxygen generated from the decomposition of H_2O_2 by ammonium molybdate to oxidize the enol ether **334** in the final step. The conditions used for the final oxidative rearrangement to **5** were suitable for large-scale production.

7.1.10 Giannis' total synthesis of (+)-artemisinin and antipode (−)-artemisinin. In 2018, Giannis and co-workers reported the total synthesis of (−)-artemisinin and (+)-artemisinin utilizing *S*-(+)- and *R*-(−)-citronellene (**335**) as starting materials, respectively (Scheme 38).[221] After five steps, conversion of *S*-(+)-citronellene to a triene mixture (**336**) was achieved; this mixture was subjected to a thermal Diels–Alder reaction to generate artemisinic acid derivatives **337** and **338**. Then, the alcohols of **337** and **338** were treated with Martin sulfurane to generate α,β-unsaturated esters, which were reduced by $NiCl_2/NaBH_4$ and Li/NH_3 to produce esters **339** and **340**, respectively. Subsequently, a previously reported procedure was applied to convert **339** and **340** to 9-desmethyl-(−)-artemisinin, which underwent methylation to produce (−)-artemisinin (**341**).

Although great advances in the total synthesis of artemisinin have been made by academic researchers over the past five decades, because of the complex structure of artemisinin and its derivatives and the drawbacks of the expensive starting material, long reaction routes, and excessive protecting group operations, no synthetic strategy is economically efficient enough for pharmaceutical industry-scale production to date. Therefore, more efforts are needed to design a total synthesis strategy that can be used by industry.

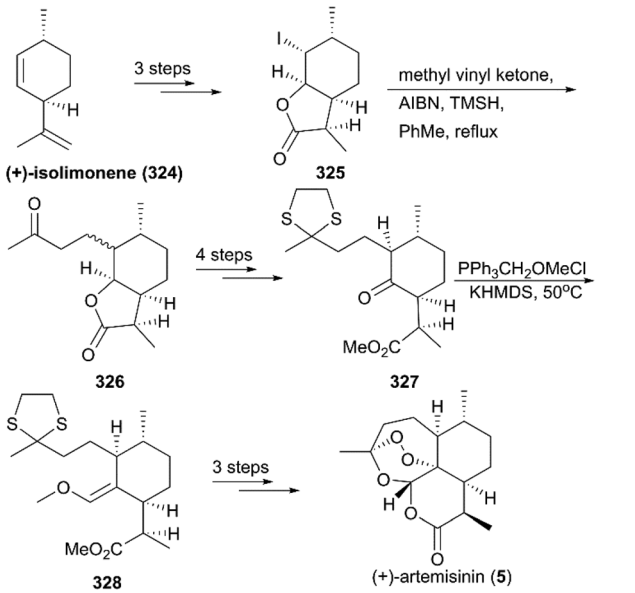

Scheme 35 Total synthesis of (+)-artemisinin by Yadav.

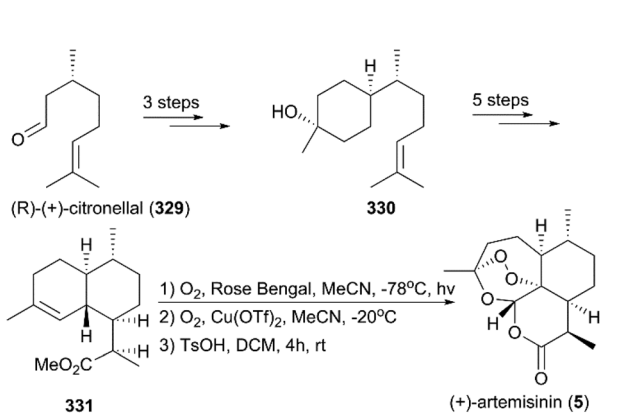

Scheme 36 Alternative total synthesis of (+)-artemisinin by Yadav.

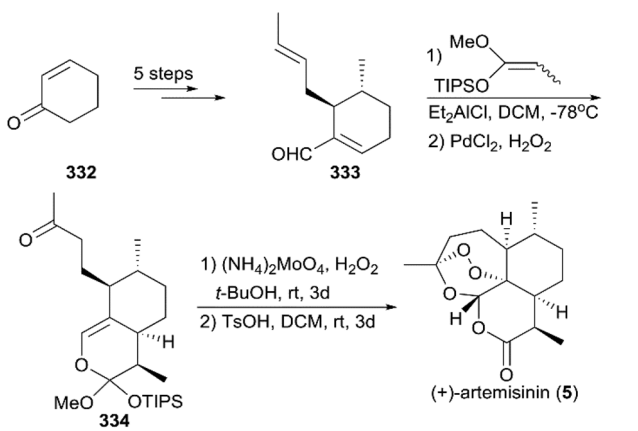

Scheme 37 Total synthesis of (+)-artemisinin by Cook.

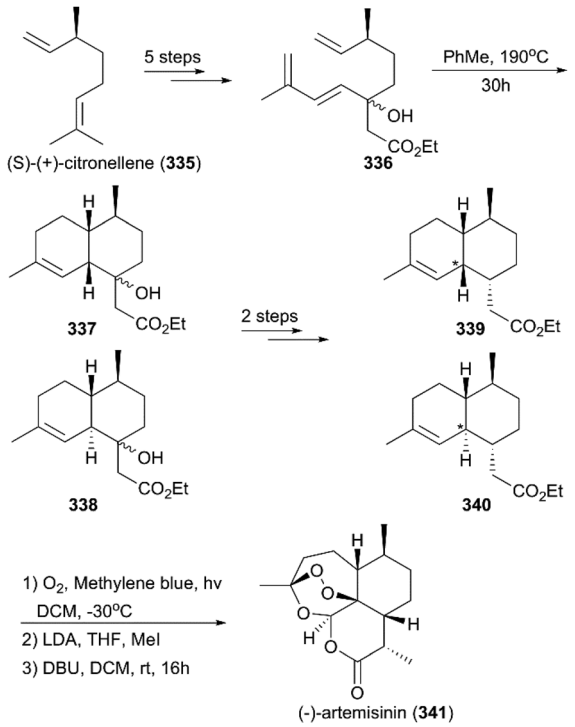

Scheme 38 Total synthesis of (–)-artemisinin by Giannis.

7.2 Structure–activity relationships of artemisinin derivatives

Since the discovery of artemisinin (**5**) as an excellent antimalaria agent, the structural analogs such as dihydroartemisinin (**294**), artemether (**296**), arteether (**342**), artesunic acid (**295**), and sodium artesunate (**343**) have been investigated (Fig. 14); this is because the poor physicochemical properties of artemisinin (**6**), including its low solubility in both oil and water, and short half-life ($t_{1/2}$), limits its first-line clinical use. A large number of artemisinin derivatives and analogs have been explored in systematic SAR studies as part of an effort to seek more potential drug candidates.[222–229]

In 2008, the first resistance to artemisinin was reported in Africa. Because of its worldwide use for a long time, WHO recommends artemisinin-based combination therapy (ACT) with different mechanisms and longer half-life instead of monotherapy using artemisinin to avoid the development and spread of resistance to artemisinin. The first-generation artemisinin-derived analogs dihydroartemisinin (**294**), artemether (**296**), arteether (**342**), artesunic acid (**295**), and sodium artesunate (**343**) were prepared by semisynthetic modifications at C10 with an acetal linkage; these analogs have improved physicochemical properties compared with their parent molecule, such as higher water-solubility. They are recommended by WHO to be used in combination with therapies such as ASAQ Winthrop (sodium artesunate-amodiaquine), Eurartesim (dihydroartemisinin-piperaquine), and ASMQ (sodium artesunate-mefloquine) for the treatment of malaria.

However, the drawbacks of analogs with the acid-sensitive acetal linkage include a short half-life and neurotoxicity. To overcome these drawbacks, the second-generation analogs without acetal groups were designed to improve the drug-like properties; in particular compounds **347** and **348** showed better activity (Fig. 15).[230]

The essential role of the peroxy bridge of artemisinin, which is the pharmacophore, in the development of antimalarials was established early after its discovery, and it was confirmed by the inactive analog deoxoartemisinin **349**.[231] The orientation of the peroxide bond in the chemical scaffold of analogs is also important. For example, the tricyclic analog **350**, which has a flexible

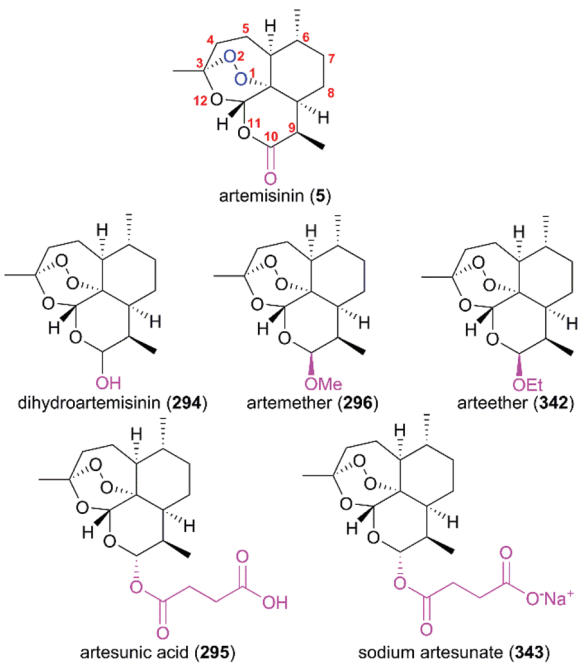

Fig. 14 The first-generation artemisinin derivatives.

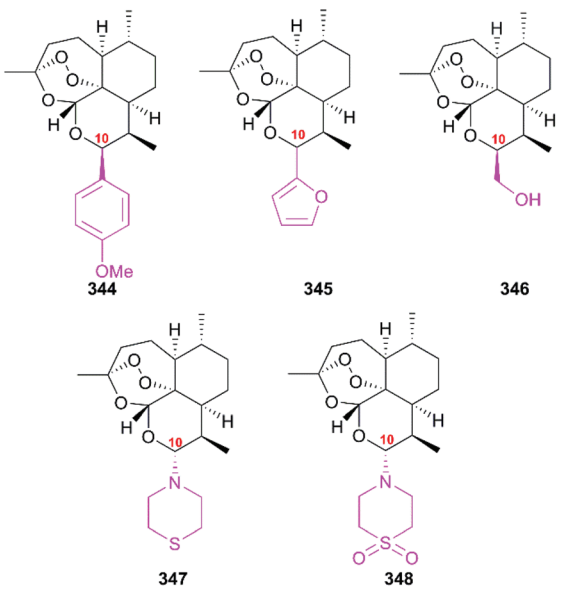

Fig. 15 The second-generation artemisinin derivatives.

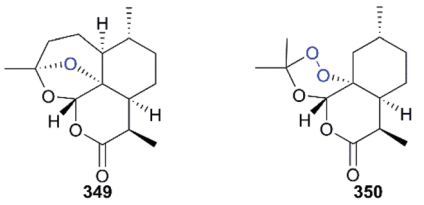

Fig. 16 Examples of artemisinin analogs.

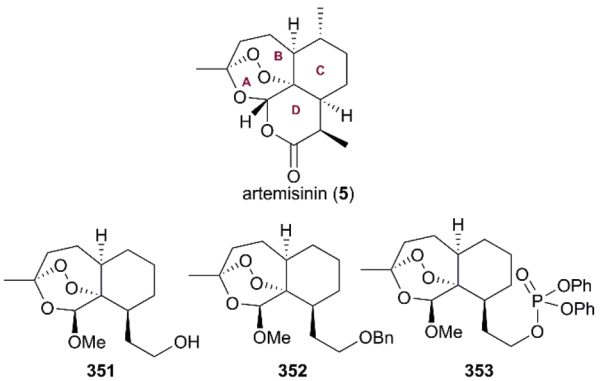

Fig. 17 Examples of peroxy bridge-containing artemisinin analogs.

peroxide ring displayed weaker antimalarial activity compared with the parent molecule artemisinin (Fig. 16).[232]

A number of semisynthetic analogs with tricyclic 1,2,4-trioxaanes in a rigid scaffold lacking the D ring of artemisinin were developed, and many of them exhibited potential antimalarial activities in lower nanomolar ranges, such as analogs **351**, **352**, and **353** (Fig. 17).

Most semisynthetic drug-like analogs with complex chemical scaffolds are probably not suitable for pharmaceutical industry-scale production. The natural product yingzhausu A (**354**) has an accessible endoperoxide ring and displays good antimalarial activity. Spurred by this finding, a large number of simple analogs with endoperoxides have been designed and some of them display good antimalarial activity and offer great potential as drug candidates (Fig. 18).[233,234]

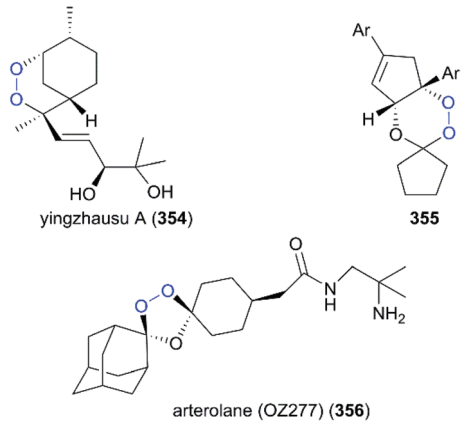

Fig. 18 Yingzhausu A and examples of analogs.

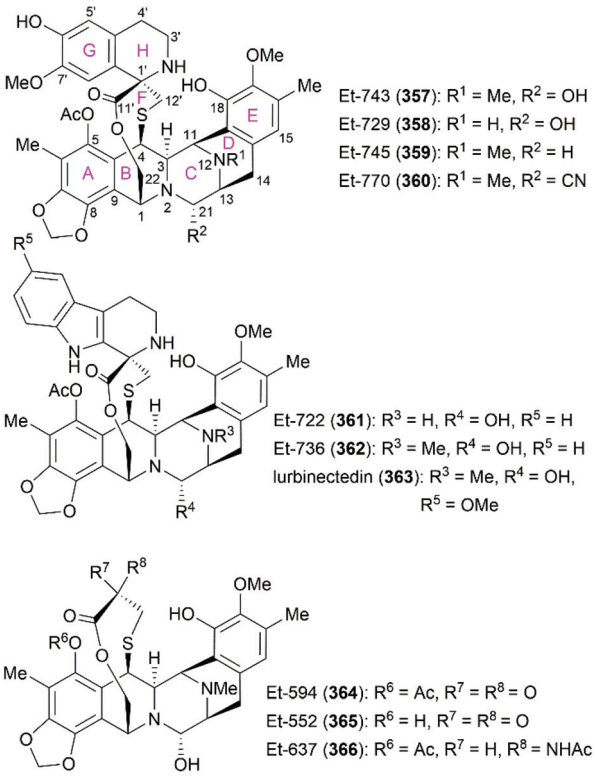

Fig. 19 Representative ecteinascidins and ecteinascidin derivatives and their ring lettering and carbon numbering system.

8. Ecteinascidins

Ecteinascidins are a family of marine natural products containing two or three tetrahydroisoquinoline subunits (Fig. 19). Many ecteinascidin members show antiproliferative activity against several tumor cell lines.[235,236] Among these bioactive ecteinascidins, ecteinascidin 743 (Et-743, trabectedin, **357**) was approved in 2007 for the treatment of advanced soft-tissue sarcoma and ovarian cancer, and lurbinectedin (**363**), one synthetic ecteinascidin derivative, was approved in 2020 for the treatment of metastatic small cell lung cancer.[237,238] Et-743 was first isolated in 1990 from a Caribbean tunicate *Ecteinascidia turbinate* and its absolute stereochemistry was determined in 1992 with the help of the X-ray crystal structure of its *N*12-oxide derivative.[239,240] Extensive studies of Et-743 show that this molecule functions by forming covalent adducts with DNA after binding to the minor groove of DNA and alkylating DNA at the N2 position of guanine.[241–243] The adducts can bend the DNA structure toward the major groove,[244,245] disrupt the interaction between DNA and DNA-binding proteins,[246] and induce double-strand breaks (DBSs),[247] all of which contribute to Et-743's antiproliferative activity on various cancer cell lines.

However, the natural source of Et-743 is limited: only 1.0 g of Et-743 can be isolated from about 1.0 ton of tunicate, which

hampered its preliminary clinical studies.[235,236] In 1996, Corey and co-workers reported the first synthetic route for Et-743, which was initially used for its industrial production.[248] A semisynthetic route relying on Corey's synthetic route was developed in 2000 for the commercial manufacture of Et-743.[249] Apart from its biological function, Et-743 also has several structural features that make it a quite challenging but attractive synthetic target: (1) three tetrahydroisoquinoline moieties with different substitution patterns; (2) eight rings including one bridged 10-membered lactone ring containing a sulfur atom; (3) seven chiral centers including one spiro center; and (4) a labile carbinolamine functional group. Continuous efforts from the synthetic community have led to outstanding achievements in the total synthesis of Et-743 and we discuss them in the following section.

8.1 Total synthesis of Et-743

8.1.1 Corey's total synthesis of Et-743. Corey and co-workers achieved the first total synthesis of Et-743 and later (in 2000) they reported a more efficient synthetic route to the key intermediate **373** (Scheme 39).[248,250] In their synthesis strategy, the chiral C13 (Et-743 numbering) stereocenter was established through enantioselective hydrogenation of the α,β-unsaturated ester **367** to generate the tyrosine derivative **368** with 96% ee. A similar approach was applied to the synthesis of another tyrosine derivative **370**, which was transformed into the bridged lactone **371** through an intramolecular Mannich reaction. Condensation between the two tyrosine derivatives **369** and **371** and subsequent manipulation of the lactone led to lactol **372**. Methanesulfonic acid promoted Mannich bisannulation of **372**, leading to the successful construction of a bridged C/D ring system with establishment of the C11 stereocenter. Then, a Strecker reaction was used to construct amino nitrile **373**, and subsequent manipulations led to pentacyclic compound **374** with the required methyl group on ring E.

Position-selective hydroxylation with benzeneseleninic anhydride followed by the introduction of the cysteine derivative **375** generated **376**, which was ready for the construction of the challenging 10-membered bridged lactone ring F. The con-

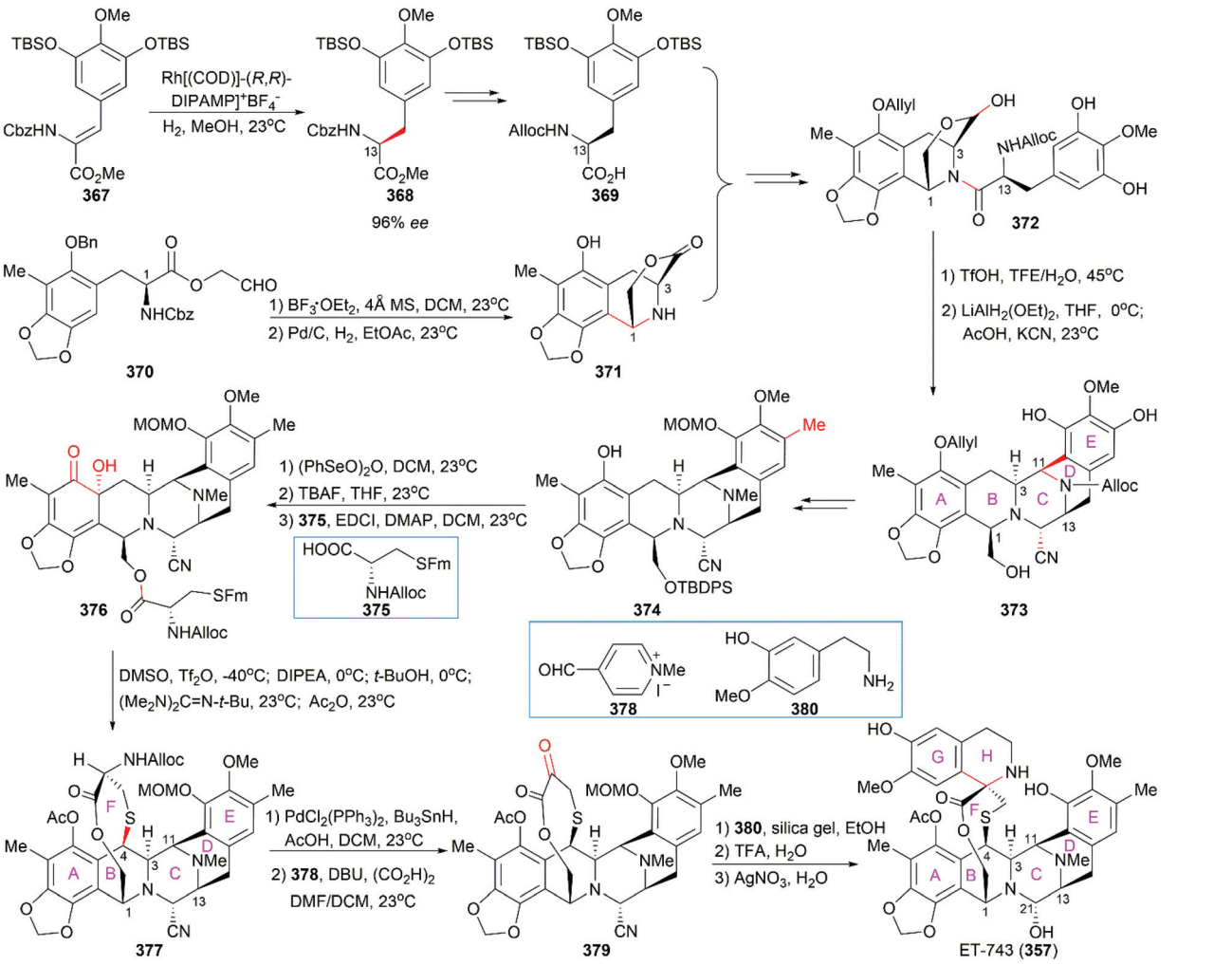

Scheme 39 Corey's synthetic route.

struction of **377** from **376** involved a series of transformations: (1) activation of the tertial hydroxy group with the *in situ*-generated Swern reagent from Tf_2O and DMSO, followed by addition of i-Pr_2NEt, which led to *o*-quinone methide; (2) Barton's base-mediated removal of the Fm protecting group, and the subsequent nucleophilic addition of a sulfur ion to the quinone methide generating ring F; and (3) acetylation of the resulting phenoxide group with Ac_2O. Removal of the Alloc protecting group and the subsequent transamination with **378** generated the keto lactone **379**, which was utilized for the introduction of the third tetrahydroisoquinoline moiety through a Pictet–Spengler reaction with **380**. Removal of the MOM protecting group from the C18 phenolic hydroxy group and stereoselective introduction of the C21 hydroxy group completed the total synthesis of Et-743.

8.1.2 Fukuyama's total synthesis of Et-743. Fukuyama and co-workers reported their first-generation synthetic route to Et-743 in 2002 and continuous efforts in their lab led to a separate synthetic strategy in 2013.[251,252] In their first-generation synthetic design,[251] the C13 chiral stereocenter in the tyrosine derivative **382** was established through enantioselective hydrogenation, while a Mannich-type reaction between **383** and chiral template **384** stereoselectively constructed the C1 chiral center (Scheme 40). A four-component Ugi reaction including **382**, **386**, *p*-methoxyphenyl isocyanide (**387**) and acetaldehyde led to **388**, which was transformed into the enamide compound **389** containing ring C. An intramolecular Heck reaction was applied for the formation of the bridged C/D ring system in tetracyclic compound **390**, which was converted to aldehyde **391** after several manipulations. Subsequent hydrogenolytic removal of the benzyl group led to spontaneous cyclization to form the pentacyclic compound **392** with the desired stereoconfiguration at C4. Protecting group manipulations followed by the introduction of the cysteine derivative provided **393**, which was utilized for the installation of the crucial ring F. Selective removal of the acetyl group gave thiol, which cyclized to form the ring F upon exposure to TFA under high dilution conditions in TFE, presumably *via* the *o*-quinone methide intermediate. Subsequent acetylation of the phenolic hydroxy group gave rise to **394**, which could be converted to Et-743 in a manner similar to that utilized in Corey's total synthesis.

In their optimized second-generation synthetic route, the diacetylated diketopiperazine **395**, which was derived from

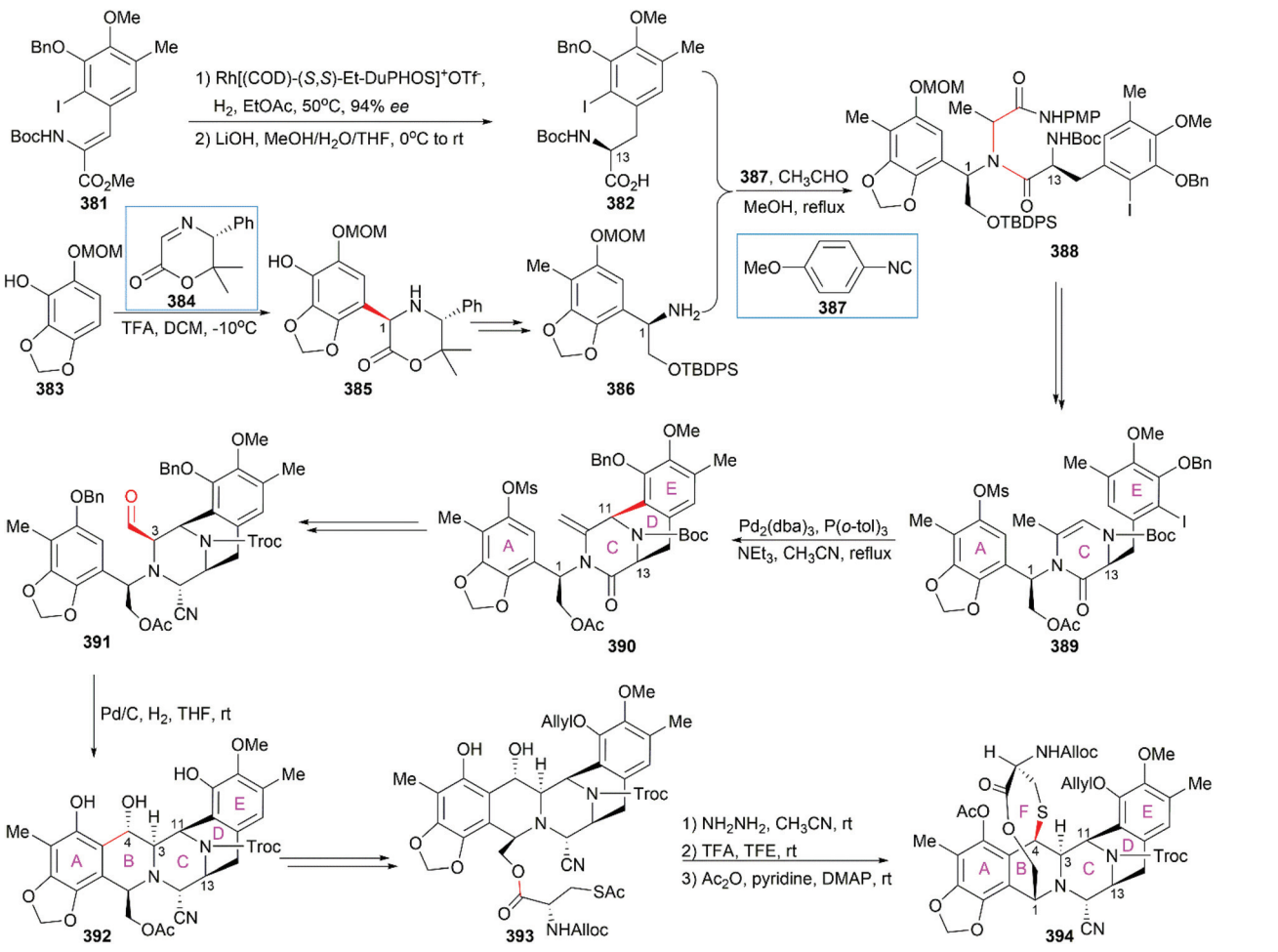

Scheme 40 Fukuyama's first-generation synthetic route.

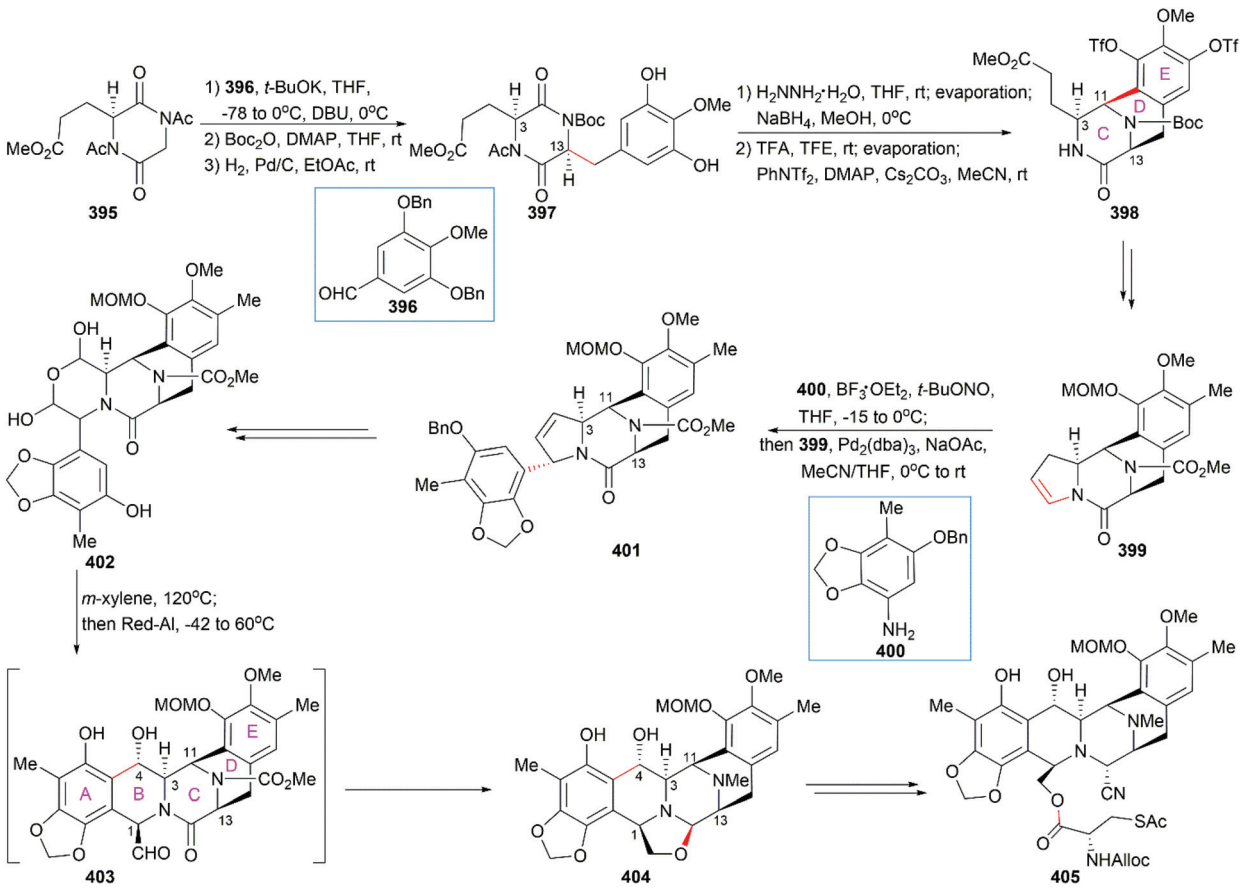

Scheme 41 Fukuyama's second-generation synthetic route.

L-glutamic acid, was the only chiral source (Scheme 41).[252] Perkin condensation of **395** with aldehyde **396** followed by protection of the amide and hydrogenation stereoselectively constructed the C13 chiral center. Selective reduction of the imide carbonyl group after hydrazinolysis of the acetyl group converted **397** to a suitable intermediate for construction of the bridged C/D ring system through Mannich-type reaction, which was performed in the presence of TFA. Tetracyclic enamide **399**, which was derived from **398** with the installation of the methyl group on ring E and several other manipulations, was used as a platform for the introduction of ring A. A regio- and stereo-selective Heck reaction of **399** with a diazonium salt derived from amine **400** successfully led to **401**. Manipulation of **401** led to the dialdehyde equivalent **402**, which cyclized to form the pentacyclic compound **403** upon heating in *m*-xylene. Reduction of **403** with Red-Al gave oxazolidine **404**, a suitable precursor for the introduction of the cysteine derivative to give **405**, an analog of **393**, which could be similarly converted to Et-743.

8.1.3 Zhu's total synthesis of Et-743. Zhu's synthesis of Et-743 started with preparing the right tetrahydroisoquinoline moiety (D/E ring system) by condensation of chiral amino alcohol **406** with Garner's aldehyde (*S*)-**407** (Scheme 42).[253] It is worth noting that the stereochemistry of the newly generated chiral center C11 was solely controlled by the absolute configuration of **406**. Assembly of **409** with racemic **410** gave coupled product **411** in 68% yield with its C1 epimer in 23% yield, the diastereoselectivity of which may be explained by an S_N1 mechanism. Construction of the piperazine ring C was achieved through oxidation of the hydroxy group of **412** followed by $ZnCl_2$-catalyzed Strecker reaction to give **413**. TFA-promoted cyclization of **414** concomitant with MOM protecting group removal successfully installed ring B in **415** with the desired stereoconfiguration at C4, which was similar to the ring B formation strategy utilized in Fukuyama's first-generation synthetic route. Removal of the acetate group followed by the introduction of the cysteine derivative led to **416**, from which ring F was installed through a one-pot deprotection/cyclization mediated by TFA. Compound **417** could be converted into Et-743 following Corey's protocol.

8.1.4 Danishefsky's formal total synthesis of Et-743. Starting with asymmetric reduction of the ketone moiety in **418** using Noyori transfer-hydrogenation conditions followed by a Mitsunobu reaction with diphenylphosphorylazide securely fashioned the C1 stereoconfiguration in **421** (Scheme 43).[254] The left tetrahydroisoquinoline moiety (A/B ring) was formed from **421** through an acid-promoted Pomerantz–Fritsch reaction. Condensation of **422** with the chiral tyrosine derivative **423** afforded **424**, which was converted into the cyclization precursor **425**. Aldehyde **425** suc-

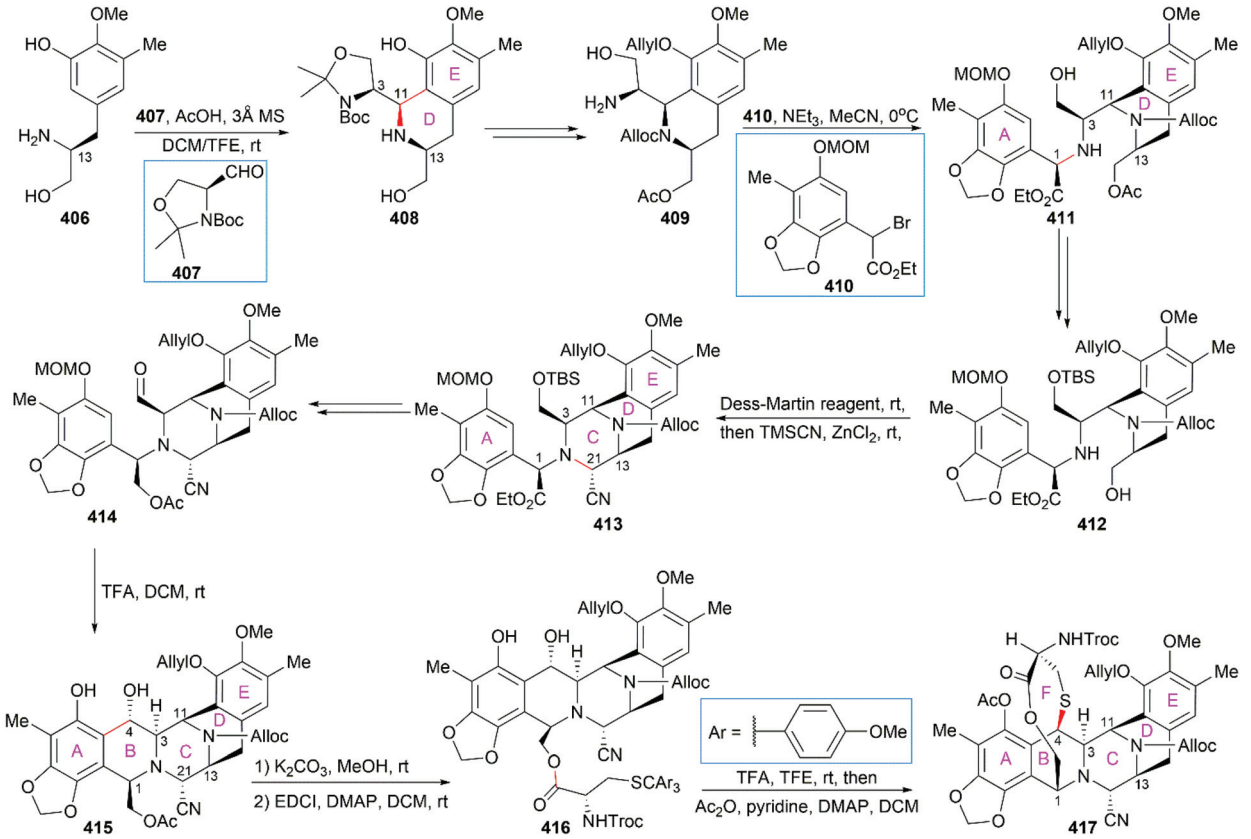

Scheme 42 Zhu's synthetic route.

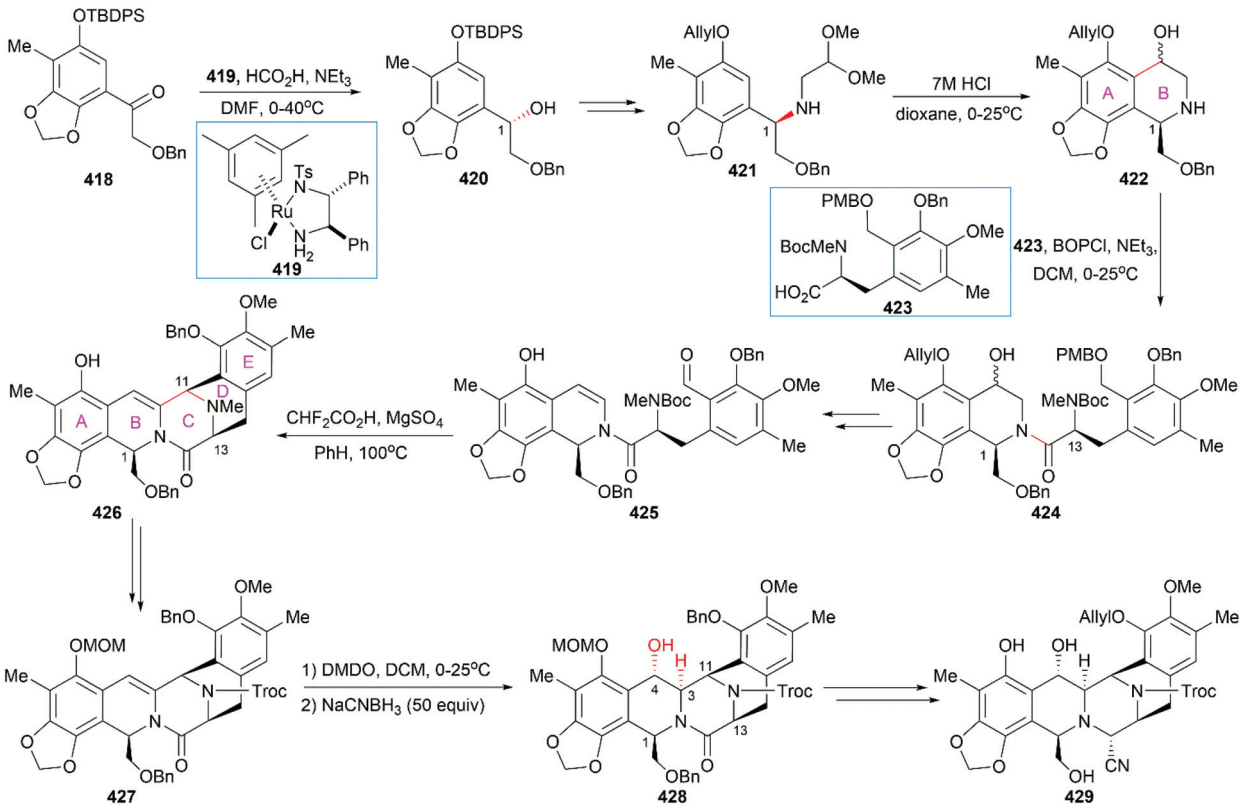

Scheme 43 Danishefsky's synthetic route.

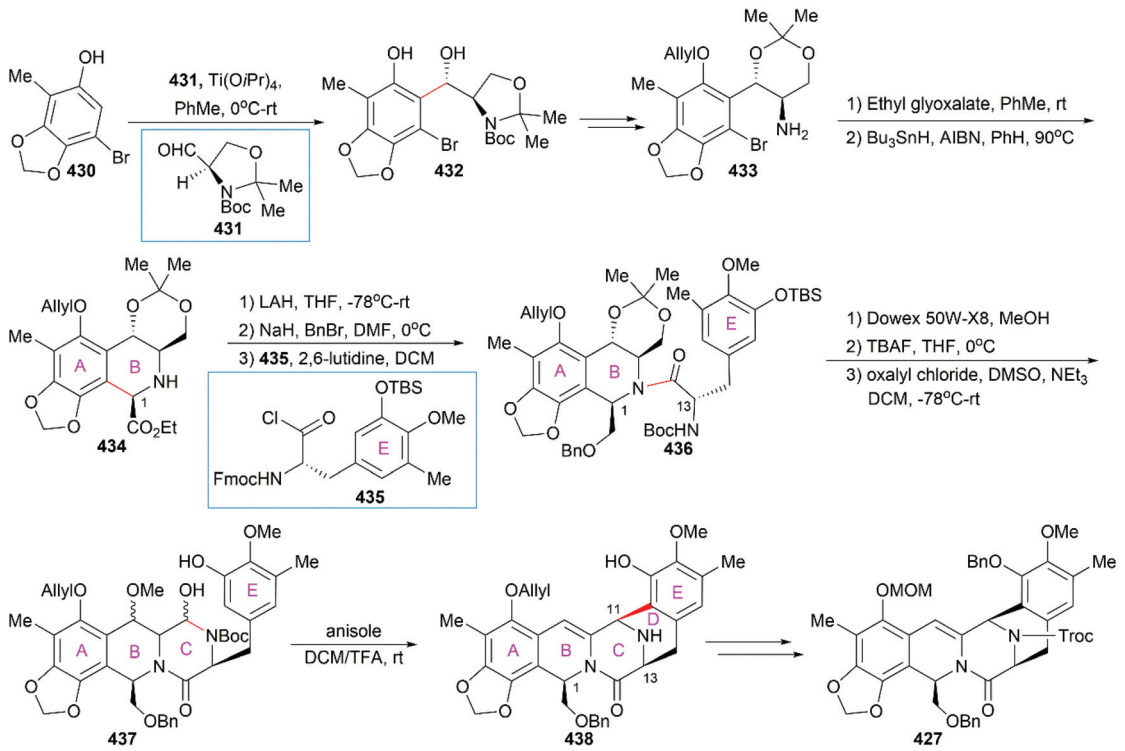

Scheme 44 Williams' synthetic route.

cessfully cyclized to give rise to the pentacyclic compound **426** through a CHF_2CO_2H-promoted vinylogous Pictet–Spengler reaction. DMDO-mediated epoxidation of the double bond in the advanced intermediate **427** followed by amide nitrogen atom-promoted epoxide ring-opening and subsequent reduction of the iminiumion produced compound **428** with

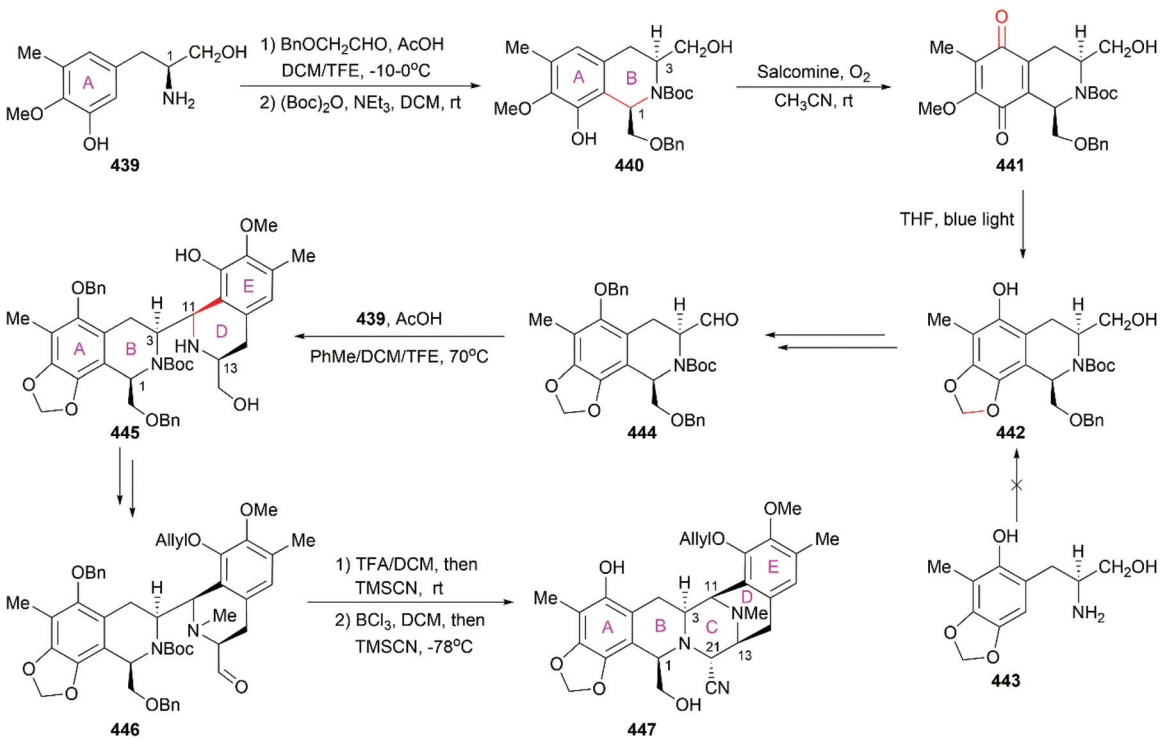

Scheme 45 Ma's synthetic route.

the desired stereoconfiguration at C3 and C4. It is worth noting that a large excess of sodium cyanoborohydride was required for the high yield of **428**. Further manipulations on **428** led to **429**, which was an intermediate in Fukuyama's total synthesis of Et-743.[251]

8.1.5 Williams' formal total synthesis of Et-743. In Williams' synthetic route,[255] stereoselective condensation of the phenol **430** with (*R*)-Garner's aldehyde **431** in the presence of Ti $(OiPr)_4$ produced the anti-product **432** (Scheme 44). Condensation of the chiral amine **433** with ethyl glyoxalate led to an imine intermediate, which proceeded to form the left tetrahydroisoquinoline **434** with the desired C1 stereocenter established through an AIBN/Bu_3SnH-mediated radical cyclization. Removal of the acetonide from **436** with Dowex 50W-X8 cationic resin in methanol followed by desilylation and subsequent Swern oxidation produced **437**. When treated with TFA, **437** successfully underwent a Pictet–Spengler reaction to give the pentacyclic compound **438**, although with low regioselectivity on the E ring. Since several protecting group manipulations could transform **438** into **427**, which was an advanced intermediate in Danishefsky's formal total synthesis, Williams and co-workers completed their formal total synthesis of Et-743.

8.1.6 Ma's total synthesis of Et-743. In 2019, Ma and co-workers reported an efficient total synthetic route to Et-743 and lurbinectedin, in which the left and right tetrahydroisoquinoline moieties were constructed from the common intermediate **439** (Scheme 45).[256] Starting from the chiral amino alcohol **439**, which was prepared from Cbz-protected (*S*)-tyrosine, a precursor for the left tetrahydroisoquinoline moiety **440** was obtained through a Pictet–Spengler reaction. After oxidation of the phenol **440** to quinone **441**, the authors carried out detailed screenings for optimized conditions to form benzo[1,3]dioxole through a light-mediated remote C–H bond activation. They finally found that blue-LED irradiation of a THF solution of **441** could smoothly transform quinone **441** into phenol **442**. It should be pointed out that this transformation was an essential step in their synthesis because the attempts to synthesize **442** from **443** through a direct Pictet–Spengler reaction under

Table 2 Cytotoxicities of Et-770 and related derivatives to three carcinoma cell lines[a]

		IC_{50} (nM)		
Entry	Compound	HCT116[b]	QG56[b]	DU145[b]
1	Et-770 (**360**)	0.71	1.6	1.6
2	Et-788 (**449**)	3.5×10^2	1.3×10^3	9.9×10^2
3	**450**	54	1.6×10^2	1.0×10^2
4	**451**	1.3	9.5	4.4
5	**452**	0.50	1.8	1.2
6	**453**	0.13	0.40	0.72
7	**454**	0.014	0.071	0.087
8	**455**	0.053	0.33	0.24
9	**456**	0.010	0.12	0.041
10	**457**	0.26	0.96	0.37
11	**458**	0.31	1.7	0.62
12	**459**	15	36	16
13	**460**	13	36	24
14	**461**	0.20	1.0	0.51

[a] Values given are IC_{50} in nM and original activity data can be found in ref. 259–262. [b] HCT116: human colon cancer cell line; QG56: human lung cancer cell line; DU145: human prostate cancer cell line.

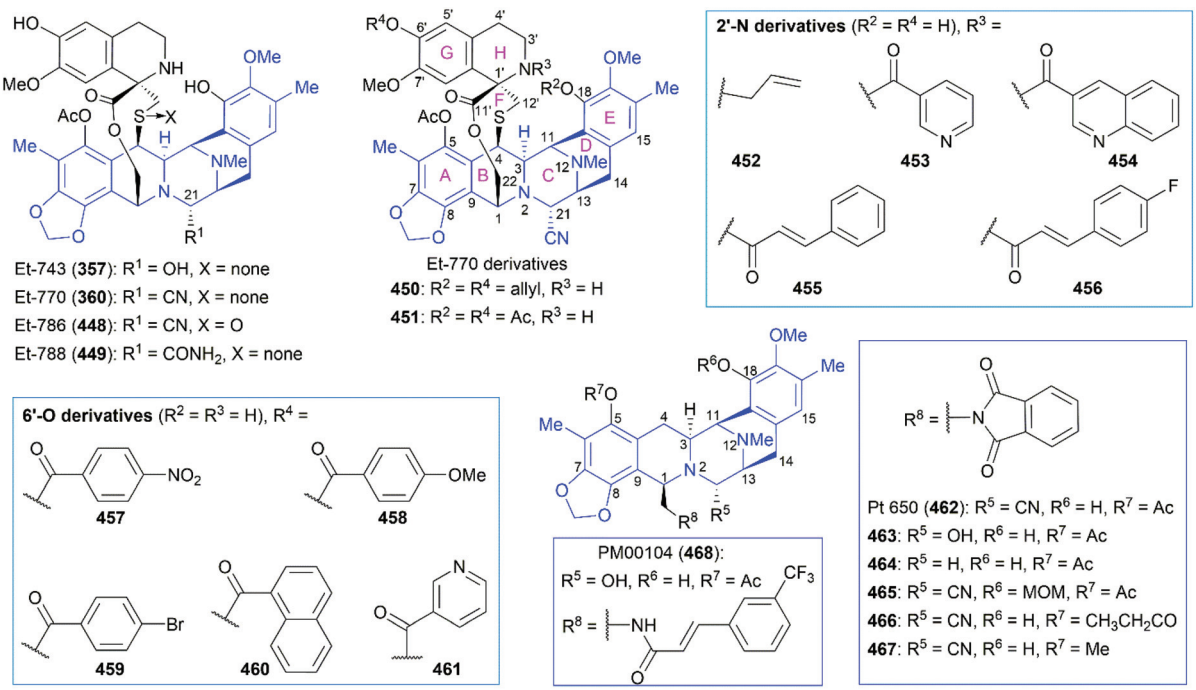

Fig. 20 Representative ecteinascidin derivatives for SAR study.

various conditions failed. Condensation of aldehyde **444** with amine **439** successfully provided **445**, which contained the desired two tetrahydroisoquinoline moieties. TFA-promoted deprotection of **446** followed by Strecker reaction and BCl_3-mediated removal of the two benzyl groups produced amino nitrile **447**, which could be transformed into Et-743 in a manner similar to that in Corey's synthetic route.

8.2 Structure–activity relationships of ecteinascidin derivatives

Although the reported total synthetic routes are not amenable to scaling-up for manufacturing ET-743 on an industrial scale, transformations developed in these studies provide access to diverse ecteinascidin derivatives, some of which are listed in Fig. 20. These synthesized ecteinascidin derivatives make SAR studies of Et-743 possible and have led to the development of more anti-tumor molecules including the approved drug lurbinectedin (**363**) and PM00104 (**468**), which is in phase II clinical trials. We give a short discussion about the SAR studies on ecteinascidin derivatives in the following section (Fig. 20 and Tables 2, 3).

Table 3 Cytotoxicities of Pt 650 and related derivatives to four carcinoma cell lines[a]

Entry	Compound	IC_{50} (nM)			
		A-549[b]	HCT116[b]	A375[b]	PC-3[b]
1	Et-743 (**357**)	1.0	0.50	0.15	0.70
2	Pt 650 (**462**)	0.95	0.38	0.17	0.55
3	**463**	1.0	0.61	0.20	0.53
4	**464**	2.2×10^3	1.1×10^3	6.1×10^2	8.5×10^2
5	**465**	2.3×10^2	74	66	98
6	**466**	2.1	1.2	0.51	2.9
7	**467**	3.1	1.4	0.55	3.1

[a] Values given are IC_{50} in nM and original activity data can be found in ref. 257. [b] A-549: human lung cancer cell line; HCT116: human colon cancer cell line; A375: human melanoma cell line; PC-3: human prostate cancer cell line.

After achieving the first total synthesis of Et-743, Corey and co-workers synthesized a series of Et-743 analogs from a common intermediate, which led to the discovery of one simpler and more stable anti-tumor molecule named Pt 650 (phthalascidin, **462**).[257] In 2002, Saito and co-workers isolated Et-770 (**360**), an analog of Et-743, from the pretreated Thai tunicate *Ecteinascidia thurstoni* with potassium cyanide.[258] Both Pt 650 and Et-770 showed antiproliferative activities on various cancer cell lines. Synthesis and evaluation of more synthesized analogs of Pt 650 and Et-770 revealed the structural features for high potent biological activities.[257–263]

A cyano or a hydroxy group at the C21 position is essential and is responsible for alkylating DNA. Et-788 (**449**) with an amide group at C21 and **464** with hydrogen at C21 showed a significant decrease in activity compared with their corresponding parent compounds.[257,261] Oxidation of the sulfur atom in Et-770 led to Et-786, which resulted in dramatically diminished cytotoxicity.[259] Protection of the C18 and C6′ phenolic hydroxy groups with allyl (**450**) or acetate (**451**) decreased cytotoxicity.[259,260] Protection of the C18 phenolic hydroxy group with MOM (**465**) also resulted in diminished antitumor activity.[257]

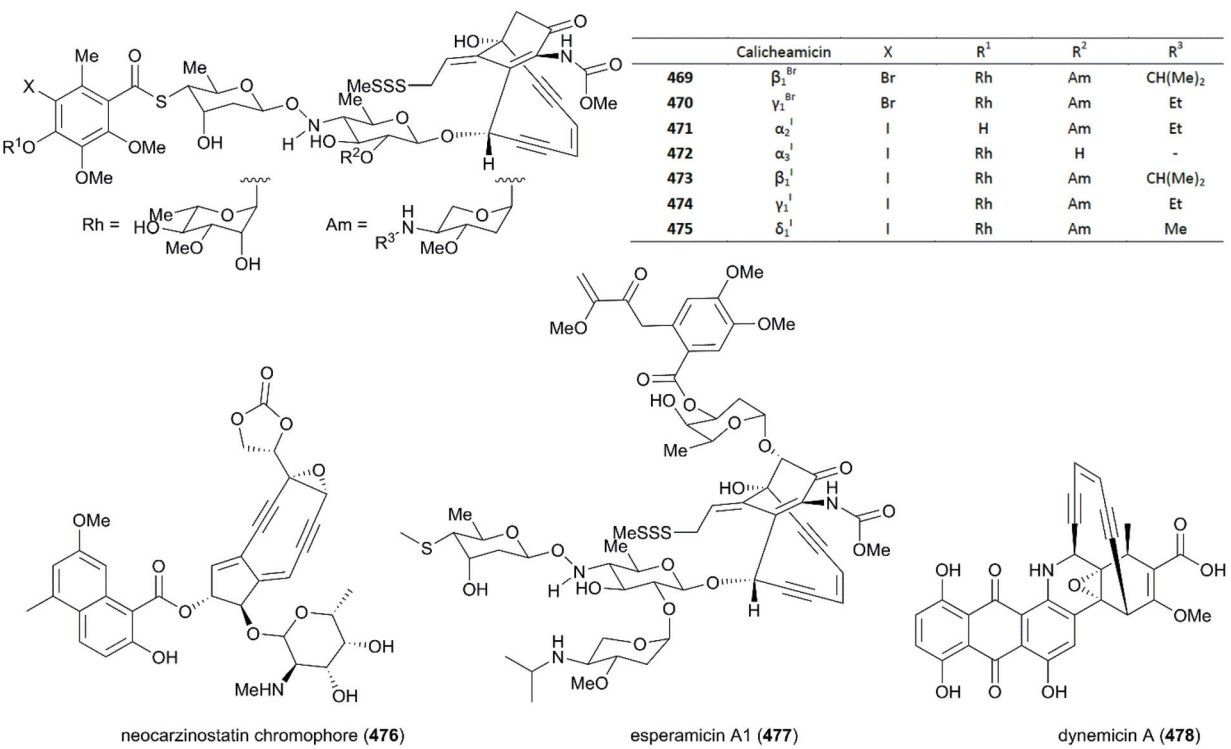

	Calicheamicin	X	R^1	R^2	R^3
469	β_1^{Br}	Br	Rh	Am	$CH(Me)_2$
470	γ_1^{Br}	Br	Rh	Am	Et
471	α_2^{I}	I	H	Am	Et
472	α_3^{I}	I	Rh	H	-
473	β_1^{I}	I	Rh	Am	$CH(Me)_2$
474	γ_1^{I}	I	Rh	Am	Et
475	δ_1^{I}	I	Rh	Am	Me

Fig. 21 Examples of natural products containing enediyne.

Modifications at the 2′-*N* position revealed that the 2′-*N*-allylated compound **452** showed activity similar to that of Et-770 (**360**), while several 2′-*N* amide derivatives including nitrogen-containing heterocycles (**453** and **454**) and cinnamoyl derivatives (**455** and **456**) exhibited improved cytotoxicity.[260–262] Notably, **454** and **456**, respectively, exhibited approximately 50- and 70-fold higher cytotoxicity to the HCT116 cancer cell line than Et-770 (**360**).[261]

Evaluation of the cytotoxicity of a series of C6′ aromatic ester derivatives showed that **457** and **458** with a nitro group or a methoxy group on the benzene ring exhibited activities similar to Et-770 (**360**).[262] However, derivatives with a bromo group on the benzene ring (**459**) or a naphthyl group (**460**) showed significantly decreased cytotoxicity. The incorporation of a nitrogen-containing heterocyclic ester group (**461**) resulted in a moderate increase in activity. For Pt 650 analogs, derivatives possessing a propionyl (**466**) or a methyl (**467**) protecting group on the C5 phenolic hydroxy group were slightly less effective than the parent compound Pt 650 (**462**).[257] These results indicate the promising role of total synthesis in the future development of ecteinascidin-type and related natural products into drugs.

9. Calicheamicin γ_1^I

Calicheamicin γ_1^I (**474**) is a potent antitumor antibiotic that was isolated from *Micromonospora echinospora* ssp in 1986. One year later, its structure was defined as an enediyne with a bicyclo [7.3.1]tridec-9-ene-2,6-diyne system, a unique N–O glycosidic linkage, and a methyl trisulfide moiety; other members of the calicheamicin family were also discovered (Fig. 21).[264–266] Several natural products containing the enediyne were also found in the 1980s, such as Neocarzinostatin chromophore (**476**),[267] Esperamicin A1 (**477**),[268] and Dynemicin A (**478**)[269] (Fig. 21). Calicheamicin γ_1^I displays excellent activity against Gram-negative and -positive bacteria at concentrations lower than 1 pg mL^{-1}. It demonstrated extreme toxicity to all cells, indicating that it has extraordinary potency against cancer cells. Investigation of its mechanism showed that calicheamicin γ_1^I targets and binds to the DNA minor groove, and then undergoes the Bergman cyclization after bioreductive activation to produce a biradical, 1,4-didehydrobenzene, which subsequently abstracts hydrogen atoms from the deoxyribose backbone of DNA to generate sugar radicals. The latter undergo oxygen-dependent reactions and finally

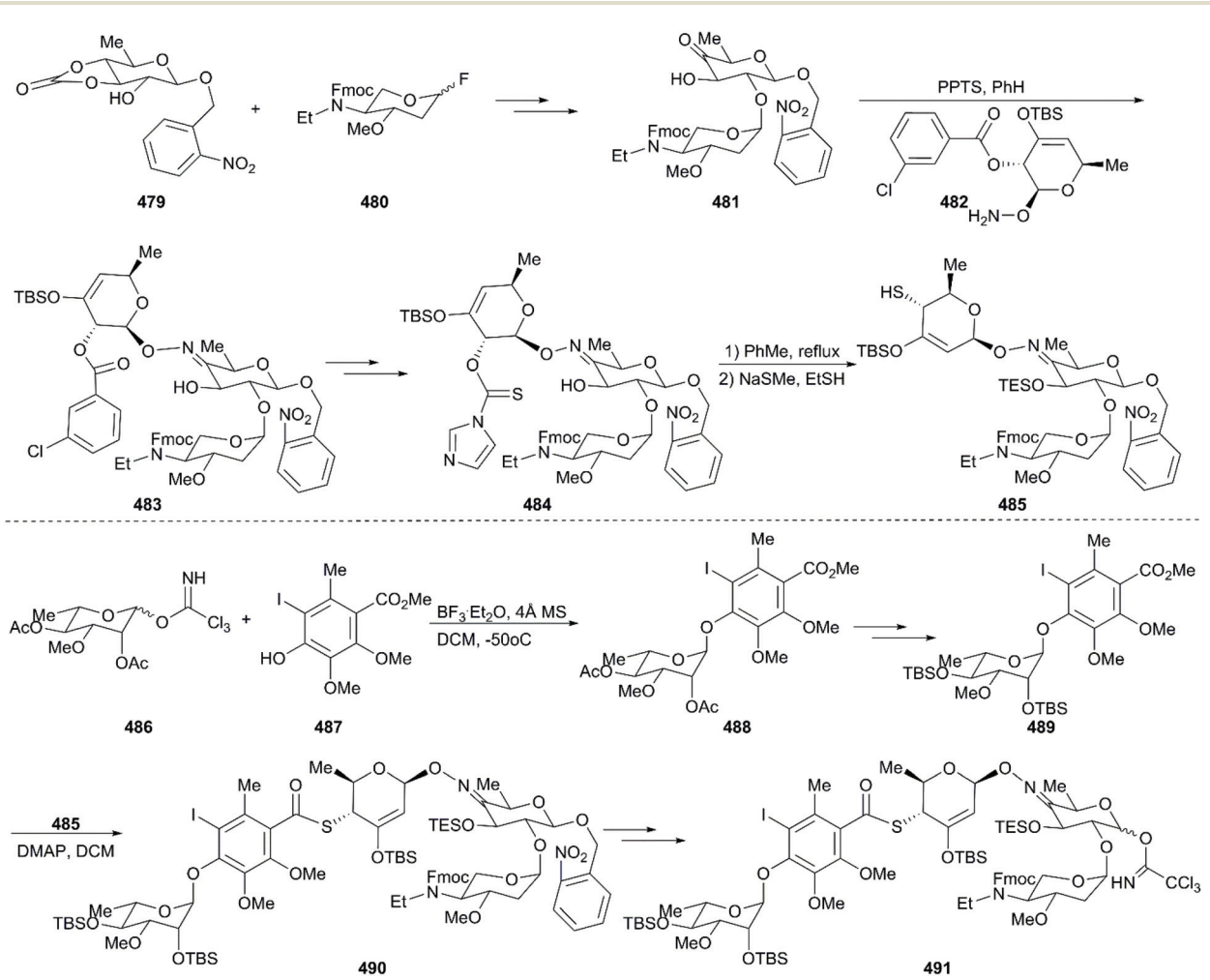

Scheme 46 Nicolaou's preparation of tetrasaccharide building block.

induce double-strand DNA breaks.[270–272] Because of its excellent activity and site-specific targeting, gemtuzumab ozogamicin (Mylotag®), a calicheamicin γ_1^I derivative, was approved by the FDA in 2000 as an antibody–drug conjugate (ADC) to treat CD-33-positive myeloid leukemia. Unfortunately, 10 years later it was withdrawn from the market because of its serious side effects. In 2017, inotuzumab ozogamicin (Besponsa®), also derived from calicheamicin γ_1^I, was approved by the FDA as an ADC medication to treat relapsed or refractory CD22-positive B-cell precursor acute lymphoblastic leukemia. All in all, the fascinating structure and highly potent drug-likeness characteristics of calicheamicin γ_1^I have spurred chemists to meet the huge challenge of developing strategies for the total synthesis of calicheamicin γ_1^I.

9.1 Total synthesis of calicheamicin γ_1^I

9.1.1 Nicolaou's total synthesis of calicheamicin γ_1^I. In 1992, Nicolaou and co-workers reported the first approach for the synthesis of calicheamicin γ_1^I using the strategy of splitting the parent molecule into two advanced intermediates, an oligosaccharide fragment and an aglycon precursor.[273–276] First, the building blocks **479** and **480** were glycosylated in the presence of $AgClO_4$ and $SnCl_2$ to produce α-disaccharide as the major product, which underwent selective deprotection followed by regioselective oxidation of C4-OH to generate hydroxy ketone **481**. The active ketone was successfully condensated with hydroxylamine **482** using PPTS as a catalyst to produce trisaccharide **483**. The introduction of thionoimidazolide instead of benzoyl generated **484**, which proceeded the [3,3]-sigmatropic rearrangement and removal of the imidazoformyl to forge trisaccharide **485** for coupling with aryl saccharide **489**. The latter was prepared by the glycosidation of saccharide unit **486** with fully substituted phenol **487** and subsequent interconversion of protecting groups. Photodeprotection of an *o*-nitrobenzyl glycoside of trisaccharide **490** generated lactol, and

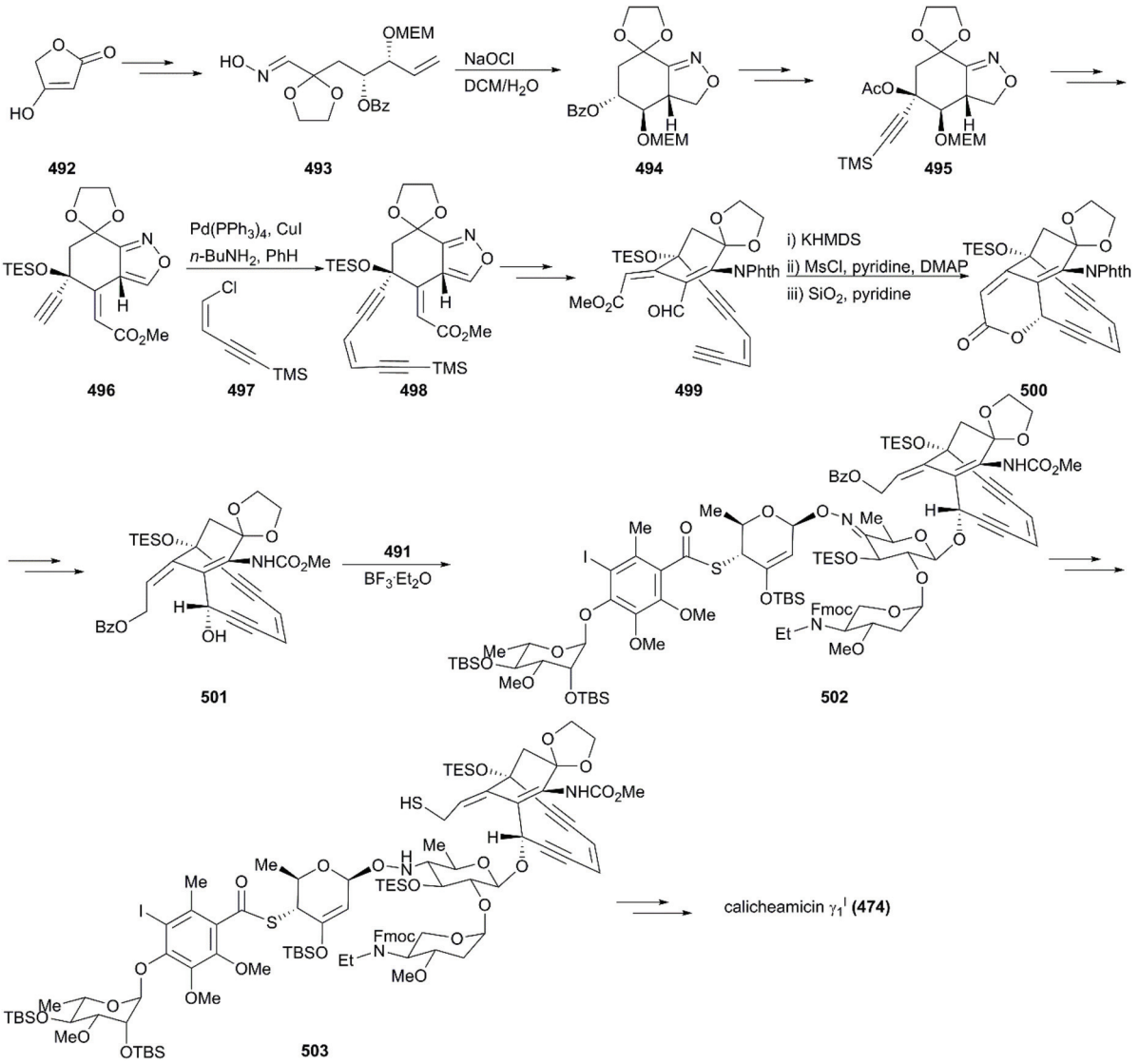

Scheme 47 Total synthesis of calicheamicin γ_1^I by Nicolaou.

Schmidt's protocol was used to generate the trichloroacetimidate **491** from **490** (Scheme 46).

The critical synthesis of aglycon portion is to construct the cyclohexenone precursor of the bicyclic enediyne scaffold using the [3 + 2] nitrile oxide cycloaddition reaction (Scheme 47). The commercially available tetronic acid **492** was used to prepare the aldoxime precursor **493**, which underwent an intramolecular 1,3-dipolar cycloaddition reaction using aqueous sodium hypochlorite solution in DCM as an oxidation system to generate isoxazoline **494**. After removal of the benzoate group and the Jones oxidation of the resultant secondary hydroxy group, the ketone intermediate was produced. Subsequent addition of lithium(trimethylsilyl)acetylide and acetylation generated intermediate **495** with high stereoselectivity. After careful removal of MEM ether, the resultant secondary alcohol was subjected to Swern oxidation, generating keto isoxazole which was treated with methyl (triphenylphosphoranylidene)acetate followed by protecting group interconversions to generate the olefination product **496** as a single geometrical isomer. This product was subsequently coupled with (*Z*)-chloroenyne using a $Pd(PPh_3)_4$-CuI catalytic system to produce the protected enediyne **498**. Cleavage of the isoxazole with molybdenum hexacarbonyl ($Mo(CO)_6$), removal of the TMS group, and phthaloylation of amine gave rise to the desired intermediate **499**. The new secondary hydroxy group produced through exposure of **499** to potassium hexamethyldisilazide in toluene was mesylated and subsequently inverted by a neighboring ester group to furnish the lactone **500** in high yield. After exchanging protecting groups and double reduction using DIBAL/$NaBH_4$, the required aglycon intermediate **501** was produced by benzoylation. With the tetrasaccharide donor **491** and aglycon **501** in hand, Schmidt glycosidation was applied to form the coupled product **502** as a single isomer. Then, the target molecule calicheamicin γ_1^I (**474**) was generated after multi-step transformations.

9.1.2 Danishefsky's total synthesis of calicheamicin γ_1^I. Three years after Nicolaou's work, Danishefsky and co-workers also finished the total synthesis of calicheamicin γ_1^I (**474**).[277–281] As shown in Scheme 48 tetrasaccharide **516** was constructed from the coupling of two disaccharide building blocks **508** and **514**. After deiodination and triflation, the first disaccharide building block **508** was prepared from disaccharide fragment **507**, which was forged by the coupling of glycal **506** and **505** in the presence of collidine-complexed iodonium perchlorate. For the second disaccharide, glycosyl donor **509** and acceptor **510** were subjected to the Schmidt procedure to build the aryl glycoside **511** with excellent yield. Subsequently, **511** was converted to acyl chloride **512**, which was then successfully coupled with

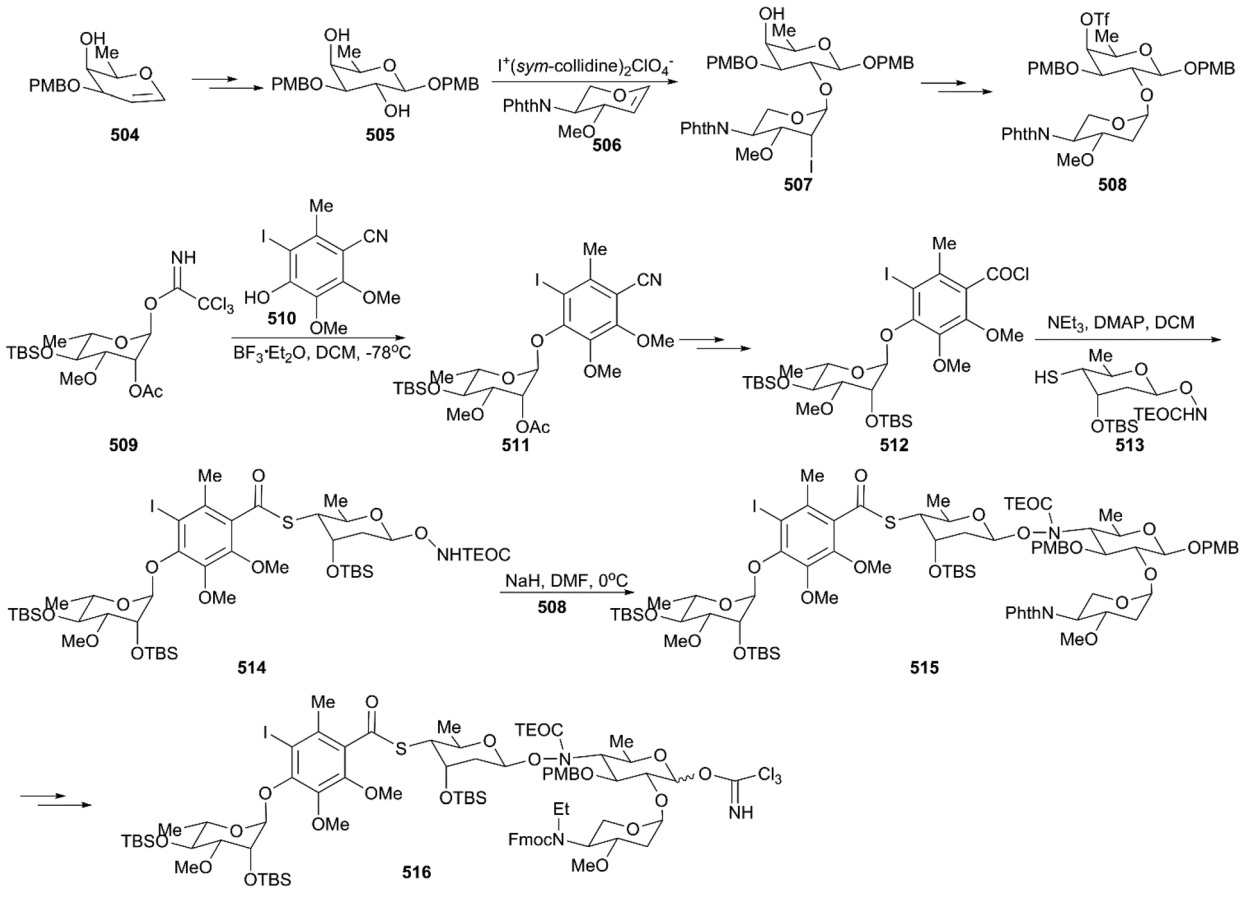

Scheme 48 Danishefsky's preparation of tetrasaccharide building block.

thiol **513** to provide disaccharide **514**. Deprotonation of the carbamate nitrogen of disaccharide **514** using NaH as the base and subsequent alkylation with triflate **508** afforded tetrasaccharide **515**, which was converted to glycosyl donor **516**.

The synthesis of the aglycon unit started with the synthesis of unstable triol **518** from the commercially available benzoate **517**; **518** was subjected to Becker oxidation to generate an epoxide and, following Dess–Martin oxidation, aldehyde **519** was obtained (Scheme 49). The aldehyde **519** was protected by treating with lithium *N*-methylanilide, and the keto group was attacked by the lithium acetylide generated from the parent enediyne to give adduct **520** after silylation of the newly formed alcohol by utilizing trimethylsilyl triflate. Then, **520** was subjected to potassium 3-ethyl-3-pentoxide, and the core skeleton **521** was obtained. Protecting group interconversions, acetolysis, and oxidative cleavage were employed to convert **521** to **522**. Exposure of **522** to a solution of sodium azide afforded the desired product, azidoenone **523**, which underwent subsequent key transformations including reduction of azide, an intramolecular Horner–Wadsworth–Emmons reaction, reduction using $NaBH_4$, and a Mitsunobu reaction, generating trisulfide **524**. Remarkably, the Schmidt protocol using silver triflate and molecular sieves was employed to couple trisulfide **524** with the tetrasaccharide donor **516** to forge **525** as a single isomer with moderate yield.

Not long after the discovery of calicheamicin γ_1^I, the structural analogs of calicheamicin, shishijimicin A (**526**)[282] and namenamicin (**527**),[283] were isolated from marine organisms (Fig. 22). Biological assays showed that they both displayed highly potent antitumor activity. Very recently, Nicolaou and co-workers finished the total synthesis of shishijimicin A (**526**)[284,285] and namenamicin (**527**)[286] using a protocol they developed previously, with some modifications. The details of

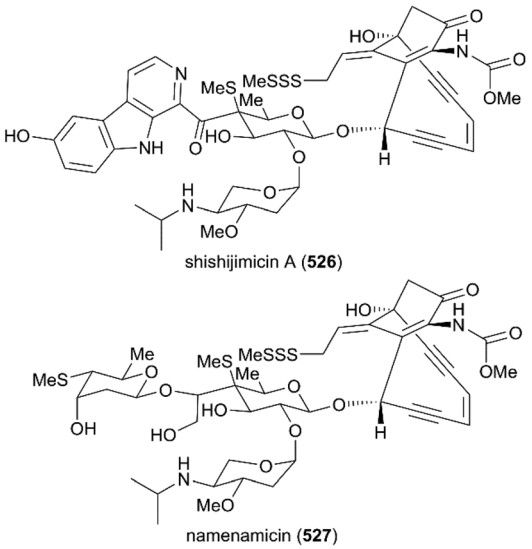

Fig. 22 The structures of shishijimicin A and namenamicin.

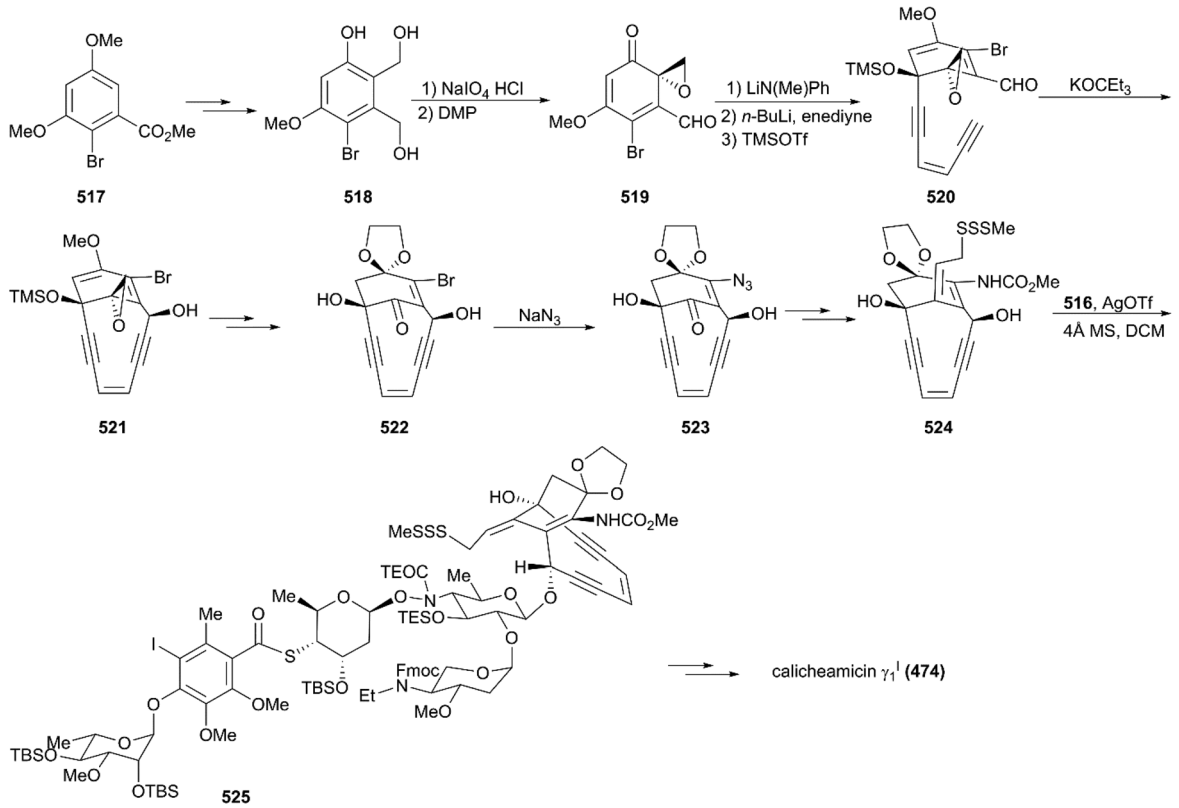

Scheme 49 Total synthesis of calicheamicin γ_1^I by Danishefsky.

these approaches are not discussed here. The derivatives and analogs of shishijimicin A were also constructed using the total synthesis strategy to explore the ADC payloads for clinical trials against tumors.[287]

9.2 Structure–activity relationships of calicheamicin γ_1^I derivatives

As mentioned above, since calicheamicin γ_1^I was discovered as a 10-membered enediyne with highly potent cytotoxicity against tumors, a number of synthetic analogs have been designed and used as ADC payloads in preclinical evaluations and clinical tests against tumors. According to the mechanism of action described, the enediyne subunit of calicheamicin γ_1^I that plays an irreplaceable role in the generation of DNA lesions through the Bergman rearrangement is unchangeable, and the allylic trisulfide serves as a trigger to induce cycloaromatization. Studies of the semisynthetic aglycon analogs revealed that the role of carbohydrate fragments is to facilitate DNA binding and confer target specificity.[270,288] To date, SAR research has mainly focused on the modification and simplification of oligosaccharide fragments or trisulfide groups.

The four calicheamicin γ_1^I analogs (Fig. 23), the natural products **471** and **472** and synthetic compounds **528** and **529**, were all conjugated to CT-M-01 and the resultant derivatives were tested for therapeutic efficacy against MX-1 xenograft tumors. The results showed that compounds **472** and **528** with

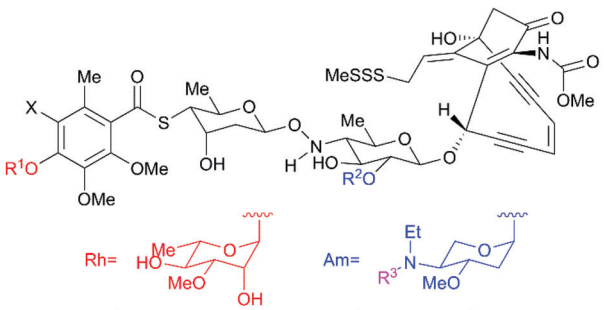

	Calicheamicin	R^1	R^2	R^3
474	γ_1^I	Rh	Am	H
471	α_2^I	H	Am	H
472	α_3^I	Rh	H	-
528	N-Ac-γ_1^I	Rh	Am	Ac
529	PSAG	H	H	-

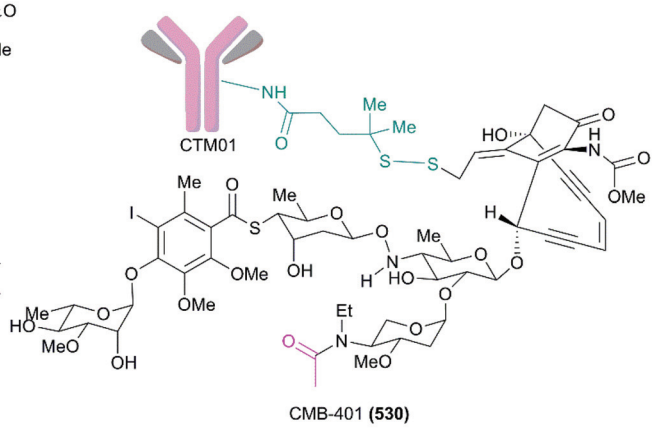

Fig. 23 Examples of calicheamicin γ_1^I derivatives(I).

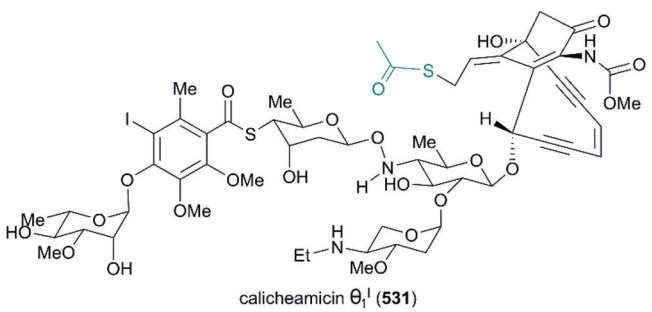

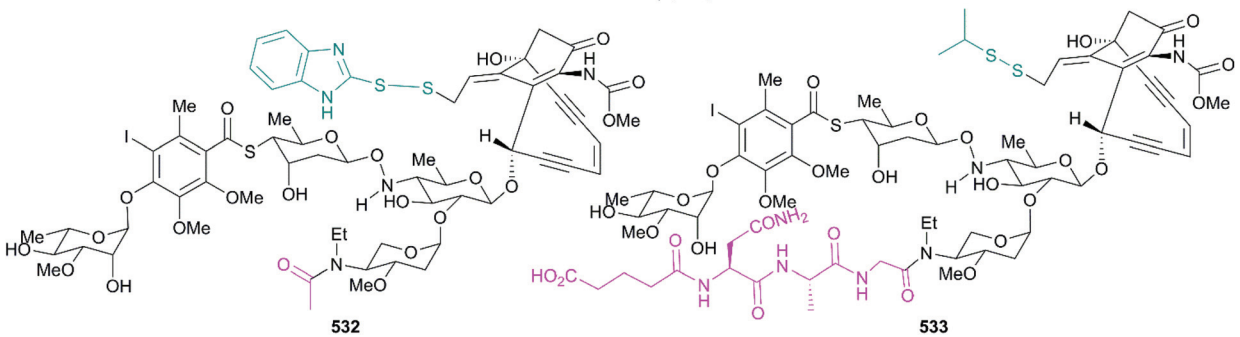

Fig. 24 Examples of calicheamicin γ_1^I derivatives(II).

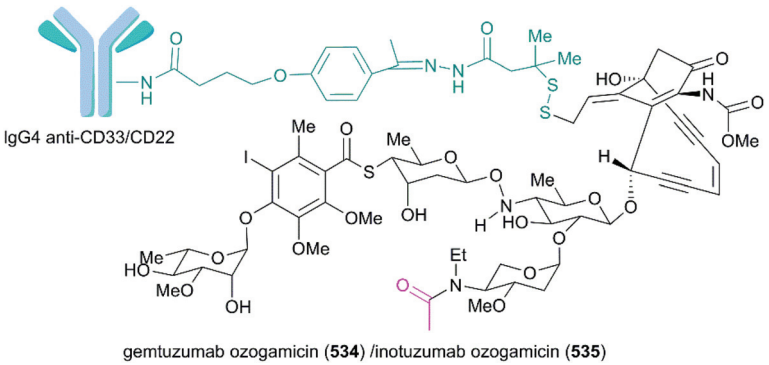

Fig. 25 Structures of the marketed ADC drugs gemtuzumab ozogamicin and inotuzumab ozogamicin.

the DNA binding unit and the lack or modifications of amino sugar fragments showed stronger therapeutic efficacy than the parent molecule **474** and the derivatives **471** and **529**, which missed the rhamnose at the DNA binding region. This result suggested that a rhamnose at the end of the binding region is required for ADC medications.[289] CMB-401 (**530**) was further developed using a more stable amide-disulfide-based linker to conjugate it with hCTMO1 based on the structure of compound **528**, and this compound was tested in phase I and phase II studies against epithelial ovarian cancer. However, no patients had objective responses in the phase II investigation. Scientists speculated that the sterically hindered disulfide failed to release the drug from the ADC payload.[288]

Calicheamicin θ_1^I (Fig. 24, **531**), a novel derivative of calicheamicin γ_1^I, was developed using thioester to replace the methyl trisulfide and prepared through total synthesis by the Nicolaou group. After the test, calicheamicin θ_1^I was hypothesized to be a powerful biological tool for generating specific DNA lesions because of its highly potent and selective DNA cleaving, apoptosis-inducing, and cytotoxic properties.[290] It was also discovered that calicheamicin θ_1^I (**531**) effectively suppressed liver metastases in a novel syngeneic model of murine neuroblastoma and CD19-positive malignancies.[291,292] In some analogs, the allylic trisulfide was replaced by isopropyl disulfide or functionalized to improve the stability and solubility (Fig. 24, **532** and **533**).[293,294] Gemtuzumab ozogamicin (Mylotag®, **534**) and inotuzumab ozogamicin (Besponsa®, **535**) are ADC drugs approved to treat myeloid leukemia and B-cell malignancies by the FDA in 2000 and 2017, respectively. Because of the important role that the linker plays in the effective release of the calicheamicin derivative from the conjugation product, allowing it to access the DNA target, a linker, 4-(4-acetylphenoxy)butanoic acid, was added to condensate drug and antibody. This conjugate showed stability in physiological buffer (pH 7.4) and the calicheamicin derivative was efficiently released inside lysosomes (pH 4.0) (Fig. 25).[295]

10. Conclusions

In this review, we discussed the total synthesis and SAR studies of eight representative families of natural products applied in the treatment of various human diseases. Although just the tip of the iceberg, these examples demonstrate the essential role of total synthesis in natural product drugs' discovery: development of efficient transformations for natural products synthesis, especially the deep-seated structural modifications that are otherwise tough to achieve; and providing adequate and sustainable supplies of natural products and their analogs for clinical studies and use. From another standpoint, total syntheses of natural products, which often contain complex structural features, also promote the development of synthetic chemistry by inspiring the discovery of new reactions and reagents for rapid molecular assembly and structural diversifications. In combination with the development of other disciplines, such as synthetic biology and chemical biology, chemical synthesis will continue to play a profound role in functional mechanism elucidation, new biological target identification, and natural product medicinal chemistry.

Abbreviations

AcOH	Acetic acid
AIBN	2,2′-Azobisisobutyronitrile
BHT	Butylated hydroxytoluene
Boc_2O	Di-*tert*-butyl dicarbonate
BOPCl	Bis(2-oxo-3-oxazolidinyl)phosphinic chloride
BPO	Benzoyl peroxide
CSA	Camphorsulfonic acid
DABCO	1,4-Diazabicyclo[2.2.2]octane
DBU	1,8-Diazabicyclo[5.4.0]undec-7-ene
DCM	Dichloromethane
DEAD	Diethyl azodicarboxylate
1,2-DFB	1,2-Difluorobenzene
DIPAMP	(Ethane-1,2-diyl)bis[(2-methoxyphenyl)(phenyl)phosphine]
DIPEA	*N*,*N*-Diisopropylethylamine
DMAP	4-(*N*,*N*-Dimethylamino)pyridine
DMDO	Dimethyldioxirane
DME	1,2-Dimethoxyethane
DMF	*N*,*N*-Dimethylformamide
DMSO	Dimethyl sulfoxide

Dppp	1,3-Bis(diphenylphosphino)propane
DTBMP	2,6-Di-*tert*-butyl-4-methylpyridine
EDCI	*N*-(3-Dimethylaminopropyl)-*N*′-ethylcarbodiimide hydrochloride
HFIP	Hexafluoroisopropanol
HMPA	Hexamethylphosphoramide
IBX	2-Iodoxybenzoic acid
KHMDS	Potassium bis(trimethylsilyl)amide
LDA	Lithium diisopropylamide
LICA	Lithium *N*-isopropylcyclohexylamide
LiDBB	Lithium di-*tert*-butylbiphenyl
LiHMDS	Lithium bis(trimethylsilyl)amide
LTMP	Lithium tetramethylpiperidide
m-CPBA	*meta*-Chloroperoxybenzoic acid
MesLi	Mesityllithium
MS	Molecular sieve
MsCl	Methanesulfonyl chloride
NaHMDS	Sodium bis(trimethylsilyl)amide
NBS	*N*-Bromosuccinimide
NMO	4-Methylmorpholine *N*-oxide
NTf_2	Bis(trifluoromethylsulfonyl)imide
$Pd_2(dba)_2$	Bis(dibenzylideneacetone)palladium
$PhNTf_2$	Bis(trifluoromethanesulfonyl)aniline
PMP	1,2,2,6,6-Pentamethylpiperidine
PPTS	Pyridinium *p*-toluenesulfonate
Red-Al	Sodium bis(2-methoxyethoxy)aluminiumhydride
$[Rh(COD)Cl]_2$	Chloro(1,5-cyclooctadiene)rhodium(I) dimer
Rt	Room temperature
SARs	Structure–activity relationships
TBAF	*tert*-Butylammonium fluoride
TBAI	*tert*-Butylammonium iodide
TBSOTf	*tert*-Butyldimethylsilyl trifluoromethanesulfonate
TESOH	Triethylsilanol
Tf_2O	Trifluoromethanesulfonic anhydride
TFA	Trifluoroacetic acid
TFAA	Trifluoroacetic anhydride
TFE	2,2,2-Trifluoroethanol
TfOH	Trifluoromethanesulfonic acid
THF	Tetrahydrofuran
TMEDA	Tetramethylethylenediamine
TMSCl	Chlorotrimethylsilane
TMSCN	Trimethylsilyl cyanide
TMSH	Trimethylsulfonium hydroxide
TMSimid	1-(Trimethylsilyl)imidazole
TMSOH	Trimethylsilanol
TPAP	Tetrapropylammonium perruthenate
TPP	Triphenylphosphine
TsOH	*p*-Toluenesulfonic acid

Author contributions

X. Q. conceived the study; G. L., M. L. and X. Q. prepared the manuscript; all authors discussed the contents and commented on the manuscript.

Conflicts of interest

The authors declare no conflict of interests.

Acknowledgements

This work was supported by the National Natural Science Foundation of China (NSFC) (Grant No. 21971018). We gratefully acknowledge the Beijing Municipal Government and Tsinghua University for financial support.

References

1 G. M. Cragg and D. J. Newman, Natural products: a continuing source of novel drug leads, *Biochim. Biophys. Acta, Gen. Subj.*, 2013, **1830**, 3670–3695.
2 N. R. Farnsworth, O. Akerele, A. S. Bingel, D. D. Soejarto and Z. Guo, Medicinal plants in therapy, *Bull. W. H. O.*, 1985, **63**, 965–981.
3 D. T. Courtwright, *Forces of habit: drugs and the making of the modern world*, Harvard University Press, 2002, P36.
4 V. Cechinel-Filho, *Plant Bioactives and drug discovery John Wiley & Sons*, Hoboken, New Jersey, 2011.
5 G. M. Cragg, D. J. Newman and K. M. Snader, Natural products in drug discovery and development, *J. Nat. Prod.*, 1997, **60**, 52–60.
6 K. S. Lam, New aspects of natural products in drug discovery, *Trends Microbiol.*, 2007, **15**, 279–289.
7 B. L. DeCorte, Underexplored opportunities for natural products in drug discovery, *J. Med. Chem.*, 2016, **59**, 9295–9304.
8 Z.-C. Wu and D. L. Boger, The quest for supernatural products: the impact of total synthesis in complex natural products medicinal chemistry, *Nat. Prod. Rep.*, 2020, **37**, 1511–1531.
9 A. G. Atanasov, S. B. Zotchev, V. M. Dirsch, the International Natural Product Sciences Taskforce and C. T. Supuran, Natural products in drug discovery: advances and opportunities, *Nat. Rev. Drug Discovery*, 2021, **20**, 200–216.
10 M.-J. U. Ferreira, Natural products in drug discovery and human health, *Phytochem. Rev.*, 2021, **20**, 1–4.
11 C. A. Dehelean, I. Marcovici, C. Soica, M. Mioc, D. Coricovac, S. Iurciuc, O. M. Cretu and I. Pinzaru, Plant-derived anticancer compounds as new perspectives in drug discovery and alternative therapy, *Molecules*, 2021, **26**, 1109–1138.
12 A. Nelson and G. Karageorgis, Natural product-informed exploration of chemical space to enable bioactive molecular discovery, *RSC Med. Chem.*, 2021, **12**, 353–362.
13 J. Skubnik, V. Pavlickova, T. Ruml and S. Rimpelova, Current Perspectives on Taxanes: Focus on Their Bioactivity, Delivery and Combination Therapy, *Plants*, 2021, **10**, 569–603.

14 C. Hobson, A. N. Chan and G. D. Wright, The antibiotic resistome: a guide for the discovery of natural products as antimicrobial agents, *Chem. Rev.*, 2021, **121**, 3464–3494.
15 P. Fernandes and E. Martens, Antibiotics in late clinical development, *Biochem. Pharmacol.*, 2017, **133**, 152–163.
16 R. I. Aminov, A brief history of the antibiotic era: lessons learned and challenges for the future, *Front. Microbiol.*, 2010, **1**, 1–7.
17 G. M. Cragg, P. G. Grothaus and D. J. Newman, Impact of natural products on developing new anti-cancer agents, *Chem. Rev.*, 2009, **109**, 3012–3043.
18 P. Kittakoop, *Anticancer drugs and potential anticancer leads inspired by natural products*, Elsevier B.V., 2015.
19 A. Mazumder, C. Cerell and M. Diederich, Natural scaffolds in anticancer therapy and precision medicine, *Biotechnol. Adv.*, 2018, **36**, 1563–1585.
20 M. Huang, J.-J. Lu and J. Ding, Natural Products in Cancer Therapy: Past, Present and Future, *Nat. Prod. Bioprospect.*, 2021, **11**, 5–13.
21 A. J. Goodman, B. L. Bourdonnec and R. E. Dolle, Mu opioid receptor antagonists: recent developments, *ChemMedChem*, 2007, **2**, 1552–1570.
22 H. Buschmann, T. Christoph, E. Friderichs, C. Maul and B. Sundermann, *Analgesics-from chemistry and pharmacology to clinical application*, Wiley-VCH, Weinheim, Germany, 2002.
23 L. H. Miller and X. Su, Artemisinin: discovery from the Chinese herbal garden, *Cell*, 2011, **146**, 855–858.
24 N. S. Tibon, C. H. Ng and S. L. Cheong, Current progress in antimalarial pharmacotherapy and multi-target drug discovery, *Eur. J. Med. Chem.*, 2020, **188**, 111983–112007.
25 H. Madhav and N. Hoda, An insight into the recent development of the clinical candidates for the treatment of malaria and their target proteins, *Eur. J. Med. Chem.*, 2021, **210**, 112955–112995.
26 D. J. Newman, G. M. Cragg and K. M. Snader, Natural products as sources of new drugs over the period 1981–2002, *J. Nat. Prod.*, 2003, **66**, 1022–1037.
27 D. J. Newman and G. M. Cragg, Natural products as sources of new drugs over the last 25 Years, *J. Nat. Prod.*, 2007, **70**, 461–477.
28 D. J. Newman and G. M. Cragg, Natural products as sources of new drugs from 1981 to 2014, *J. Nat. Prod.*, 2016, **79**, 629–661.
29 D. J. Newman and G. M. Cragg, Natural products as sources of new drugs over the nearly four decades from 01/1981 to 09/2019, *J. Nat. Prod.*, 2020, **83**, 770–803.
30 F. W. Serturner, Darstellung der reinen Mohnsäure (Opiumsaure) nebst einer Chemischen Untersuchung des Opiums mit vorzüglicher Hinsicht auf einen darin neuentdeckten Stoff und die dahin gehörigen Bemerkungen, *J. Pharm.*, 1806, **14**, 47–93.
31 B. H. Novak, T. Hudlicky, J. W. Reed, J. Mulzer and D. Trauner, Morphine synthesis and biosynthesis—an update, *Curr. Org. Chem.*, 2000, **4**, 343–362.
32 P. R. Blakemorea and J. D. White, Morphine, the proteus of organic molecules, *Chem. Commun.*, 2002, 1159–1168.
33 J. Zezula and T. Hudlicky, Recent progress in the synthesis of morphine alkaloids, *Synlett*, 2005, 388–405.
34 U. Rinner and T. Hudlicky, in *Alkaloid synthesis*, ed. H.-J. Knolker, Springer Science & Business Media, 2012, vol. 309, pp. 33–66.
35 A. S. Yekkirala, A. E. Kalyuzhny and P. S. Portoghese, Standard opioid agonists activate heteromeric opioid receptors: evidence for morphine and [d-Ala(2)-MePhe(4)-Glyol(5)]enkephalin as selective μ-δ agonists, *ACS Chem. Neurosci.*, 2010, **1**, 146–154.
36 A. S. Yekkirala, M. L. Banks, M. M. Lunzer, S. S. Negus, K. C. Rice and P. S. Portoghese, Clinically employed opioid analgesics produce antinociception via μ-δ opioid receptor heteromers in Rhesus monkeys, *ACS Chem. Neurosci.*, 2012, **3**, 720–727.
37 J. W. Reed and T. Hudlicky, The quest for a practical synthesis of morphine alkaloids and their derivatives by chemoenzymatic methods, *Acc. Chem. Res.*, 2015, **48**, 674–687.
38 T. M. Kutchan, in *The alkaloids: chemistry and biology*, ed. G. A. Cordell, Academic Press, London, 1998, vol. 50, pp. 257–316.
39 S. Galanie, K. Thodey, I. J. Trenchard, M. F. Interrante and C. D. Smolke, Complete biosynthesis of opioids in yeast, *Science*, 2015, **349**, 6252–6257.
40 J. M. Gulland and R. Robinson, *Mem. Proc. – Manchester Lit. Philos. Soc.*, 1925, **69**, 79.
41 M. Gates and G. Tschudi, The synthesis of morphine, *J. Am. Chem. Soc.*, 1952, **74**, 1109–1110.
42 M. Gates and G. Tschudi, The synthesis of morphine, *J. Am. Chem. Soc.*, 1956, **78**, 1380–1393.
43 M. F. Mackay and D. C. Hodgki, A crystallographic examination of the structure of morphine, *J. Chem. Soc.*, 1955, 3261–3267.
44 Q. Li and H. Zhang, Research progress on the synthesis of morphine alkaloids, *Chin. J. Org. Chem.*, 2017, **37**, 1629–1652.
45 S. A. Chambers, J. M. DeSousa, E. D. Huseman and S. D. Townsend, The DARK side of total synthesis: strategies and tactics in psychoactive drug production, *ACS Chem. Neurosci.*, 2018, **9**, 2307–2330.
46 C. Y. Hong, N. Kado and L. E. Overman, Asymmetric synthesis of either enantiomer of opium alkaloids and morphinans. Total synthesis of (−)- and (+)-dihydrocodeinone and (−)- and (+)-morphine, *J. Am. Chem. Soc.*, 1993, **115**, 11028–11029.
47 I. Iijima and K. C. Rice, Studies in the (+)-morphinan series I. An alternative conversion of (+)-dihydrocodeinone into (+)-codeine, *Heterocycles*, 1977, **6**, 1157–1165.
48 J. D. White, P. Hrnciar and F. Stappenbeck, Asymmetric synthesis of (+)-morphine. The phenanthrene route revisited, *J. Org. Chem.*, 1997, **62**, 5250–5251.
49 B. M. Trost and W. Tang, An efficient enantioselective synthesis of (-)-galanthamine, *Angew. Chem., Int. Ed.*, 2002, **41**, 2795–2797.
50 B. M. Trost and W. Tang, Enantioselective synthesis of (-)-codeine and (-)-morphine, *J. Am. Chem. Soc.*, 2002, **124**, 14542–14543.

51 B. M. Trost, W. Tang and F. D. Toste, Divergent enantioselective synthesis of (-)-galanthamine and (-)-morphine, *J. Am. Chem. Soc.*, 2005, **127**, 14785–14803.
52 H. Leisch, A. T. Omori, K. J. Finn, J. Gilmet, T. Bissett, D. Ilceski and T. Hudlicky, Chemoenzymatic enantiodivergent total syntheses of (+)- and (-)-codeine, *Tetrahedron*, 2009, **65**, 9862–9875.
53 M. Makarova, M. A. A. Endoma-Arias, H. E. D. Paz, R. Simionescu and T. Hudlicky, Chemoenzymatic total synthesis of ent-oxycodone: second-, third-, and fourth-generation strategies, *J. Am. Chem. Soc.*, 2019, **141**, 10883–10904.
54 Q. Zhang, F.-M. Zhang, C.-S. Zhang, S.-Z. Liu, J.-M. Tian, S.-H. Wang, X.-M. Zhang and Y.-Q. Tu, Enantioselective synthesis of cis-hydrobenzofurans bearing all-carbon quaternary stereocenters and application to total synthesis of (-)-morphine, *Nat. Commun.*, 2019, **10**, 2507–2513.
55 Y. S.-H. Hou, A. Prichina and G. Dong, Deconstructive asymmetric total synthesis of morphine-family alkaloid (-)-thebainone A, *Angew. Chem., Int. Ed.*, 2021, **60**, 13057–13064.
56 D. A. Williams, V. F. Roche and E. B. Roche, in *Foye's principles of medicinal chemistry*, ed. T. L. Lemke, D. A. Williams, V. F. Roche and S. W. Zito, Lippincott Williams & Wilkins, China, 7 edn, 2012, ch. 20, pp. 675–695.
57 K. Raynor, H. Kong, Y. Chen, K. Yasuda, L. Yu, G. I. Bell and T. Reisine, Pharmacological characterization of the cloned kappa-, delta-, and mu-opioid receptors, *Mol. Pharmacol.*, 1994, **45**, 330–334.
58 I. D. Pogozheva, A. L. Lomize and H. I. Mosberg, Opioid receptor three-dimensional structures from distance geometry calculations with hydrogen bonding constraints, *Biophys. J.*, 1998, **75**, 612–632.
59 H. E. Hassan, S. L. Mercer, C. W. Cunningham, A. Coop and N. D. Eddington, Evaluation of the P-glycoprotein (Abcb1) affinity status of a series of morphine analogs: Comparative study with meperidine analogs to identify opioids with minimal P-glycoprotein interactions, *Int. J. Pharm.*, 2009, **375**, 48–54.
60 T. H. Jukes, Some historical notes on chlortetracycline, *Rev. Infect. Dis.*, 1985, **7**(5), 702–707.
61 A. C. Finlay, G. L. Hobby, S. Y. P'an, P. P. Regna, J. B. Routien, D. B. Seeley, G. M. Shull, B. A. Sobin, I. A. Solomons, J. W. Vinson and J. H. Kane, Terramycin, a new antibiotic, *Science*, 1950, **111**, 85–87.
62 M. A. Darken, H. Berenson, R. J. Shirk and N. O. Sjolander, Production of tetracycline by Streptomyces aureofaciens in synthetic media, *Appl. Microbiol.*, 1960, **8**, 46–51.
63 J. R. D. McCormick, N. O. Sjolander, U. Hirsch, E. R. Jensen and A. P. Doerschuk, A new family of antibiotics: the demethyltetracyclines, *J. Am. Chem. Soc.*, 1957, **79**, 4561–4563.
64 I. Chopra and M. Roberts, Tetracycline antibiotics: mode of action, applications, molecular biology, and epidemiology of bacterial resistance, *Microbiol. Mol. Biol. Rev.*, 2001, **65**, 232–260.
65 D. E. Brodersen, J. William, M. Clemons, A. P. Carter, R. J. Morgan-Warren, B. T. Wimberly and V. Ramakrishnan, The structural basis for the action of the antibiotics tetracycline, pactamycin, and hygromycin B on the 30S ribosomal subunit, *Cell*, 2000, **103**, 1143–1154.
66 M. C. Roberts, Tetracycline resistance determinants: mechanisms of action, regulation of expression, genetic mobility, and distribution, *FEMS Microbiol. Rev.*, 1996, **19**, 1–24.
67 S. R. Connell, D. M. Tracz, K. H. Nierhaus and D. E. Taylor, Ribosomal protection proteins and their mechanism of tetracycline resistance, *Antimicrob. Agents Chemother.*, 2003, **47**, 3675–3681.
68 T. H. Grossman, Tetracycline antibiotics and resistance, *Cold Spring Harbor Perspect. Med.*, 2016, **6**, a025387–a025387.
69 C. R. Stephens, L. H. Conover, F. A. Hochstein, P. P. Regna, F. J. Pilgrim, K. J. Brunings and R. B. Woodward, Terramycin. VIII. Structure of aureomycin and terramycin, *J. Am. Chem. Soc.*, 1952, **74**, 4976–4977.
70 F. A. Hochstein, C. R. Stephens, L. H. Conover, P. P. Regna, R. Pasternack, P. N. Gordon, F. J. Pilgrim, K. J. Brunings and R. B. Woodward, The structure of terramycin, *J. Am. Chem. Soc.*, 1953, **75**, 5455–5475.
71 C. R. Stephens, L. H. Conover, R. Pasternack, F. A. Hochstein, W. T. Moreland, P. P. Regna, F. J. Pilgrim, K. J. Brunings and R. B. Woodward, Structure of aureomycin, *J. Am. Chem. Soc.*, 1954, **76**, 3568–3575.
72 D. L. J. Clive, Chemistry of the tetracyclines, *Q. Rev., Chem. Soc.*, 1968, **22**, 435–456.
73 T. K. Allred, F. Manoni and P. G. Harran, Exploring the boundaries of "practical": De novo syntheses of complex natural product-based drug candidates, *Chem. Rev.*, 2017, **117**, 11994–12051.
74 L. H. Conover, K. Butler, R. B. Johnston, R. B. Korst and R. B. Woodward, The total synthesis of 6-demethyl-6 deoxytetracycline, *J. Am. Chem. Soc.*, 1962, **84**, 3222–3224.
75 R. B. Woodward, The total synthesis of a tetracycline, *Pure Appl. Chem.*, 1963, **6**, 561–573.
76 J. J. Korst, J. D. Johnston, K. Butler, E. J. Bianco, L. H. Conover and R. B. Woodward, The total synthesis of dl-6-demethyl-6-deoxytetracycline, *J. Am. Chem. Soc.*, 1968, **90**, 439–457.
77 A. I. Gurevich, M. G. Karapetyan, M. N. Kolosov, V. G. Korobko, V. V. Onoprienko, S. A. Popravko and M. M. Shemyakin, Synthesis of 12a-deoxy-5a,6-anhydrotetracycline. The first total synthesis of the naturally occuring tetracycline, *Tetrahedron Lett.*, 1967, **8**, 131–134.
78 M. S. V. Wittenau, Preparation of tetracyclines by photooxidation of anhydrotetracyclines, *J. Org. Chem.*, 1964, **29**, 2746–2748.
79 H. Muxfeldt and W. Rogalski, Tetracyclines. V. A total synthesis of (±)-6-deoxy-6-demethyltetracycline, *J. Am. Chem. Soc.*, 1965, **87**, 933–934.

80 H. Muxfeldt, G. Haas, G. Hardtmann, F. Kathawala, J. B. Mooberry and E. Vedejs, Tetracyclines. 9. Total synthesis of dl-terramycin, *J. Am. Chem. Soc.*, 1979, **101**, 689–701.
81 G. Stork, J. J. L. Clair, P. Spargo, R. P. Nargund and N. Totah, Stereocontrolled synthesis of (±)-12a -deoxytetracycline, *J. Am. Chem. Soc.*, 1996, **118**, 5304–5305.
82 K. Tatsuta, T. Yoshimoto, H. Gunji, Y. Okado and M. Takahashi, The first total synthesis of natural (−)-tetracycline, *Chem. Lett.*, 2000, **29**, 646–647.
83 M. G. Charest, C. D. Lerner, J. D. Brubaker, D. R. Siegel and A. G. Myers, A convergent enantioselective route to structurally diverse 6-deoxytetracycline antibiotics, *Science*, 2005, **308**, 395–398.
84 M. G. Charest, D. R. Siegel and A. G. Myers, Synthesis of (--)-tetracycline, *J. Am. Chem. Soc.*, 2005, **127**, 8292–8293.
85 J. D. Brubaker and A. G. Myers, A practical, enantioselective synthetic route to a key precursor to the tetracycline antibiotics, *Org. Lett.*, 2007, **9**, 3523–3525.
86 C. Sun, Q. Wang, J. D. Brubaker, P. M. Wright, C. D. Lerner, K. Noson, M. Charest, D. R. Siegel, Y.-M. Wang and A. G. Myers, A robust platform for the synthesis of new tetracycline antibiotics, *J. Am. Chem. Soc.*, 2008, **130**, 17913–17927.
87 D. A. Kummer, D. Li, A. Dion and A. G. Myers, A practical, convergent route to the key precursor to the tetracycline antibiotics, *Chem. Sci.*, 2011, **2**, 1710–1718.
88 M. Ronn, Z. Zhu, P. C. Hogan, W.-Y. Zhang, J. Niu, C. E. Katz, N. Dunwoody, O. Gilicky, Y. Deng, D. K. Hunt, M. He, C.-L. Chen, C. Sun, R. B. Clark and X.-Y. Xiao, Process R&D of eravacycline: The first fully synthetic fluorocycline in clinical development, *Org. Process Res. Dev.*, 2013, **17**, 838–845.
89 A. Mullard, 2018 FDA drug approvals, *Nat. Rev. Drug Discovery*, 2019, **18**, 85–89.
90 W. Y. Zhang, C. Sun, D. Hunt, M. He, Y. Deng, Z. Zhu, C. L. Chen, C. E. Katz, J. Niu, P. C. Hogan, X. Y. Xiao, N. Dunwoody and M. Ronn, Process development and scale-up of fully synthetic tetracycline TP-2758: a potent antibacterial agent with excellent oral bioavailability, *Org. Process Res. Dev.*, 2016, **20**, 284–296.
91 G. G. Zhanel, K. Homenuik, K. Nichol, A. Noreddin, L. Vercaigne, J. Embil, A. Gin, J. A. Karlowsky and D. J. Hoban, The glycylcyclines, *Drugs*, 2004, **64**, 63–88.
92 A. R. Martin, in *Wilson and Gisvold's textbook of organic medicinal and pharmaceutical chemistry*, ed. J. N. Delgado and W. A. Remers, Lippincott-Raven Publishers, Philadelphia, 10th edn, 1998, pp. 210–215.
93 K. F. Benitz and H. F. Diermeier, Renal toxicity of tetracycline degradation products, *Exp. Biol. Med.*, 1964, **115**, 930–935.
94 M. J. Martell and J. H. Boothe, 6-deoxytetracyclines. VII. Alkylated aminotetracyclines possessing unique antibacterial activity, *J. Med. Chem.*, 1967, **10**, 44–46.
95 A. E. Yñigez-Gutierrez and B. O. Bachmann, Fixing the unfixable: the art of optimizing natural products for human medicine, *J. Med. Chem.*, 2019, **62**, 8412–8428.
96 P. E. Sum and P. Petersen, Synthesis and structure-activity relationship of novel glycylcycline derivatives leading to the discovery of GAR-936, *Bioorg. Med. Chem. Lett.*, 1999, **9**, 1459–1462.
97 P. J. Petersen, N. V. Jacobus, W. J. Weiss, P. E. Sum and R. T. Testa, In vitro and in vivo antibacterial activities of a novel glycylcycline, the 9-t-butylglycylamido derivative of minocycline (GAR-936), *Antimicrob. Agents Chemother.*, 1999, **43**, 738–744.
98 L. Honeyman, M. Ismail, M. L. Nelson, B. Bhatia, T. E. Bowser, J. Chen, R. Mechiche, K. Ohemeng, A. K. Verma, E. P. Cannon, A. Macone, S. K. Tanaka and S. Levy, Structure-activity relationship of the aminomethylcyclines and the discovery of omadacycline, *Antimicrob. Agents Chemother.*, 2015, **59**, 7044–7053.
99 R. B. Clark, D. K. Hunt, M. He, C. Achorn, C.-L. Chen, Y. Deng, C. Fyfe, T. H. Grossman, P. C. Hogan, W. J. O'Brien, L. Plamondon, M. Rönn, J. A. Sutcliffe, Z. Zhu and X.-Y. Xiao, Fluorocyclines. 2. Optimization of the C-9 side-chain for antibacterial activity and oral efficacy, *J. Med. Chem.*, 2012, **55**, 606–622.
100 P. F. Wiley, K. Gerzon, E. H. Flynn, M. V. S. Jr., O. Weaver, U. C. Quarck, R. R. Chauvette and R. Monahan, Erythromycin. X.1 Structure of erythromycin, *J. Am. Chem. Soc.*, 1957, **79**, 6062–6070.
101 R. Place, F. O. R. The, C. Growikg, T. H. Office and H. Office, Erythromycin: another antibiotic, *Lancet*, 1952, **260**, 232–233.
102 D. R. Harris, S. G. McGeachin and H. H. Mills, The structure and stereochemistry of erythromycin A, *Tetrahedron Lett.*, 1965, **6**, 679–685.
103 A. Contreras and D. Vazquez, Cooperative and antagonistic interactions of peptidyl-tRNA and antibiotics with bacterial ribosomes, *Eur. J. Biochem.*, 1977, **74**, 539–547.
104 J. A. Dunkle, L. Xiong, A. S. Mankin and J. H. D. Cate, Structures of the Escherichia coli ribosome with antibiotics bound near the peptidyl transferase center explain spectra of drug action, *Proc. Natl. Acad. Sci. U. S. A.*, 2010, **107**, 17152–17157.
105 J. Sutcliffe, A. Tait-Kamradt and L. W. Ondarck, Streptococcus pneumoniae and Streptococcus pyogenes resistantto macrolides but sensitive to clindamycin: a common resistance pattern mediated by an efflux system, *Antimicrob. Agents Chemother.*, 1996, **40**, 1817–1824.
106 D. Felminghama, R. Cantónb and S. G. Jenkins, Regional trends in β-lactam, macrolide, fluoroquinolone and telithromycin resistance among Streptococcus pneumoniae isolates 2001–2004, *J. Infect.*, 2007, **55**, 111–118.
107 A. Canu, B. Malbruny, M. L. Coquemont, T. A. Davies, P. C. Appelbaum and R. Leclercq, Diversity of ribosomal mutations conferring resistance to macrolides, clindamycin, streptogramin, and telithromycin in streptococcus pneumoniae, *Antimicrob. Agents Chemother.*, 2002, **46**, 125–131.
108 S. Pestka, R. Vince, R. LeMahieu, F. Weiss, L. Fern and J. Unowsky, Induction of erythromycin resistance in sta-

phylococcus aureus by erythromycin derivatives, *Antimicrob. Agents Chemother.*, 1976, **9**, 128–130.
109 N. E. Allen, Macrolide resistance in staphylococcus aureus: induction of macrolide-resistant protein synthesis, *Antimicrob. Agents Chemother.*, 1977, **11**, 661–668.
110 H. Ounissi and P. Courvalin, Nucleotide sequence of the gene ereA encoding the erythromycin esterase in Escherichia coli, *Gene*, 1985, **35**, 271–278.
111 M. Arthur, D. Autissier and P. Courvalin, Analysis of the nucleotide sequence of the ereB gene encoding the erythromydn esterase type II, *Nucleic Acids Res.*, 1986, **14**, 4987–4999.
112 P. Kurath, P. H. Jones, R. S. Egan and T. J. Perun, Acid degradation of erythromycin A and erythromycin B, *Experientia*, 1971, **27**, 362.
113 R. B. Woodward, E. Logusch, K. P. Nambiar, K. Sakan, D. E. Ward, B. W. Au-Yeung, P. Balaram, L. J. Browne, P. J. Card and C. H. Chen, Asymmetric total synthesis of erythromcin. 1. Synthesis of an erythronolide A secoacid derivative via asymmetric induction, *J. Am. Chem. Soc.*, 1981, **103**, 3210–3213.
114 R. B. Woodward, B. W. Au-Yeung, P. Balaram, L. J. Browne, D. E. Ward, B. W. Au-Yeung, P. Balaram, L. J. Browne, P. J. Card and C. H. Chen, Asymmetric total synthesis of erythromycin. 2. Synthesis of an erythronolide A lactone system, *J. Am. Chem. Soc.*, 1981, **103**, 3213–3215.
115 R. B. Woodward, E. Logusch, K. P. Nambiar, K. Sakan, D. E. Ward, B. W. Au-Yeung, P. Balaram, L. J. Browne, P. J. Card and C. H. Chen, Asymmetric total synthesis of erythromycin. 3. Total synthesis of erythromycin, *J. Am. Chem. Soc.*, 1981, **103**, 3215–3217.
116 P. Breton, P. J. Hergenrother, T. Hida, A. Hodgson, A. S. Judd, E. Kraynack, P. R. Kym, W. C. Lee, M. S. Loft, M. Yamashita and S. F. Martin, Total synthesis of erythromycin B, *Tetrahedron*, 2007, **63**, 5709–5729.
117 H. C. Kim and S. H. Kang, Total synthesis of azithromycin, *Angew. Chem., Int. Ed.*, 2009, **48**, 1827–1829.
118 S. Morimoto, Y. Takahashi, Y. Watanabe and S. Ōmura, Chemical modification of eryhromycins, *J. Antibiot.*, 1984, **37**, 187–189.
119 S. Djokić, G. Kobrehel, G. Lazarevski, N. Lopotar, Z. Tamburašev, B. Kamenar, A. Nagl and I. Vicković, Erythromycin series. Part 11. Ring expansion of erythromycin A oxime by the Beckmann rearrangement, *J. Chem. Soc., Perkin Trans. 1*, 1986, 1881–1890.
120 J. W. McFarland, C. M. Berger, S. A. Froshauer, S. F. Hayashi, S. J. Hecker, B. H. Jaynes, M. R. Jefson, B. J. Kamicker, C. A. Lipinski, K. M. Lundy, C. P. Reese and C. B. Vu, Quantitative structure–activity relationships among macrolide antibacterial agents: in vitro and in vivo potency against pasteurella multocida, *J. Med. Chem.*, 1997, **40**, 1340–1346.
121 W. R. Baker, J. D. Clark, R. L. Stephens and K. H. Kim, Modification of macrolide antibiotics. Synthesis of 11-deoxy-11-(carboxyamino)-6-O-methy¡erythromycin A ll,12-(Cyclic esters) via an intramolecular Michael reaction of O-carbamates with an,/9-unsaturated ketone, *J. Org. Chem.*, 1988, **53**, 2340–2345.
122 D. Bertrand, S. Bertrand, E. Neveu and P. Fernandes, Molecular characterization of off-target activities of telithromycin: a potential role for nicotinic acetylcholine receptors, *Antimicrob. Agents Chemother.*, 2010, **54**, 5399–5402.
123 R. J. Owellen, C. A. Hartke, R. M. Dickerson and F. O. Hams, Inhibition of tubulin-microtubule polymerization by drugs of the Vinca alkaloid class, *Cancer Res.*, 1976, **36**, 1499–1502.
124 R. H. Himes, Interactions of the catharanthus (Vinca) alkaloids with tubulin and microtubules, *Pharmacol. Ther.*, 1991, **51**, 257–267.
125 M. A. Jordan and L. Wilson, Microtubules as a target for anticancer drugs, *Nat. Rev. Cancer*, 2004, **4**, 253–265.
126 V. F. Roche, in *Foye's principles of Medicinal Chemistry*, ed. T. L. Lemke, D. A. Williams, V. F. Roche and S. W. Zito, Lippincott Williams & Wilkins, China, 7 edn, 2012, ch. 37, pp. 1244–1250.
127 B. Gigant, C. Wang, R. B. Ravelli, F. Roussi, M. O. Steinmetz, P. A. Curmi, A. Sobel and M. Knossow, Structural basis for the regulation of tubulin by vinblastine, *Nature*, 2005, **435**, 519–522.
128 R. L. Noble, C. T. Beer and J. H. Cutts, Role of chance observations in chemotherapy: vinca rosea, *Ann. N. Y. Acad. Sci.*, 1958, **76**, 882–894.
129 G. H. Svoboda, N. Neuss and M. Gorman, Alkaloids of vinca rosea Linn. (Catharanthus roseus G. Don.) V.: Preparation and characterization of alkaloids, *J. Am. Pharm. Assoc., Sci. Ed.*, 1959, **48**, 659–666.
130 G. H. Svoboda, Alkaloids of Vinca rosea. IX. Extraction and characterization of leurosidine and leurocristine, *Lloydia*, 1961, **24**, 173–178.
131 J. W. Moncrief and W. N. Lipscomb, Structures of leurocristine (vincristine) and vincaleukoblastine. X-ray analysis of leurocristine methiodide, *J. Am. Chem. Soc.*, 1965, **87**, 4963–4964.
132 N. Langlois, F. Gueritte, Y. Langlois and P. Potier, Application of a modification of the Polonovski reaction to the synthesis of vinblastine-type alkaloids, *J. Am. Chem. Soc.*, 1976, **98**, 7017–7024.
133 P. Mangeney, R. Z. Andriamialisoa, N. Langlois, Y. Langlois and P. Potier, Preparation of vinblastine, vincristine, and leurosidine, antitumor alkaloids from Catharanthus species (Apocynaceae), *J. Am. Chem. Soc.*, 1979, **101**, 2243–2245.
134 J. P. Kutney, L. S. L. Choi, J. Nakano, H. Tsukamoto, M. McHugh and C. A. Boulet, A highly efficient and commercially important synthesis of the antimuor Catharanthus alkaloids vinblastine and leurosidine from catharanthine and vindoline, *Heterocycles*, 1988, **27**, 1845–1853.
135 M. E. Kuehne, P. A. Matson and W. G. Bornmann, Enantioselective syntheses of vinblastine, leurosidine, vin-

covaline, and 20′-epi-vincovaline, *J. Org. Chem.*, 1991, **56**, 513–528.

136 W. G. Bornmann and M. E. Kuehne, A common intermediate providing syntheses of ψ-tabersonine, coronaridine, iboxyphylline, ibophyllidine, vinamidine, and vinblastine, *J. Org. Chem.*, 1992, **57**, 1752–1760.

137 P. Magnus, J. S. Mendoza, A. Stamford, M. Ladlow and P. Willis, Nonoxidative coupling methodology for the synthesis of the antitumor bisindole alkaloid vinblastine and a lower-half analogue: solvent effect on the stereochemistry of the crucial C-15/C-18′ bond, *J. Am. Chem. Soc.*, 1992, **114**, 10232–10245.

138 S. Kobayashi, T. Ueda and T. Fukuyama, An efficient total synthesis of (-)-vindoline, *Synlett*, 2000, 883–886.

139 S. Yokoshima, T. Ueda, S. Kobayashi, A. Sato, T. Kuboyama, H. Tokuyama and T. Fukuyama, Stereocontrolled total synthesis of (+)-vinblastine, *J. Am. Chem. Soc.*, 2002, **124**, 2137–2139.

140 T. Kuboyama, S. Yokoshima, H. Tokuyama and T. Fukuyama, Stereocontrolled total synthesis of (+)-vincristine, *Proc. Natl. Acad. Sci. U. S. A.*, 2004, **101**, 11966–11970.

141 T. Miyazaki, S. Yokoshima, S. Simizu, H. Osada, H. Tokuyama and T. Fukuyama, Synthesis of (+)-vinblastine and its analogues, *Org. Lett.*, 2007, **9**, 4737–4740.

142 H. Ishikawa, G. I. Elliott, J. Velcicky, Y. Choi and D. L. Boger, Total synthesis of (-)- and ent-(+)-vindoline and related alkaloids, *J. Am. Chem. Soc.*, 2006, **128**, 10596–10612.

143 H. Ishikawa, D. A. Colby and D. L. Boger, Direct coupling of catharanthine and vindoline to provide vinblastine: total synthesis of (+)- and ent-(-)-vinblastine, *J. Am. Chem. Soc.*, 2008, **130**, 420–421.

144 H. Gotoh, J. E. Sears, A. Eschenmoser and D. L. Boger, New insights into the mechanism and an expanded scope of the Fe(III)-mediated vinblastine coupling reaction, *J. Am. Chem. Soc.*, 2012, **134**, 13240–13243.

145 H. Ishikawa, D. A. Colby, S. Seto, P. Va, A. Tam, H. Kakei, T. J. Rayl, I. Hwang and D. L. Boger, Total synthesis of vinblastine, vincristine, related natural products, and key structural analogues, *J. Am. Chem. Soc.*, 2009, **131**, 4904–4916.

146 N. Wang, J. Liu, C. Wang, L. Bai and X. Jiang, Asymmetric total syntheses of (-)-jerantinines A, C, and E, (-)-16-methoxytabersonine, (-)-vindoline, and (+)-vinblastine, *Org. Lett.*, 2018, **20**, 292–295.

147 L. S. Borman and M. E. Kuehne, in *The Alkaloids*, ed. A. Brossi and M. Suffness, Academic, San Diego, 1990, vol. 37, pp. 133–144.

148 H. L. Pearce, in *The Alkaloids*, ed. A. Brossi and M. Suffness, Academic, San Diego, 1990, vol. 37, pp. 145–204.

149 J. Fahy, Modifications in the "upper" or velbenamine part of the vinca alkaloids have major implications for tubulin interacting activities, *Curr. Pharm. Des.*, 2001, **7**, 1181–1197.

150 J. E. Sears and D. L. Boger, Total synthesis of vinblastine, related natural products, and key analogues and development of inspired methodology suitable for the systematic study of their structure-function properties, *Acc. Chem. Res.*, 2015, **48**, 653–662.

151 H. Gotoh, K. K. Duncan, W. M. Robertson and D. L. Boger, 10′-Fluorovinblastine and 10′-fluorovincristine: synthesis of a key series of modified vinca alkaloids, *ACS Med. Chem. Lett.*, 2011, **2**, 948–952.

152 T. J. Barker, K. K. Duncan, K. Otrubova and D. L. Boger, Potent vinblastine C20′ ureas displaying additionally improved activity against a vinblastine-resistant cancer cell line, *ACS Med. Chem. Lett.*, 2013, **4**, 985–988.

153 E. K. Leggans, K. K. Duncan, T. J. Barker, K. D. Schleicher and D. L. Boger, A remarkable series of vinblastine analogues displaying enhanced activity and an unprecedented tubulin binding steric tolerance: C20′ urea derivatives, *J. Med. Chem.*, 2013, **56**, 628–639.

154 A. Tam, H. Gotoh, W. M. Robertson and D. L. Boger, Catharanthine C16 substituent effects on the biomimetic coupling with vindoline: preparation and evaluation of a key series of vinblastine analogues, *Bioorg. Med. Chem. Lett.*, 2010, **20**, 6408–6410.

155 K. D. Schleicher, Y. Sasaki, A. Tam, D. Kato, K. K. Duncan and D. L. Boger, Total synthesis and evaluation of vinblastine analogues containing systematic deep-seated modifications in the vindoline subunit ring system: core redesign, *J. Med. Chem.*, 2013, **56**, 483–495.

156 M. C. Wani, H. L. Taylor, M. E. Wall, P. Coggon and A. T. McPhail, Plant antitumor agents. VI. Isolation and structure of taxol, a novel antileukemic and antitumor agent from Taxus brevifolia, *J. Am. Chem. Soc.*, 1971, **93**, 2325–2327.

157 M. A. Jordan, Mechanism of action of antitumor drugs that interact with microtubules and tubulin, *Curr. Med. Chem.: Anti-Cancer Agents*, 2002, **2**, 1–17.

158 M. A. Jordan and L. Wilson, Microtubules as a target for anticancer drugs, *Nat. Rev. Cancer*, 2004, **4**, 253–265.

159 A. Todd, P. W. Groundwater and J. H. Gill, in *Anticancer Therapeutics: From Drug Discovery to Clinical Applications*, John Wiley & Sons Ltd, 2018, pp. 211–232.

160 R. A. Holton, C. Somoza, H. B. Kim, F. Liang, R. J. Biediger, P. D. Boatman, M. Shindo, C. C. Smith and S. Kim, First total synthesis of taxol. 1. Functionalization of the B ring, *J. Am. Chem. Soc.*, 1994, **116**, 1597–1598.

161 R. A. Holton, H. B. Kim, C. Somoza, F. Liang, R. J. Biediger, P. D. Boatman, M. Shindo, C. C. Smith and S. Kim, First total synthesis of taxol. 2. Completion of the C and D rings, *J. Am. Chem. Soc.*, 1994, **116**, 1599–1600.

162 K. C. Nicolaou, Z. Yang, J. J. Liu, H. Ueno, P. G. Nantermet, R. K. Guy, C. F. Claiborne, J. Renaud, E. A. Couladouros, K. Paulvannan and E. J. Sorensen, Total synthesis of taxol, *Nature*, 1994, **367**, 630–634.

163 K. C. Nicolaou, P. G. Nantermet and H. Ueno, Novel chemistry of taxol. Retrosynthetic and synthetic studies, *J. Chem. Soc., Chem. Commun.*, 1994, 295–296.

164 S. J. Danishefsky, J. J. Masters, W. B. Young, J. T. Link, L. B. Snyder, T. V. Magee, D. K. Jung, R. C. A. Isaacs,

W. G. Bornmann, C. A. Alaimo, C. A. Coburn and M. J. D. Grandi, Total synthesis of baccatin III and taxol, *J. Am. Chem. Soc.*, 1996, **118**, 2843–2859.

165 P. A. Wender, N. F. Badham, S. P. Conway, P. E. Floreancig, T. E. Glass, C. Gränicher, J. B. Houze, J. Jänichen, D. Lee, D. G. Marquess, P. L. McGrane, W. Meng, T. P. Mucciaro, M. Mühlebach, M. G. Natchus, H. Paulsen, D. B. Rawlins, J. Satkofsky, A. J. Shuker, J. C. Sutton, R. E. Taylor and K. Tomooka, The pinene path to taxanes. 5. Stereocontrolled synthesis of a versatile taxane precursor, *J. Am. Chem. Soc.*, 1997, **119**, 2755–2756.

166 P. A. Wender, N. F. Badham, S. P. Conway, P. E. Floreancig, T. E. Glass, J. B. Houze, N. E. Krauss, D. Lee, D. G. Marquess, P. L. McGrane, W. Meng, M. G. Natchus, A. J. Shuker, J. C. Sutton and R. E. Taylor, The pinene path to taxanes. 6. A concise stereocontrolled synthesis of taxol, *J. Am. Chem. Soc.*, 1997, **119**, 2757–2758.

167 K. Morihira, R. Hara, S. Kawahara, T. Nishimori, N. Nakamura, H. Kusama and I. Kuwajima, Enantioselective total synthesis of taxol, *J. Am. Chem. Soc.*, 1998, **120**, 12980–12981.

168 H. Kusama, R. Hara, S. Kawahara, T. Nishimori, H. Kashima, N. Nakamura, K. Morihira and I. Kuwajima, Enantioselective total synthesis of (−)-taxol, *J. Am. Chem. Soc.*, 2000, **122**, 3811–3820.

169 T. Mukaiyama, I. Shiina, H. Iwadare, H. Sakoh, Y. Tani, M. Hasegawa and K. Satoh, Asymmetric total synthesis of Taxol, *Chem. – Eur. J.*, 1999, **5**, 121–161.

170 T. Doi, S. Fuse, S. Miyamoto, K. Nakai, D. Sasuga and T. Takahashi, A formal total synthesis of taxol aided by an automated synthesizer, *Chem. – Asian J.*, 2006, **1**, 370–383.

171 S. Hirai, M. Utsugi, M. Iwamoto and M. Nakada, Formal total synthesis of (−)-taxol through Pd-catalyzed eight-membered carbocyclic ring formation, *Chem. – Eur. J.*, 2015, **21**, 355–359.

172 K. Fukaya, Y. Tanaka, A. C. Sato, K. Kodama, H. Yamazaki, T. Ishimoto, Y. Nozaki, Y. M. Iwaki, Y. Yuki, K. Umei, T. Sugai, Y. Yamaguchi, A. Watanabe, T. Oishi, T. Sato and N. Chida, Synthesis of Paclitaxel. 1. Synthesis of the ABC ring of Paclitaxel by SmI2-mediated cyclization, *Org. Lett.*, 2015, **17**, 2570–2573.

173 K. Fukaya, K. Kodama, Y. Tanaka, H. Yamazaki, T. Sugai, Y. Yamaguchi, A. Watanabe, T. Oishi, T. Sato and N. Chida, Synthesis of paclitaxel. 2. Construction of the ABCD ring and formal synthesis, *Org. Lett.*, 2015, **17**, 2574–2577.

174 S. Jennewein, M. R. Wildung, M. Chau, K. Walker and R. Croteau, Random sequencing of an induced Taxus cell cDNA library for identification of clones involved in Taxol biosynthesis, *Proc. Natl. Acad. Sci. U. S. A.*, 2004, **101**, 9149–9154.

175 R. Croteau, R. E. Ketchum, R. M. Long, R. Kaspera and M. R. Wildung, Taxol biosynthesis and molecular genetics, *Phytochem. Rev.*, 2006, **5**, 75–97.

176 Y. Kanda, H. Nakamura, S. Umemiya, R. K. Puthukanoori, V. R. M. Appala, G. K. Gaddamanugu, B. R. Paraselli and P. S. Baran, Two-phase synthesis of taxol, *J. Am. Chem. Soc.*, 2020, **142**, 10526–10533.

177 Y. Kanda, Y. Ishihara, N. C. Wilde and P. S. Baran, Two-phase total synthesis of taxanes: tactics and strategies, *J. Org. Chem.*, 2020, **85**, 10293–10320.

178 A. Mendoza, Y. Ishihara and P. S. Baran, Scalable enantioselective total synthesis of taxanes, *Nat. Chem.*, 2012, **4**, 21–25.

179 D. G. I. Kingston, Taxol: The chemistry and structure-activity relationships of a novel anticancer agent, *Trends Biotechnol.*, 1994, **12**, 222–227.

180 W.-S. Fang and X.-T. Liang, Recent progress in structure activity relationship and mechanistic studies of taxol analogues, *Mini-Rev. Med. Chem.*, 2005, **5**, 1–12.

181 D. G. I. Kingston, The shape of things to come: structural and synthetic studies of taxol and related compounds, *Phytochemistry*, 2007, **68**, 1844–1854.

182 Y. Fu, S. Li, Y. Zu, G. Yang, Z. Yang, M. Luo, S. Jiang, M. Wink and T. Efferth, Medicinal chemistry of paclitaxel and its analogues, *Curr. Med. Chem.*, 2009, **16**, 3966–3985.

183 J. Żwawiak and L. Zaprutko, A brief history of taxol, *J. Med. Sci.*, 2014, **83**, 47–52.

184 D. G. I. Kingston, M. D. Chordia, P. G. Jagtap, J. Liang, Y.-C. Shen, B. H. Long, C. R. Fairchild and K. A. Johnston, Synthesis and biological evaluation of 1-deoxypaclitaxel analogues, *J. Org. Chem.*, 1999, **64**, 1814–1822.

185 H. Yuan, C. R. Fairchild, X. Liang and D. G. I. Kingston, Synthesis and biological activity of C-6 and C-7 modified paclitaxels, *Tetrahedron*, 2000, **56**, 6407–6414.

186 Q. Cheng, T. Oritani, T. Horiguchi, T. Yamada and Y. Mong, Synthesis and biological evaluation of novel 9-functional heterocyclic coupled 7-deoxy-9-Dihydropaclitaxel analogue, *Bioorg. Med. Chem. Lett.*, 2000, **10**, 517–521.

187 L. L. Klein, Synthesis of 9-dihydrotaxol: a novel bioactive taxane, *Tetrahedron Lett.*, 1993, **34**, 2047–2050.

188 H. Ge, V. Vasandani, J. K. Huff, K. L. Audus, R. H. Himes, A. Seelig and G. I. Georg, Synthesis and interactions of 7-deoxy-, 10-deacetoxy, and 10-deacetoxy-7-deoxypaclitaxel with NCI/ADR-RES cancer cells and bovine brain microvessel endothelial cells, *Bioorg. Med. Chem. Lett.*, 2006, **16**, 433–436.

189 S. H. Chen, J. M. Wei and V. Farina, Taxol structure-activity relationships: synthesis and biological evaluation of 2-deoxytaxol, *Tetrahedron Lett.*, 1993, **34**, 3205–3206.

190 A. Datta, L. R. Jayasinghe and G. I. Georg, 4-Deacetyltaxol and 10-acetyl-4-deacetyltaxotere: synthesis and biological evaluation, *J. Med. Chem.*, 1994, **37**, 4258–4260.

191 K. A. Neidigh, M. M. Gharpure, J. M. Rimoldi, D. G. I. Kingston, Y. Q. Jiang and E. Hamel, Synthesis and biological evaluation of 4-deacetylpaclitaxel, *Tetrahedron Lett.*, 1994, **35**, 6839–6842.

192 R. Marder-Karsenti, J. Dubois, L. Bricard, D. Guénard and F. Guéritte-Voegelein, Synthesis and biological evaluation of D-ring-modified taxanes: 15(20)-azadocetaxel analogs, *J. Org. Chem.*, 1997, **62**, 6631–6637.

193 A. A. L. Gunatilaka, F. D. Ramdayal, M. H. Sarragiotto, D. G. I. Kingston, D. L. Sackett and E. Hamel, Synthesis and biological evaluation of novel paclitaxel (taxol) D-ring modified analogues, *J. Org. Chem.*, 1999, **64**, 2694–2703.

194 I. Ojima, J. C. Slater, E. Michaud, S. D. Kuduk, P.-Y. Bounaud, P. Vrignaud, M.-C. Bissery, J. M. Veith, P. Pera and R. J. Bernacki, Syntheses and structure–-activity relationships of the second-generation antitumor taxoids: exceptional activity against drug-resistant cancer cells, *J. Med. Chem.*, 1996, **39**, 3889–3896.

195 S. M. Ali, M. Z. Hoemann, J. Aube, L. A. Mitscher, G. I. Georg, R. McCall and L. R. Jayasinghe, Novel cytotoxic 3′-(tert-Butyl) 3′-diphenyl analogs of paclitaxel and docetaxel, *J. Med. Chem.*, 1995, **38**, 3821–3828.

196 T. C. Boge, R. H. Himes, D. G. V. Velde and G. I. Georg, The effect of the aromatic rings of taxol on biological activity and solution conformation: synthesis and evaluation of saturated taxol and taxotere analogs, *J. Med. Chem.*, 1994, **37**, 3337–3343.

197 I. Ojima and S. Lin, Efficient asymmetric syntheses of β-lactams bearing a cyclopropane or an epoxide moiety and their application to the syntheses of novel isoserines and taxoids, *J. Org. Chem.*, 1998, **63**, 224–225.

198 I. Ojima, T. Inoue and S. Chakravarty, Enantiopure fluorine-containing taxoids: potent anticancer agents and versatile probes for biomedical problems, *J. Fluor. Chem.*, 1999, **97**, 3–10.

199 J. Wang, C. Xu, Y. K. Wong, Y. Li, F. Liao, T. Jiang and Y. Tu, Artemisinin, the magic drug discovered from traditional Chinese medicine, *Engineering*, 2019, **5**, 32–39.

200 A. Robert, F. Benoit-Vical, C. Claparols and B. Meunier, The antimalarial drug artemisinin alkylates heme in infected mice, *Proc. Natl. Acad. Sci. U. S. A.*, 2005, **102**, 13676–13680.

201 F. T. Aweeka and P. I. German, Clinical pharmacology of artemisinin-based combination therapies, *Clin. Pharmacokinet.*, 2008, **47**, 91–102.

202 L. Cui and X. Z. Su, Discovery, mechanisms of action and combination therapy of artemisinin, *Expert Rev. Anti-Infect. Ther.*, 2009, **7**, 999–1013.

203 J. Wang, C.-J. Zhang, W. N. Chia, C. C. Y. Loh, Z. Li, Y. M. Lee, Y. He, L.-X. Yuan, T. K. Lim, M. Liu, C. X. Liew, Y. Q. Lee, J. Zhang, N. Lu, C. T. Lim, Z.-C. Hua, B. Liu, H.-M. Shen, K. S. W. Tan and Q. Lin, Haem-activated promiscuous targeting of artemisinin in Plasmodium falciparum, *Nat. Commun.*, 2015, **6**, 10111–10122.

204 L. Tilley, J. Straimer, N. F. Gnädig, S. A. Ralph and D. A. Fidock, Artemisinin action and resistance in plasmodium falciparum, *Trends Parasitol.*, 2016, **32**, 282–296.

205 M. Ouji, J.-M. Augereau, L. Paloque and F. Benoit-Vical, Plasmodium falciparum resistance to artemisinin-based combination therapies: A sword of Damocles in the path toward malaria elimination, *Parasite*, 2018, **25**, 1–12.

206 C. H. Sibley, Understanding artemisinin resistance, *Science*, 2015, **347**, 373–374.

207 A. A. Mbengue, S. S. Bhattacharjee, T. T. Pandharkar, H. Liu, G. Estiu, R. V. Stahelin, S. S. Rizk, D. L. Njimoh, Y. Ryan, K. Chotivanich, C. Nguon, M. Ghorbal, J. J. Lopez-Rubio, M. Pfrender, S. Emrich, N. Mohandas, A. M. Dondorp, O. Wiest and K. Haldar, A molecular mechanism of artemisinin resistance in Plasmodium falciparum malaria, *Nature*, 2015, **520**, 683–687.

208 Z. Wang, L. Yang, X. Yang and X. Zhang, Advances in the chemical synthesis of artemisinin, *Synth. Commun.*, 2014, **44**, 1987–2003.

209 S. K. Sahu, P. K. Behera, P. Choudhury, S. Panda and L. Rout, Strategy and problems for synthesis of antimalaria artemisinin (qinghaosu), *ChemistrySelect*, 2020, **5**, 12333–12344.

210 G. Schmid and W. Hofheinz, Total synthesis of qinghaosu, *J. Am. Chem. Soc.*, 1983, **105**, 624–625.

211 X.-X. Xu, J. Zhu, D.-Z. Huang and W.-S. Zhou, Total synthesis of arteannuin and deoxyarteannuin, *Tetrahedron*, 1986, **42**, 819–828.

212 M. A. Avery, C. Jennings-White and W. K. M. Chong, The total synthesis of (+)-artemisinin and (+)-9-desmethyltemesinin, *Tetrahedron Lett.*, 1987, **20**, 4629–4632.

213 M. A. Avery, W. K. M. Chong and C. Jennings-White, Stereoselective total synthesis of (+)-artemisinin, the antimalarial constituent of Artemisia annua L, *J. Am. Chem. Soc.*, 1992, **114**, 974–979.

214 T. Ravindranathan, M. A. Kumar, R. B. Menon and S. V. Hiremath, Stereoselective synthesis of artemisinin, *Tetrahedron Lett.*, 1990, **31**, 755–758.

215 H. J. Liu, W. L. Yeh and S. Yeu Chew, A total synthesis of the antimarial natural product (+)-qinghaosu, *Tetrahedron Lett.*, 1993, **34**, 4435–4438.

216 J. B. Bhonsle, B. Pandey, V. H. Deshpande and T. Ravindranathan, New synthetic strategies towards (+)-artemisinin, *Tetrahedron Lett.*, 1994, **35**, 5489–5492.

217 M. G. Constantino, M. B. Jr., G. V. J. Silva and J. Zukerman-Schpector, A novel asymmetric total synthesis of (+)-artemisinin, *Synth. Commun.*, 1196, **26**, 321–329.

218 J. S. Yadav, R. S. Babu and G. Sabitha, Stereoselective total synthesis of (+)-artemisinin, *Tetrahedron Lett.*, 2003, **44**, 387–389.

219 J. S. Yadav, B. Thirupathaiah and P. Srihari, A concise stereoselective total synthesis of (+)-artemisinin, *Tetrahedron*, 2010, **66**, 2005–2009.

220 C. Zhu and S. P. Cook, A concise synthesis of (+)-artemisinin, *J. Am. Chem. Soc.*, 2012, **134**, 13577–13579.

221 J. Krieger, T. Smeilus, M. Kaiser, E.-J. Seo, T. Efferth and A. Giannis, Total synthesis and biological investigation of (−)-artemisinin: the antimalarial activity of artemisinin is not stereospecific, *Angew. Chem., Int. Ed.*, 2018, **57**, 8293–8296.

222 J. N. Cumming, D. Wang, S. B. Park, T. A. Shapiro and G. H. Posner, Design, synthesis, derivatization, and structure–activity relationships of simplified, tricyclic, 1,2,4-trioxane alcohol analogues of the antimalarial artemisinin, *J. Med. Chem.*, 1998, **41**, 952–964.

223 M. A. Avery, M. Alvim-Gaston, C. R. Rodrigues, E. J. Barreiro, F. E. Cohen, Y. A. Sabnis and J. R. Woolfrey, Structure–activity relationships of the antimalarial agent artemisinin. 6. The development of predictive in vitro potency models using CoMFA and HQSAR methodologies, *J. Med. Chem.*, 2002, **45**, 292–303.

224 M. A. Avery, S. Mehrotra, T. L. Johnson, J. D. Bonk, J. A. Vroman and R. Miller, Structure–activity relationships of the antimalarial agent artemisinin. 5. Analogs of 10-deoxoartemisinin substituted at C-3 and C-9, *J. Med. Chem.*, 1996, **39**, 4149–4155.

225 M. A. Avery, P. Fan, J. M. Karle, J. D. Bonk, R. Miller and D. K. Goins, Structure–activity relationships of the antimalarial agent artemisinin. 3. Total synthesis of (+)-13-carbaartemisinin and related tetra- and tricyclic structures, *J. Med. Chem.*, 1996, **39**, 1885–1897.

226 M. A. Avery, S. Mehrotra, J. D. Bonk, J. A. Vroman, D. K. Goins and R. Miller, Structure–activity relationships of the antimalarial agent artemisinin. 4. Effect of substitution at C-3, *J. Med. Chem.*, 1996, **39**, 2900–2906.

227 M. A. Avery, J. D. Bonk, W. K. M. Chong, S. Mehrotra, R. Miller, W. Milhous, D. K. Goins, S. Venkatesan and C. Wyandt, Structure-activity relationships of the antimalarial agent artemisinin. 2. Effect of heteroatom substitution at O-11: synthesis and bioassay of N-alkyl-11-aza-9-desmethylartemisinins, *J. Med. Chem.*, 1995, **38**, 5038–5044.

228 M. A. Avery, F. Gao, W. K. M. Chong, S. Mehrotra and W. K. Milhous, Structure-activity relationships of the antimalarial agent artemisinin. 1. Synthesis and comparative molecular field analysis of C-9 analogs of artemisinin and 10-deoxoartemisinin, *J. Med. Chem.*, 1993, **36**, 4264–4275.

229 M. K. Tiwari and S. Chaudhary, Artemisinin-derived antimalarial endoperoxides from bench-side to bed-side: Chronological advancements and future challenges, *Med. Res. Rev.*, 2020, **40**, 1220–1275.

230 R. K. Haynes, B. Fugmann, J. Stetter, K. Rieckmann, H.-D. Heilmann, H.-W. Chan, M.-K. Cheung, W.-L. Lam, H.-N. Wong, S. L. Croft, L. Vivas, L. Rattray, L. Stewart, W. Peters, B. L. Robinson, M. D. Edstein, B. Kotecka, D. E. Kyle, B. Beckermann, M. Gerisch, M. Radtke, G. Schmuck, W. Steinke, U. Wollborn, K. Schmeer and A. Römer, Artemisone—a highly active antimalarial drug of the artemisinin class, *Angew. Chem., Int. Ed.*, 2006, **45**, 2082–2088.

231 Y. Tu, *From Artemisia annua L. to artemisinins: the discovery and development of artemisinins and antimalarial agents*, Academic Press, 2017.

232 M. A. Avery, F. Gao, W. K. M. Chong, T. F. Hendrickson, W. D. Inman and P. Crews, Synthesis, conformational analysis, and antimalarial activity of tricyclic analogs of artemisinin, *Tetrahedron*, 1994, **50**, 957–972.

233 T. N. C. Wells, R. H. V. Huijsduijnen and W. C. V. Voorhis, Malaria medicines: a glass half full?, *Nat. Rev. Drug Discovery*, 2015, **14**, 424–442.

234 S. L. Rawe, in *Antimalarial Agents*, Elsevier Ltd, 2020, pp. 99–132.

235 C. Cuevas and A. Francesch, Development of Yondelis (trabectedin, ET-743). A semisynthetic process solves the supply problem, *Nat. Prod. Rep.*, 2009, **26**, 322–337.

236 V. H. Le, M. Inai, R. M. Williams and T. Kan, Ecteinascidins. A review of the chemistry, biology and clinical utility of potent tetrahydroisoquinoline antitumor antibiotics, *Nat. Prod. Rep.*, 2015, **32**, 328–347.

237 S. Yuan, Y.-Q. Luo, J.-H. Zuo, H. Liu, F. Li and B. Yu, New drug approvals for 2020: Synthesis and clinical applications, *Eur. J. Med. Chem.*, 2021, **215**, 113284–113317.

238 K. K. C. Liu, S. M. Sakya, C. J. O'Donnell and J. Li, Synthetic approaches to the 2007 new drugs, *Mini-Rev. Med. Chem.*, 2008, **8**, 1526–1548.

239 K. L. Rinehart, T. G. Holt, N. L. Fregeau, J. G. Stroh, P. A. Keifer, F. Sun, L. H. Li and D. G. Martin, Ecteinascidins 729, 743, 745, 759A, 759B, and 770: potent antitumor agents from the Caribbean tunicate Ecteinascidia turbinata, *J. Org. Chem.*, 1990, **55**, 4512–4515.

240 R. Sakai, K. L. Rinehart, Y. Guan and A. H.-J. Wang, Additional antitumor ecteinascidins from a Caribbean tunicate: crystal structures and activities in vivo, *Proc. Natl. Acad. Sci. U. S. A.*, 1992, **89**, 11456–11460.

241 Y. Pommier, G. Kohlhagen, C. Bailly, M. Waring, A. Mazumder and K. W. Kohn, DNA sequence- and structure-selective alkylation of guanine N2 in the DNA minor groove by ecteinascidin 743, a potent antitumor compound from the caribbean tunicate Ecteinascidia turbinata, *Biochemistry*, 1996, **35**, 13303–13309.

242 B. M. Moore, F. C. Seaman and L. H. Hurley, NMR-based model of an ecteinascidin 743-DNA adduct, *J. Am. Chem. Soc.*, 1997, **119**, 5475–5476.

243 B. M. Moore, F. C. Seaman, R. T. Wheelhouse and L. H. Hurley, Mechanism for the catalytic activation of ecteinascidin 743 and its subsequent alkylation of guanine N2, *J. Am. Chem. Soc.*, 1998, **120**, 2490–2491.

244 R. Garcia-Nieto, I. Manzanares, C. Cuevas and F. Gago, Bending of DNA upon binding of ecteinascidin 743 and phthalascidin 650 studied by unrestrained molecular dynamics simulations, *J. Am. Chem. Soc.*, 2000, **122**, 7172–7182.

245 M. Zewail-Foote and L. H. Hurley, Ecteinascidin 743: a minor groove alkylator that bends DNA toward the major groove, *J. Med. Chem.*, 1999, **42**, 2493–2497.

246 A. B. Herrero, C. Martin-Castellanos, E. Marco, F. Gago and S. Moreno, Cross-talk between nucleotide excision and homologous recombination DNA repair pathways in the mechanism of action of antitumor trabectedin, *Cancer Res.*, 2006, **66**, 8155–8162.

247 D. G. Soares, A. E. Escargueil, V. Poindessous, A. Sarasin, A. D. Gramont, D. Bonatto, J. A. P. Henriques and A. K. Larsen, Replication and homologous recombination repair regulate DNA double-strand break formation by the antitumor alkylator ecteinascidin 743, *Proc. Natl. Acad. Sci. U. S. A.*, 2007, **104**, 13062–13067.

248 E. J. Corey, D. Y. Gin and R. S. Kania, Enantioselective total synthesis of ecteinascidin 743, *J. Am. Chem. Soc.*, 1996, **118**, 9202–9203.
249 C. Cuevas, M. Perez, M. J. Martin, J. L. Chicharro, C. Fernandez-Rivas, M. Flores, A. Francesch, P. Gallego, M. Zarzuelo, F. D. L. Calle, J. Garcia, C. Polanco, I. Rodriguez and I. Manzanares, Synthesis of ecteinascidin ET-743 and phthalascidin Pt-650 from cyanosafracin B, *Org. Lett.*, 2000, **2**, 2545–2548.
250 E. J. Martinez and E. J. Corey, A new, more efficient, and effective process for the synthesis of a key pentacyclic intermediate for production of ecteinascidin and phthalascidin antitumor agents, *Org. Lett.*, 2000, **2**, 993–996.
251 A. Endo, A. Yanagisawa, M. Abe, S. Tohma, T. Kan and T. Fukuyama, Total synthesis of ecteinascidin 743, *J. Am. Chem. Soc.*, 2002, **124**, 6552–6554.
252 F. Kawagishi, T. Toma, T. Inui, S. Yokoshima and T. Fukuyama, Total synthesis of ecteinascidin 743, *J. Am. Chem. Soc.*, 2013, **135**, 13684–13687.
253 J. Chen, X. Chen, M. Bois-Choussy and J. Zhu, Total synthesis of ecteinascidin 743, *J. Am. Chem. Soc.*, 2006, **128**, 87–89.
254 S. Zheng, C. Chan, T. Furuuchi, B. J. D. Wright, B. Zhou, J. Guo and S. J. Danishefsky, Stereospecific formal total synthesis of ecteinascidin 743, *Angew. Chem., Int. Ed.*, 2006, **45**, 1754–1759.
255 D. Fishlock and R. M. Williams, Synthetic studies on Et-743. Assembly of the pentacyclic core and a formal total synthesis, *J. Org. Chem.*, 2008, **73**, 9594–9600.
256 W. He, Z. Zhang and D. Ma, A scalable total synthesis of the antitumor agents Et-743 and lurbinectedin, *Angew. Chem., Int. Ed.*, 2019, **58**, 3972–3975.
257 E. J. Martinez, T. Owa, S. L. Schreiber and E. J. Corey, Phthalascidin, a synthetic antitumor agent with potency and mode of action comparable to ecteinascidin 743, *Proc. Natl. Acad. Sci. U. S. A.*, 1999, **96**, 3496–3501.
258 K. Suwanborirux, K. Charupant, S. Amnuoypol, S. Pummangura, A. Kubo and N. Saito, Ecteinascidins 770 and 786 from the Thai Tunicate Ecteinascidia thurstoni, *J. Nat. Prod.*, 2002, **65**, 935–937.
259 P. Puthongking, C. Patarapanich, S. Amnuoypol, K. Suwanborirux, A. Kubo and N. Saito, Chemistry of ecteinascidins. Part 2. Preparation of 6′-O-acyl derivatives of stable ecteinascidin and evaluation of cytotoxicity, *Chem. Pharm. Bull.*, 2006, **54**, 1010–1016.
260 P. Saktrakulkla, S. Toriumi, M. Tsujimoto, C. Patarapanich, K. Suwanborirux and N. Saito, Chemistry of ecteinascidins. Part 3: preparation of 2′-N-acyl derivatives of ecteinascidin 770 and evaluation of cytotoxicity, *Bioorg. Med. Chem.*, 2011, **19**, 4421–4436.
261 M. Tsujimoto, W. Lowtangkitcharoen, N. Mori, W. Pangkruang, P. Putongking, K. Suwanborirux and N. Saito, Chemistry of ecteinascidins. Part 4: preparation of 2′-N-acyl ecteinascidin 770 derivatives with improved cytotoxicity profiles, *Chem. Pharm. Bull.*, 2013, **61**, 1052–1064.
262 R. Toyoshima, N. Mori, T. Suzuki, W. Lowtangkitcharoen, K. Suwanborirux and N. Saito, Chemistry of ecteinascidins. Part 5: an additional proof of cytotoxicity evaluation of ecteinascidin 770 derivatives, *Chem. Pharm. Bull.*, 2016, **64**, 966–969.
263 N. Saito, Chemical research on antitumor isoquinoline marine natural products and related compounds, *Chem. Pharm. Bull.*, 2021, **69**, 155–177.
264 M. D. Lee, T. S. Dunne, M. M. Siegel, C. C. Chang, G. O. Morton and D. B. Borders, Calichemicins, a novel family of antitumor antibiotics. 1. Chemistry and partial structure of calichemicin .gamma.1I, *J. Am. Chem. Soc.*, 1987, **109**, 3464–3466.
265 M. D. Lee, T. S. Dunne, C. C. Chang, G. A. Ellestad, M. M. Siegel, G. O. Morton, W. J. McGahren and D. B. Borders, Calichemicins, a novel family of antitumor antibiotics. 2. Chemistry and structure of calichemicin . gamma.1I, *J. Am. Chem. Soc.*, 1987, **109**, 3466–3468.
266 M. D. Lee, J. K. Manning, D. R. Williams, N. A. Kuck, R. T. Testa and D. B. Borders, Calicheamicins, a novel family of antitumor antibiotics, *J. Antibiot.*, 1989, **42**, 1070–1087.
267 K. Edo, M. Mizugaki, Y. Koide, H. Seto, K. Furihata, N. Ōtake and N. Ishida, The structure of neocarzinostatin chromophore possessing a novel bicyclo-[7,3,0]dodecadiyne system, *Tetrahedron Lett.*, 1985, **26**, 331–334.
268 J. Golik, G. Dubay, G. Groenewold, H. Kawaguchi, M. Konishi, B. Krishnan, H. Ohkuma, K. Saitoh and T. W. Doyle, Esperamicins, a novel class of potent antitumor antibiotics. 3. Structures of esperamicins A1, A2, and A1b, *J. Am. Chem. Soc.*, 1987, **109**, 3462–3464.
269 M. Konishi, H. Ohkuma, K. Matsumoto, T. Tsuno, H. Kamei, T. Miyaki, T. Oki, H. Kawaguchi, G. D. Vanduyne and J. Clardy, Dynemicin A, a novel antibiotic with the anthraquinone and 1,5-diyn-3-ene subunit, *J. Antibiot.*, 1989, **42**, 1449–1452.
270 S. Walker, R. Landovitz, W. D. Ding, G. A. Ellestad and D. Kahne, Cleavage behavior of calicheamicin gamma 1 and calicheamicin T, *Proc. Natl. Acad. Sci. U. S. A.*, 1992, **89**, 4608–4612.
271 R. Gébleux and G. Casi, Antibody-drug conjugates: Current status and future perspectives, *Pharmacol. Ther.*, 2016, **167**, 48–59.
272 S. Yaghoubi, M. H. Karimi, M. Lotfinia, T. Gharibi, M. Mahi-Birjand, E. Kavi, F. Hosseini, K. S. Sepehr, M. Khatami, N. Bagheri and M. Abdollahpour-Alitappeh, Potential drugs used in the antibody–drug conjugate (ADC) architecture for cancer therapy, *J. Cell. Physiol.*, 2020, **235**, 31–64.
273 K. C. Nicolaou, C. W. Hummel, E. N. Pitsinos, M. Nakada, A. L. Smith, K. Shibayama and H. Saimoto, Total synthesis of calicheamicin .gamma.1I, *J. Am. Chem. Soc.*, 1992, **114**, 10082–10084.
274 R. D. Groneberg, T. Miyazaki, N. A. Stylianides, T. J. Schulze, W. Stahl, E. P. Schreiner, T. Suzuki, Y. Iwabuchi, A. L. Smith and K. C. Nicolaou, Total syn-

thesis of calicheamicin .gamma.1I. 1. Synthesis of the oligosaccharide fragment, *J. Am. Chem. Soc.*, 1993, **115**, 7593–7611.

275 A. L. Smith, E. N. Pitsinos, C. K. Hwang, Y. Mizuno, H. Saimoto, G. R. Scarlato, T. Suzuki and K. C. Nicolaou, Total synthesis of calicheamicin .gamma.1I. 2. Development of an enantioselective route to (-)-calicheamicinone, *J. Am. Chem. Soc.*, 1993, **115**, 7612–7624.

276 K. C. Nicolaou, C. W. Hummel, M. Nakada, K. Shibayama, E. N. Pitsinos, H. Saimoto, Y. Mizuno, K. U. Baldenius and A. L. Smith, Total synthesis of calicheamicin . gamma.1I. 3. The final stages, *J. Am. Chem. Soc.*, 1993, **115**, 7625–7635.

277 M. P. Cabal, R. S. Coleman and S. J. Danishefsky, Total synthesis of calicheamicinone: a solution to the problem of the elusive urethane, *J. Am. Chem. Soc.*, 1990, **112**, 3253–3255.

278 J. N. Haseltine, M. P. Cabal, N. B. Mantlo, N. Iwasawa, D. S. Yamashita, R. S. Coleman, S. J. Danishefsky and G. K. Schulte, Total synthesis of calicheamicinone: new arrangements for actuation of the reductive cycloaromatization of aglycon congeners, *J. Am. Chem. Soc.*, 1991, **113**, 3850–3866.

279 S. A. Hitchcock, S. H. Boyer, M. Y. Chu-Moyer, S. H. Olson and S. J. Danishefsky, A convergent total synthesis of calicheamicin γ1′, *Angew. Chem., Int. Ed.*, 1994, **33**, 858–862.

280 R. L. Halcomb, S. H. Boyer, M. D. Wittman, S. H. Olson, D. J. Denhart, K. K. C. Liu and S. J. Danishefsky, Studies related to the carbohydrate sectors of esperamicin and calicheamicin: definition of the stability limits of the esperamicin domain and fashioning of a glycosyl donor from the calicheamicin domain, *J. Am. Chem. Soc.*, 1995, **117**, 5720–5749.

281 S. A. Hitchcock, M. Y. Chu-Moyer, S. H. Boyer, S. H. Olson and S. J. Danishefsky, A remarkable glycosidation reaction: the total synthesis of calicheamicin .gamma.1I, *J. Am. Chem. Soc.*, 1995, **117**, 5750–5756.

282 N. Oku, S. Matsunaga and N. Fusetani, Shishijimicins A–C, novel enediyne antitumor antibiotics from the ascidian didemnum proliferum1, *J. Am. Chem. Soc.*, 2003, **125**, 2044–2045.

283 L. A. McDonald, T. L. Capson, G. Krishnamurthy, W.-D. Ding, G. A. Ellestad, V. S. Bernan, W. M. Maiese, P. Lassota, R. A. Kramer and C. M. Ireland, Namenamicin, a new enediyne antitumor antibiotic from the marine ascidian polysyncraton lithostrotum, *J. Am. Chem. Soc.*, 1996, **118**, 10898–10899.

284 K. C. Nicolaou, Z. Lu, R. Li, J. R. Woods and T.-I. Sohn, Total synthesis of shishijimicin A, *J. Am. Chem. Soc.*, 2015, **137**, 8716–8719.

285 K. C. Nicolaou, R. Li, Z. Lu, E. N. Pitsinos, L. B. Alemany, M. Aujay, C. Lee, J. Sandoval and J. Gavrilyuk, Streamlined total synthesis of shishijimicin A and its application to the design, synthesis, and biological evaluation of analogues thereof and practical syntheses of PhthNSSMe and related sulfenylating reagents, *J. Am. Chem. Soc.*, 2018, **140**, 12120–12136.

286 K. C. Nicolaou, R. Li, Z. Lu, E. N. Pitsinos and L. B. Alemany, Total synthesis and full structural assignment of namenamicin, *J. Am. Chem. Soc.*, 2018, **140**, 8091–8095.

287 K. C. Nicolaou, R. Li, Q. Chen, Z. Lu, E. N. Pitsinos, A. Schammel, B. Lin, C. Gu, H. Sarvaiya, R. Tchelepi, A. Valdiosera, J. Clubb, N. Barbour, V. Sisodiya, J. Sandoval, C. Lee, M. Aujay and J. Gavrilyuk, Synthesis and biological evaluation of shishijimicin A-type linker-drugs and antibody–drug conjugates, *J. Am. Chem. Soc.*, 2020, **142**, 12890–12899.

288 A. M. Gillespie, T. J. Broadhead, S. Y. Chan, J. Owen, A. P. Farnsworth, M. Sopwith and R. E. Coleman, Phase I open study of the effects of ascending doses of the cytotoxic immunoconjugate CMB-401 (hCTMO1-calicheamicin) in patients with epithelial ovarian cancer, *Ann. Oncol.*, 2000, **11**, 735–741.

289 L. M. Hinman, P. R. Hamann, R. Wallace, A. T. Menendez, F. E. Durr and J. Upeslacis, Preparation and characterization of monoclonal antibody conjugates of the calicheamicins: a novel and potent family of antitumor antibiotics, *Cancer Res.*, 1993, **53**, 3336–3342.

290 K. C. Nicolaou, T. Li, M. Nakada, C. W. Hummel, A. Hiatt and W. Wrasidlo, Calicheamicin θ1′: A rationally designed molecule with extremely potent and selective DNA cleaving properties and apoptosis inducing activity, *Angew. Chem., Int. Ed.*, 1994, **33**, 183–186.

291 H. N. Lode, R. A. Reisfeld, R. Handgretinger, K. C. Nicolaou, G. Gaedicke and W. Wrasidlo, Targeted therapy with a novel enediyene antibiotic calicheamicin ϑI1 effectively suppresses growth and dissemination of liver metastases in a syngeneic model of murine neuroblastoma, *Cancer Res.*, 1998, **58**, 2925–2928.

292 K. M. Bernt, A. Prokop, N. Huebener, G. Gaedicke, W. Wrasidlo and H. N. Lode, Eradication of CD19+ leukemia by targeted calicheamicin θ, *Bioconjugate Chem.*, 2009, **20**, 1587–1594.

293 G. Chen, B. K. Alisher, H. Zhang, T. Zhu and Z. Miao, Calicheamicin antibody drug conjugates linking and amidoacetyl group to a sugar moiety on calicheamicin, WO/2017/172907, 2017.

294 T. Pillow, Calicheamicin-antibody-drug conjugates and methods of use, WO/2017/068511, 2017.

295 A. D. Ricart, Antibody-drug conjugates of calicheamicin derivative: gemtuzumab ozogamicin and inotuzumab ozogamicin, *Clin. Cancer Res.*, 2011, **17**, 6417–6427.